Identification and function analysis of genes involved in development of intermuscular bone of wuchang bream (Megalobrama amblycephala)

Wan, Shiming

UNIVERSTY OF ZAGREB
FACULTY OF AGRICULTURE

HUAZHONG AGRICULTURAL UNIVERSITY
COLLEGE OF FISHERIES

Shiming Wan

IDENTIFICATION AND FUNCTION ANALYSIS OF GENES INVOLVED IN DEVELOPMENT OF INTERMUSCULAR BONE OF WUCHANG BREAM (*MEGALOBRAMA AMBLYCEPHALA*)

INTERNATIONAL DUAL DOCTORATE

Zagreb, 2020.

UNIVERSTY OF ZAGREB
FACULTY OF AGRICULTURE

HUAZHONG AGRICULTURAL UNIVERSITY
COLLEGE OF FISHERIES

Shiming Wan

IDENTIFICATION AND FUNCTION ANALYSIS OF GENES INVOLVED IN DEVELOPMENT OF INTERMUSCULAR BONE OF WUCHANG BREAM (*MEGALOBRAMA AMBLYCEPHALA*)

INTERNATIONAL DUAL DOCTORATE

Supervisors:

Tea Tomljanović

Zexia Gao

Zagreb, 2020.

PhD assessment

This dissertation was evaluated by the committee:

1. Professor. Tomislav Treer, PhD
2. Assisstant professor. Daniel Matulić, PhD
3. Professor. Kaijian Wei, PhD
4. Professor. Hong Liu, PhD
5. Professor. Jingou Tong, PhD

The dissertation is defended at Huazhong Agricultural University, College of Fisheries, China and University of Zagreb Faculty of Agriculture by ZOOM on line meeting 22. May 2020. by the committee:

1. Professor Tomislav Treer, PhD

2.Assisstant Professor Daniel Matulić, PhD

3. Professor Kaijian Wei, PhD

4. Professor Hong Liu, PhD

5. Professor Jingou Tong, PhD

Information about mentors

Mentor 1: Tea Tomljanović PhD Associate Professor

Tea Tomljanović was born in Split, where she finished elementary and high school. She graduated in 2000. at the Faculty of Agriculture, University of Zagreb. Since 2000 she has been employed at the Department of Fisheries, Beekeeping and Special Zoology at the Faculty of Agriculture, where she defended her Master's thesis in 2004. Since her main scientific interest is molecular genetics in fisheries, the topic of her doctoral thesis defended in 2010 is "Morphological and genetic analyzes of carp populations (*Cyprinus carpio* L.) in the Republic of Croatia".

Basic scientific interest of Tea Tomljanović is a molecular genetic study of fish and their genetic relationships. In her scientific training, she has worked with a number of molecular molecular genetics researchers in Slovenia, Austria, Hungary, the Czech Republic, P.R. China. In addition to this, she has worked in other areas, especially in the field of open water and fish ecology. So far, she has published 24 papers of group a1, 22 papers of group a2 and 11 papers of group a3. In addition, she has participated in numerous international and national scientific conferences.

Intensive international cooperation Asst. Tee Tomljanovic is also well-known for his active participation in 8 international scientific projects. In addition, he has been involved in national scientific projects since the beginning of his work. He is the head of an international and national scientific project. She is the editor-in-chief of the Croatian Journal of Fisheries.

Mentor 2: Zexia Gao PhD Associate Professor

Professor Gao was Ph.D. student in the College of Fisheries, Huazhong Agriculture University Wuhan, Hubei, PR China where she contined her professional carier.

Professor Gao research areas are genetic selection and breeding in aquaculture, fish genomics and molecular genetics. She started her carier at 2010. as a lecturer of the Department of Fish Molecular Breeding, College of Fisheries, Huazhong Agricultural University where she still working as a professor at Department of Fish Molecular Breeding, College of Fisheries, Huazhong Agricultural University. Professor Gao had a working experiences in University of California, Davis, USA (2016-2017) and Nofima, Norway (2015). She is Associate Editor for Journal of World Aquaculture Society and Croatian Journal of Fisheries, Director Member of Zoology and Animal Society of Hubei Province and Wuhan City and reviewer for several international journals, such as BMC Genomics, Plos One, Aquaculture, Aquaculture Research, Journal of Fish Biology, Biological Invasions, Journal of World Aquaculture Society, Marine Biodiversity, etc.

SUMMARY

IDENTIFICATION AND FUNCTION ANALYSIS OF GENES INVOLVED IN DEVELOPMENT OF INTERMUSCULAR BONE OF WUCHANG BREAM (*MEGALOBRAMA AMBLYCEPHALA*)

Intermuscular bones (IB), which occur only in the myosepta of the lower teleosts, are segmental, serially homologous ossifications from connective tissue in the myosepta. Most of the freshwater aquaculture fishes around the world, especially Cyprinidae species, possess a certain amount of IB. These IB have brought about many adverse impacts on the deep processing and food value of a fish species, because they are difficult to remove and make the fish unpleasant to eat. Meanwhile, IB reduces the economic value of a fish species, resulting in low price and exports. Main results and conclusions are as follows:
The results of tissue section observation revealed the microstructural features of IB, CT and muscle tissue, indicating that IB has a potential differentiation relationship with CT. The miRNA comparative analysis between IB and connective tissue finally obtained a total of 218 known miRNAs belong to 97 miRNA families. Of them, 188 miRNAs were expressed in both tissues, while 13 and 17 miRNAs were specifically expressed in IB and connective tissue, respectively.
On the basis of fthis key development stages of IB (S1: IB haven't emerged; S2: a few IB with small length emerged in the tail; S3: more IB of greater length gradually emerged in the tail; S4: all of the IB in the tail have a mature morphology and length. IB have also emerged throughout the body of the fish from the tail to the head), it is constructed a reference transcriptome to analyze miRNA and mRNA expression profiles over fthis IB developmental stages. The wild-type construct GLO-*runx2b* was not reduced by miR-206-3p mimics, which showed the inaccuracy of software prediction and the necessity of experimental verification.
Considering significant enrichment of BMP signaling pathway in previous studies, it is verified the function of *bmpr2a*/*2b* receptors through CRISPR-Cas9 technology and focused on its role in intermuscular bone and skeleton development. Phylogenetic and genomic structure analysis indicated that the sequence characteristics of *bmpr2a* and *bmpr2b* genes in zebrafish were differentiated in the evolutionary process. Gene knockout results showed that the loss of bmpr2a and bmpr2b function did not cause significant changes in the IB phenotype, but *bmpr2b*$^{-/-}$ mutant showed different degrees and types of mineralized bone malformations. The significant changes in the expression levels of BMP-Smad signaling molecules and various bone development genes, and the phenotypic changes in *bmpr2b*$^{-/-}$ individuals revealed an important role for bmpr2b in bone mineralization of zebrafish.

Keywords: *Megalobrama amblycephala*; intermuscular bone; development; miRNA; gene expression; gene function

PROŠIRENI SAŽETAK

IDENTIFIKACIJA I FUNKCIJSKA ANALIZA GENA KOJI SU UKLJUČENI U RAZVOJ INTERMUSKULARNIH KOSTIJU WUCHANG DEVERIKE (*MEGALOBRAMA AMBLYCEPHALA)*

U ovom istraživanju otkrivena je mikrostruktura i potencijalni odnos diferencijacije intermuskularnih kostiju i okolnog vezivnog tkiva u miosepti kod vrste wuchang deverike. Na temelju razlika u strukturi tkiva i usporedne analize transkripta, otkrivena je specifična ekspresija miRNA u različitim tkivima i ciljanim genima. Analizom KEGG staze otkriven je veliki broj specifičnih gena značajnih za skeletni razvoj. Genetski podaci intermuskularnih kostiju identificirani su kroz diferencijaciju tkiva.

Korelacijska analiza ekspresije mRNA i miRNA u ključnim razvojnim fazama intermuskularnih kostiju otkrila je mRNA i miRNA koje su posebno eksprimirane u različitim razvojnim fazama, kao i različito eksprimirane gene i miRNA između različitih razvojnih stadija, uključujući gene za TGF-β putove čija se razina ekspresije nastavlja smanjivati / povećavati u različitim razvojnim fazama. Utvrđena je uska veza TGF-β sa signalnim putovima MAPK i ERK kojima se reguliraa diferencijacija osteoblasta. Istraživanje je otkrilo veliku količinu genetskih informacija o intermuskularnim kostima iz razvojne perspektive.

Analiza interakcije miRNA-mRNA otkrila je veliki broj miRNA i mRNA povezanih s razvojem kostiju. Validacijom odnosa između skeniranih razvojnih miRNA i mRNA na temelju dualnog luciferaznog gena otkrila je da miR-133b-3p značajno inhibira 3'UTR ekspresiju tgfbrla i runx2a te da miR-206-3p značajno inhibira ekspresiju 'UTR sekvence. Međutim, eksperimentalni rezultati također su pokazali da prekomjerna ekspresija miR-206-3p nije uzrokovala supresiju ekspresije plazmida GLO-runx2b, što sugerira nesigurnost ciljnih gena predviđenih softverom i nužnost daljnjih eksperimenta za validaciju.

Funkcionalna provjera gena kandidata na temelju CRISPR-Cas9 otkrila je ulogu bmpr2b u mineralizaciji kostiju model riba zebrica, ali nije pronađen izravan regulatorni učinak na fenotip intermuskularnih kostiju.

U ovom radu postignuto je više istraživačkih inovacija. Prvi put je promatrana mikrostruktura intermuskularnih kostiju i srodnih tkiva, istražena je njihova potencijalna diferencijacija i konstruirana je baza podataka mRNA i miRNA transkriptora intermuskularnih kostiju i potencijalno diferenciranog tkiva. Također je na temelju karakteristika razvoja intermuskularnih kostiju, konstruirama je transkriptna baza podataka o mRNA i miRNA, otkrivajući potencijalni regulatorni odnos između miRNA i mRNA u razvoju intermuskularnih kostiju. Prvi put je sustavno proučavan mehanizam molekularne regulacije intermuskularnih kostiju riba kombinirajući morfologiju, histologiju, transkriptomiju i tehnologiju uređivanja gena CRISPR-Cas9

Stoga je ostvaren i predviđeni znanstveni doprinos u sveobuhvatnoj izgradi genetičke baze intermuskularnih kostiju wuchang deverike i generalizacije važnih genetskih informacija vezanih uz nastanak i razvoj intermuskularnih kostiju koje se mogu koristiti za

daljnje istraživanje molekularnog mehanizma razvoja intermuskularnih kostiju i molekularno genetskih tehnika kod uzgoja wuchang deverike.

Ključne riječi: *Megalobrama amblycephala*; intermuskularne kosti; ravoj; miRNA; ekspresija gena; funkcija gena

Contents

Contents 1
List of abbreviation 3
1 INTRODUCTION 4
1.1. Microstructural observation and miRNA transcriptome analysis of IBs and CT in the *M. amblycephala* 4
1.2. Correlation analysis and validation of mRNA and miRNA expression patterns in key developmental stages of IBs 6
1.3. Functional verification of BMP II receptor genes in zebrafish bone development 8
1.4. Objective and hypotheses of research 10
2 Materiels and Methods 11
2.1 Animals and Tissue Collection 11
2.2 Morphological observation 11
2.3 Small RNA Isolation and cDNA Library Construction 11
2.4 Small RNA Sequence Analysis 12
2.5 Differential Expression Analysis of miRNAs 13
2.6 Prediction of miRNA Target Genes 14
2.7 Experimental animals and tissue collection 15
2.8 Total RNA isolation and cDNA library construction 17
2.9 De novo assembly and functional annotation 17
2.10 Gene expression profiling of different development stages 18
2.11 MiRNA sequencing and differential expression analysis 18
2.12 Quantitative PCR for miRNA and mRNA expression 19
2.13 Vector Construction and Dual Luciferase reporter assays 20
2.14. Phylogenetic Analysis and Genomic Structure Analysis 20
2.15 Fish Strain, Design of bmpr2a and bmpr2b gRNAs for CRISPR/Cas9, Generation and Genotyping of Mutants 21
2.16 Phenotypic and Developmental Observation of Mutant Fish 22
2.17 Comparative Transcriptome Analysis 23
2.18 Quantitative real-time PCR for BMP-Smad Pathway Genes and Skeletal Development-Related Genes 24
2.19. Protein Expression Analysis by Western Blot 25
3 RESULTS 26
3.1. Tissue section and staining observation results 26
3.2 General Features of Small RNAs 27
3.3 Identification of Conserved miRNAs 28
3.4 Statistics of Multiple IsomiRs in *M. amblycephala* 31
3.5 Differentially Expressed miRNAs 33
3.6 Prediction of Potential Targets of Differentially-Expressed miRNA 35
3.7 Function Analysis of Target Genes of Differentially-Expressed miRNAs 36
3.8 Assembly and annotation of reference transcriptome 38
3.9 Expression profiling of IBs development-dependent genes 40

3.10 Functional analysis of DEGs and SEGs during the fthis developmental stages . . . 43
3.11 Sequence and expression profiling of IB development-dependent microRNAs. . . . 44
3.12 Analysis of miRNA-mRNA interaction . . . 47
3.13 Quantitative analysis of miRNA and mRNA expression . . . 49
3.14 Target verification of miR-133b-3p and miR-206-3p . . . 51
3.15 Chromosome synteny analysis and conservation analysis of *bmpr2* genes . . . 52
3.16 Generation of *bmpr2a* and *bmpr2b* mutant zebrafish . . . 54
3.17 *bmpr2a*$^{-/-}$与 *bmpr2b*$^{-/-}$ zebrafish with normal IBs . . . 54
3.18 *bmpr2b*$^{-/-}$ zebrafish showed varying degrees of mineralized bone malformations . . . 55
3.19 Expression of BMP-Smad signaling molecule significantly Down-Regulated in *bmpr2b*$^{-/-}$ mutants . . . 57
4 DISCUSSION. . . . 61
5. CONCLUSIONS. . . . 65
Key Findings:. . . . 65
Research Innovation . . . 66
6 REFERENCES . . . 67
Additional file 1 miRNA reverse transcription-specific stem-loop primers . . . 81
Additional file 2 miRNAs qRT-PCR froward primers . . . 81
Additional file 3 miRNA reverse transcription-specific stem-loop primers . . . 82
Additional file 4 miRNAs qRT-PCR froward primers . . . 82
Additional file 5 Protocols for fast DNA extraction . . . 82
Additional file 6 Bone and cartilage staining method. . . . 83
Additional file 7 Wild and bmpr2a mutant zebrafish sequence . . . 84
Additional file 8 Wild and bmpr2b mutant zebrafish sequence . . . 86

List of abbreviation

Abbreviation	English Full Name
IB	Intermuscular bones
CT	Connective tissue
TGF-β	transforming growth factor-β
dpf	day after fertilization
BMP	bone morpho-genetic proteins
MAPK	mitogen-activated protein kinase
ERK	extracellular regulated protein kinases
Runx2	runt related transcription factor 2
NR	NCBI non-redundant protein sequences
KEGG	Kyoto Encyclopedia of Genes and Genomes
KOG	eukaryotic Orthology Groups
GO	Gene Ontology
FDR	False Discovery Rate
RNA-Seq	RNA Sequencing
ncRNA	Non-coding RNA
NGS	Next-generation sequencing,
Osx	osterix
miRNA	microRNA
sRNA	Small RNA
PCR	Polymorphism Chain Reaction
RT-PCR	Reverse Transcription PCR
qRT-PCR	Quantitative real-time PCR

1 INTRODUCTION

1.1. Microstructural observation and miRNA transcriptome analysis of IBs and CT in the *M. amblycephala*

Intermuscular bones (IBs), which occur only in lower teleosts amongst vertebrates, are segmental, serially homologous ossifications in the myosepta (Patterson and Johnson, 1995). They appeared to have a function to strengthen the connection between the sarcomeres (Xie, 2010). Obviously, the ossification process and distribution of IBs was different from other axial skeletons (Bird and Mabee, 2003). The IBs develop directly from mesenchymal condensation, being totally different from the ribs, which are developed from a mesenchymal cell population derived from the ventral somite. The IBs are primordially differentiated from osteoblast in connective tissue, which is essentially different from normal muscle. Most of the freshwater aquaculture fishes around the world, especially Cyprinidae species, such as crucian carp (*Carassius carassius*), grass carp (*Ctenopharyngodon idellus*), silver carp (*Hypophthalmichthys molitrix*), etc., possess a certain amount of IBs. These IBs have brought about many adverse impacts on the economic and food value of a species, such as influencing the processing and affecting the freshness (Ma et al., 2012). Along with the evolution of fish species, the morphology tends to be more complicated, especially becoming extremely complex with the evolution of the cyprinids (Lü et al, 2007). In view of its potential value, researchers began to study IBs in fish as early as the 1960s. Bing (1962) first described the morphology of IBs in juvenile common carp (*Cyprinus carpio*). Patterson and Johnson (1995) and Johnson and Patterson (2001) have made detailed observations and analyses of the IBs for 125 teleostean fish species, including Chinese major freshwater cyprinids. Subsequently, extensive research has been undertaken focusing on the morphology, number and distribution of the IBs in many fish species (Ke et al., 2008; Jiang et al, 2008; Fang and Li (2013)). Interestingly, Li et al. (2013) documented the number of IBs in different ploidies of *C. auratus* and found significant differences among the different ploidy fishes, which indicated the possibility of decreasing the number of IBs through genetic improvement.

With the rapid development of molecular breeding technologies, it is possible to suppress IB formation by gene silencing, gene knockout and fluorescent protein methods combined with gene inhibitor technology.

It is well known that miRNA is a special kind of molecule in organisms, which regulates the level of proteins by decreasing messenger RNA (mRNA) levels or inhibiting translation by binding the 3' UTR of the target mRNA. miRNA plays an important role in various developmental, physiological and pathological conditions, such as osteoblast differentiation, development, disease, gene transcription and translation (Hobert, 2008). The description of miRNA has been recorded for several fish species, such as Atlantic salmon (*Salmo salar*), medaka (*Oryzias latipes*), rainbow trout (*Oncorhynchus mykiss*), *C. carpio*, bighead carp (*Hypophthalmichthys nobilis*), *H. molitrix*, channel catfish (*Ictalurus punctatus*) and Nile tilapia (*Oreochromis niloticus*). The progress of these studies in fish provides insight into the types of miRNAs and their possible mechanisms in sexual development (Bizuayehu et al., 2012), evolution evaluation (Chen, 2009), skeletal muscle development (Yan et al, 2012) and growth (Yi et al., 2013). Nonetheless, few studies have been conducted on the identification of miRNA for fish IBs.

Blunt snout bream (*Megalobrama amblycephala*, Yih, 1955), which is restrictively distributed in the middle and lower reaches of the Yangtze River in Central China, is a fish species with high economic value, which has been farmed in China’s freshwater polyculture systems since the 1960s (Wan et al., 2015). Intensive studies of this species have been performed, especially concerning growth, disease control and genetic resthisces (Luo et al., 2014; Li et al., 2012; Gao et al., 2012). This previous study has documented the emergent periods and morphogenesis of IBs in *M. amblycephala* (Wan et al., 2014). In the present study, it is implemented a miRNA comparative analysis to investigate the miRNAs expression and regulated pattern of IBs and connective tissue (CT), which encircle IBs, through high throughput sequencing technology. The miRNAs in two tissues of M. amblycephala were identified, and the differentially-expressed miRNAs were analyzed. The obtained miRNA resthisces from this study will contribute to a further understanding of the molecular mechanisms of IBs development and the roles that miRNAs play in regulating diverse biological processes in fish.

1.2. Correlation analysis and validation of mRNA and miRNA expression patterns in key developmental stages of IBs

It is well known that most of the freshwater aquaculture fishes around the world, especially Cyprinidae species, possessed a certain amount of intermuscular bones (IBs), which are hard-boned spicules located in the muscle tissue on both sides of the vertebrae (Patterson and Johnson, 1995). The IBs develop directly from mesenchymal condensation and consist of membranous ossifications of connective tissue in the muscular septum. IBs differ from other axial skeletons, such as the vertebral column, which develops from a mesenchymal cell population derived from the ventral somite (Bird and Mabee, 2003). IBs reduce the edibleness and economic value of a fish species (Ma et al., 2012). In view of the potential value in eliminating IBs, researchers began to study IBs in fish as early as the 1960s (Bing, 1962). Interestingly, prior studies revealed the significant differences in the number of IBs among fish of different ploidy, indicating that genetic improvement methods could have a significant effect on decreasing the number of IBs (Li et al, 2013). But so far, almost all existing studies have only focused on the morphology of IBs in fish species (Ke et al., 2008; Jiang et al., 2008; Fang et al., 2013). Few in-depth studies have been carried out and little information has been obtained regarding the molecular mechanism for development of IBs. Only one previous study has revealed the molecular properties of IBs through microRNA (miRNA) transcriptome analysis (Wan et al., 2015).

High-throughput sequencing technologies are being widely used to investigate the complete repertoire of expressed RNA transcripts in specific tissues or cells at specific stages of development, and this knowledge is helping improve this understanding of the molecule mechanism affecting expression (Guo et al, 2012), regulatory (Huang et al, 2012) and development (Yu et al, 2014). In fish, independent transcriptome profiling (RNA-seq) of miRNAs or mRNAs has been used to identify gene and miRNA expression related to various physiological functions (Yu et al, 2014; He et al, 2015; Yi et al, 201, Fu et al, 2011). As miRNAs has been reported to regulate gene expression by promoting mRNA degradation and repressing translation, the combined analyses of mRNA with miRNA expression data has been conducted in plants and mammals to infer regulatory

mechanisms associated with various physiological processes (Tang et al, 2014; Ran et al, 2015; Zeng et al, 2015). In fish species, the integrated analysis of mRNA and miRNA expression profiles has been performed on zebrafish (*Danio rerio*) for optic nerve regeneration and on darkbarbel catfish (*Pelteobagrus vachelli*) in response to hypoxia (Fuller-Carter et al, 2015; Zhang et al, 2016).

Perazza et al. 2015 has reported that specimens of tambaqui (*Colossoma macropomum*) from one culture population lack IBs, even though this fish normally has IBs. Xu et al.23 has identified an intermuscular bone-deficient grass carp (*Ctenopharyngodon idellus*) mutant in an artificial gynogenetic group. Based on these two reports, it has been speculated that there maybe one or several key genes that regulate the development of IBs.

In the present study, it is used one typical Cyprinidae species, blunt snout bream (*Megalobrama amblycephala*), for which the morphological characteristics, emergent periods and morphogenesis of IBs are known from this previous research (Wan et al, 2014). IBs gradually appear during the growth and development of *M. amblycephala*. It emerged 20 days post hatching (dph) at a body length of 1.33 cm, first in the tail and then toward the head. When fry was 40 dph with the body length of 2.36 cm, all intermuscular bones had appeared. With the aim to generate the fundamental molecular resthisces across the different developmental stages from emerging to complete formation of IBs and try to find the putative key genes or miRNAs for regulating IBs' development, the transcriptome property, mRNA and miRNA expression profiling were investigated in the fthis key stages related to IBs development of M. amblycephala in this study. A certain amount of bone-related genes, period-specific or period-differential expressed mRNAs and miRNAs were identified, and the related signaling pathways were uncovered through the comparisons of the fthis development stages. Meanwhile, some interaction networks and regulatory modes of mRNAs and miRNAs were also revealed based on the integrated analysis of miRNA and mRNA expression profiles.

1.3. Functional verification of BMP II receptor genes in zebrafish bone development

The skeleton is a complex living structure composed of bone and cartilage, which serve a variety of functions in internal organ protection, hematopoietic, mineral storage, muscle attachment, movement and joint protection (Meyer and Wiesmann, 2006; Berendsen and Olsen, 2015). Endochondral ossification and intramembranous ossification are two distinct developmental process of bone formation. Many genes and associated signaling pathways have been recruited as core regulators in these process (Karsenty, 2003; Kronenberg, 2003), such as bone morphogenic protein (BMP) pathway, which has widely recognized roles in animal skeletal development (Chen et al., 2012; Salazar et al., 2016; Kobayashi et al., 2005; Yi et al., 2000). In mammals, *Bmpr2* (BMP type II receptor) has been shown to be the essential molecule that activates the canonical BMP-Smad signaling in response to BMP ligands binding (Miyazono et al., 2010). Previous studies have revealed that mutations in *Bmpr2* are associated with familial primary pulmonary hypertension in human (Lane et al., 2000). However, the conventional knockout of *Bmpr2* will lead to mouse embryonic death (Beppu et al., 2000), which limits the functional exploration of bmpr2 in systemic physiology and skeletal systems. Only limited conditional knockout experiments explored the role of *Bmpr2* in mammalian skeletal development, showed that deletion of *Bmpr2* in mouse skeletal progenitor cells can result in increased bone formation rate and high bone mass (Lowery et al., 2015).

Zebrafish has become a powerful model for studying the function of mammal homologs because many zebrafish knockout mutants survive longer than their mouse counterparts allowing for a more ththisogh analysis of homologs function in skeletal development (Apschner et al, 2011). Researchers have established the zebrafish model of human osteogenesis imperfecta at the biological and molecular levels, providing an important resthisce for the pathophysiology of the disease (Fisher et al., 2003). Study on zebrafish models of PXE (pseudoxanthoma elasticum) and GACI (generalised arterial calcification of infancy) suggested that vitamin K could be a beneficial treatment for human patients with PXE or GACI (Mackay et al., 2015). Previous study also found that *sp7* mutant

zebrafish exhibited a skeletal phenotype similar to that of patients with osteogenesis imperfecta (Lapunzina et al., 2010; Kague et al., 2016), mutations in zebrafish *edar* that affect similar residues as those mutated in human cases of HED (hypohidrotic ectodermal dysplasia) and show similar abnormal skeletal and dental phenotypic (Harris et al., 2008). Besides, zebrafish model have also been used to reveal and complement the function of *bmpr2*. Morpholino knockdown results in zebrafish suggested that *bmpr2a* and *bmpr2b* are required for the establishment of left–right asymmetry (Monteiro et al., 2008) and vascular development in early embryonic development of zebrafish (Washko et al., 2009). However, to known roles in early development, the role of the *bmpr2* in fish osteoblasts differentiation and bone formation remains to be determined.

Phylogenetic studies suggested that an additional whole genome duplication occurred in the stem lineage of ray-finned (actinopterygian) fishes, namely the fish-specific genome duplication (FSGD), which resulted in an increase of gene copy number and functional diversity (Meyer and Schartl, 2000). While tetrapodes have a signle copy of the *Bmpr2* gene, zebrafish have two, called *bmpr2a* and *bmpr2b*. Considering the signal transduction role of *bmpr2* in BMP-Smad pathway associated with skeletal development and no studies have focused on the role of *bmpr2* in fish skeletal development as this would required genetic mutants, it is conducted evolutionary analysis and sequence structure comparison between the human *Bmpr2* and two copies of *bmpr2* in zebrafish, and constructed two zebrafish mutant line for *bmpr2a* and *bmpr2b* using CRISPR-Cas9 technology. Subsequent results showed that function loss of *bmpr2a* and *bmpr2b* did not result in abnormal cartilage development, but *bmpr2b*$^{-/-}$ mutant caused abnormalities in bone mineralization and significant changes in the expression levels of BMP-Smad signaling molecules and various bone development genes, which revealed the role of bmpr2 based on bmp-smad signaling in zebrafish skeletal development and provided a promising model to explore the potential pathogenesis of human bone diseases and develop corresponding therapeutic approaches.

1.4. Objective and hypotheses of research

Hypotheses:

1. The intermuscular bones are differentiated from the surrounding connective tissue in the myosepta;
2. The initial differentiation of connective tissue into intermuscular bones and their development is controlled by key genes;
3. The differentiation and development of intermuscular bone is indirectly regulated by key non-coding RNA;
4. Loss of function of key genes can promote or inhibit the differentiation and development of intermuscular bones.

Objectives:

1. Determine differences between intermuscular bones and surrounding connective tissue
2. Determine the impact of differentially and specifically expressed genes related to initial formatting of connective tissue in the immediate environment of intermuscular bones and their growth and development
3. Determine the impact of non-coding RNA on intermuscular bones differentiation
4. Determine the impact of functional deletion of key genes on differentiation and development of intermuscular bones

2 Materiels and Methods

2.1 Animals and Tissue Collection

All animals and experiments were conducted in accordance with the “Guidelines for Experimental Animals” of the Ministry of Science and Technology (Beijing, China). The study was approved by the Institutional Animal Care and Use Ethics Committee of Huazhong Agricultural University. All efforts were made to minimize suffering.

The experimental animals were collected from an M. amblycephala selective population, which were bred in the Ezhou Fish Breeding Base of Huazhong Agricultural University (30°22'N, 114°47'E). All experimental procedures involving fish were approved by the Institution Animal Care and Use Committee of the Huazhong Agricultural University.

The IB and CT samples for small RNA sequencing were collected from six individuals at 6 months old from the same population. The maturation age of this species is normally 2–3 years, and the fish are actively growing at 6 months old. The fish were anaesthetized in well-aerated water containing the 100 mg/L concentration of tricaine methanesulfonate (MS-222) before tissue collection. The IBs and CT, which surround the IBs, were immediately collected to extract total RNA. Other tissue samples, including rib, muscle, liver, kidney, spleen, gonad and brain, were also snap-frozen in liquid nitrogen and stored at −80 °C for total RNA extraction.

2.2 Morphological observation

Separate the IBs, CT and muscle tissues, then fixed them in 4% paraformaldehyde solution for 48 h. Dehydration and embedding were then performed in accordance with conventional paraffin sectioning methods. Finally, 5 μm-thick sections and HE staining were performed on the samples.

2.3 Small RNA Isolation and cDNA Library Construction

Total RNA was isolated from the connective tissue using RNAiso Plus Reagent (TaKaRa, Dalian, China), according to the manufacturer’s protocol. The total RNA of IBs was isolated using an innovative method (Chinese Patent No. 201310673534). Briefly,

the samples of IBs were separated quickly from muscle tissues and homogenized by grinding in liquid nitrogen. Hydrosaline solution (0.8 M sodium citrate and 1.2M sodium chloride) was used for removing the protein pollution with isopropanol treatment. The total RNA pellet was washed twice with 75% ethanol by vortexing and centrifuging for 5 min at 7500× g and then dissolved in 30 μL of RNase-free water. RNA quality and quantity was measured using the NanoDrop 2000 (Thermo Scientific, Waltham, MA, USA) and Agilent 2100 Bioanalyzer (Agilent, Santa Clara, CA, USA). All of the samples were standardized to 500 ng/μL, and equal volumes of the same tissues from different individuals were combined into one pool.

For the construction of two small RNA (sRNA) libraries, small RNAs of 18–30 nt in length were first isolated from the total RNA by size fractionation in a polyacrylamide gel, and these small RNAs were ligated with 5'-RNA and 3'-RNA adapters. Afterwards, reverse transcription PCR was used to create cDNA constructs based on two adapters. The generated small cDNA libraries were amplified by PCR using primers complementary to the adaptor sequences. Subsequently, the amplified cDNA constructs were tested by the Agilent 2100 Bioanalyzer and ABI StepOnePlus Real-Time PCR System and sequenced by Illumina technology (BGI, Shenzhen, China).

2.4 Small RNA Sequence Analysis

The sequencing of cDNA libraries was based on the criteria of HiSeq 2000 SE50. By the base calling step, the basic figure from Illumina small RNA deep sequencing is converted into sequence data (raw reads), which is stored in a FASTQ format, including quality data of the reads. Before accurate analysis, low-quality reads, reads with 5' primer contaminants, reads with 3' primer, reads with polyA and reads shorter than 18 nt were eliminated. After filtering, the statistics of data quality and length distribution were performed. The common and specific reads of two samples were summarized, including the summary of unique and total reads.

Afterwards, a standard bioinformatics analysis of the high-quality sequences was implemented. The high-quality reads were blasted against the Rfam (available online: ftp://sanger.ac.uk/pub/databases/Rfam/) database and the GenBank noncoding RNA database (available online: http://blast.ncbi.nlm.nih.gov/) to annotate rRNA, tRNA, snRNA and other ncRNA sequences and aligned to the transcriptome of the M. amblycephala (Sequence Read Archive (SRA) Database: SRR1613326, SRR1612557, SRR1613325) to screen and remove the mRNA-derived degraded fragments. The selected sequences were also mapped to the zebrafish genome with a tolerance of one mismatch in the seed sequence to analyze their expression and distribution on the genome by Short Oligonucleotide Analysis Package (SOAP, available online: http://soap.genomics.org.cn/). Subsequently, miRNA identification was performed by comparing the data from two samples with the known mature miRNAs and the miRNA precursor of all fish in miRBase20.0 available online: (http://www.mirbase.org/ftp.shtml). Furthermore, the base bias had been analyzed, respectively, on the first position of identified miRNAs with a different length and on each position of all identified miRNAs. The base edit of known miRNAs (isomiRs) was conducted. The majority of identified miRNAs showed heterogeneity of length and sequence in the prior studies. The nucleotides at position 2–8 of a mature miRNA are known as the seed region, and this region is highly conserved (Fu et al., 2011; Xu et al., 2015). The target of miRNA might be different with the change of nucleotides in this region. In this analysis pipeline, miRNAs, which might have a base edit, can be detected by aligning unannotated sRNA tags with mature miRNAs from miRBase20.0, allowing one mismatch on a certain position.

2.5 Differential Expression Analysis of miRNAs

The known miRNA expression level between two samples was compared to find out the differentially-expressed miRNAs. Total miRNA counts were used for normalization, and the miRNAs of reads less than 100 were discarded on account of meaningless biological or technological errors. miRNAs that appeared as differently expressed in two libraries

were further analyzed by use of the method described in previous studies (Yi et al., 2013; Kang et al., 2013; Audic et al., 1997). Briefly, miRNAs expression in two libraries was normalized using the following formula: normalized expression = (actual miRNA sequencing reads count/total clean reads count) × 1,000,000. If the normalized expression (NE) value of a given miRNA were zero, the expression value was modified to 0.01. If the normalized expression of a given miRNA were less than 1 in both libraries, it was removed in future differential expression analyses. The fold-change and p-value were calculated from the normalized expression. When |log2ratio| ≥ 1 and p-value ≤ 0.05, it was identified as differential expression. A prerequisite for using the data for expression comparisons is that the method applied reproduces the different individual miRNA expression levels in a sample well.

Quantitative stem-loop RT-PCR with SYBR Green PCR Master Mix (TaKaRa, Dalian, China) was performed to profile the expression levels of miRNAs in 9 tissues. Eleven primers for stem-loop RT-PCR were designed according to descriptions in prior study [64] (Table S7). Total RNA from IBs, CT, rib, muscle, brain, liver, spleen, kidney and gonad of M. amblycephala was isolated using TRIzol reagent (Invitrogen) following the recommendations of the manufacturer. Real-time PCR was carried out on a Roche LightCycler 480 System II (Roche, Mannheim, Germany) according to the manufacturer's instructions, and all real-time reactions were performed in triplicate. The primers for stem-loop real-time PCR are shown in Table S7. The relative expression levels of the differentially-expressed miRNAs were measured in terms of threshold cycle value (Ct) and were normalized to 5S rRNA using the equation $2^{-\Delta\Delta Ct}$, in which $\Delta C_t = C_{t\ miRNA} - C_{t\ 5s}$。

2.6 Prediction of miRNA Target Genes

Considering that genome references of M. amblycephala are not available, the sequences of zebrafish genome and transcriptome sequences of *M. amblycephala* sequenced in this laboratory (SRA Database: SRR1613326, SRR1612557, SRR1613325) were selected to predict the target genes. Briefly, miRNAs identified in the present study were used to search for antisense hits in the reference RNA sequences. Subsequently,

mRNA sequences exhibiting perfect or near perfect complementarity with corresponding miRNAs were selected and analyzed with TargetScan (available online: http://www.targetscan.org/) and MiRanda (available online: http://www.microrna.org) to predict the target sequences. Furthermore, the biological function of the novel miRNAs was annotated with mapping targets genes to each term of the Gene Ontology database: (available online: http://www.geneontology.org/), and the gene numbers of each GO term were calculated. The main pathways of biochemical and signal transduction significantly associated with the predicted target genes of the miRNAs were determined via a KEGG pathway analysis (available online: http://www.kegg.jp/).

2.7 Experimental animals and tissue collection

Experimental fishes were selected from an artificially propagated population and grown in the recirculating aquaculture system after hatching. Before sampling, experimental animals were anaesthetized in well-aerated water containing the 100 mg/L concentration of Tricaine methanesulfonate (MS-222). This key stages for the development of IBs were selected as done for this previous research and shown in Fig. 1. Muscle tissue containing IBs in the tail (Fig. 2), which were the initial area of intermuscular bone differentiation, were sampled under an anatomical lens. The accuracy of sample collection was validated using Alizarin red and Alcian blue staining to ensure that there was no interference form fins, scales and other impurities. Composite samples of 6–10 individuals were collected to extract total RNA for every stage and each stage possessed two biological replicates. In addition, six months old fish was used to sample different tissues for gene expression analysis.

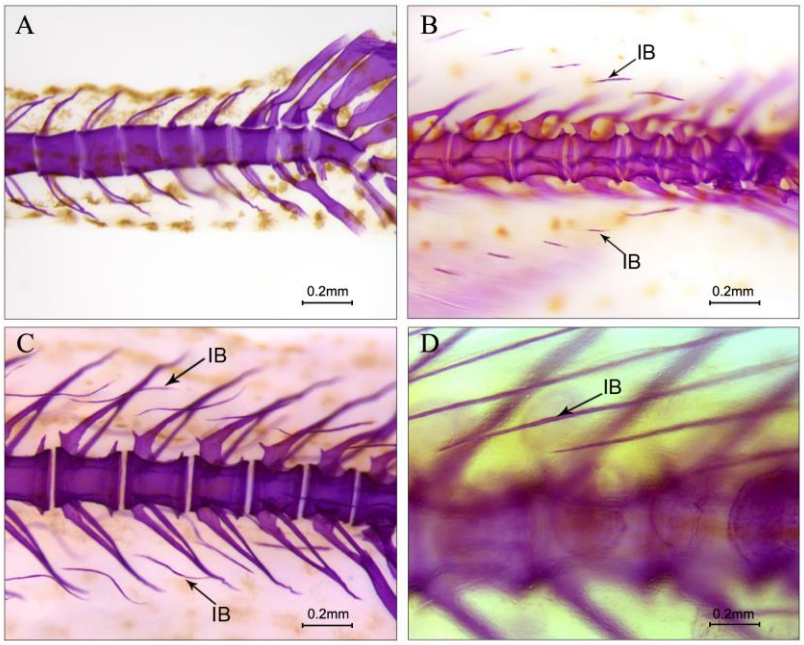

Fig. 1 Development characteristics of IB in the fthis key development stages of *M.amblycephala*. (A) Stage 1 (S1), Body Length≈11mm. 17 dph, the IB haven't emerged, but the fins and axial skeleton have developed completely, so the presence or absence of IB does not affect the development of fins and axial skeleton; (B) Stage 2 (S2), Body Length≈16mm. 24 dph, a few IB of small length have emerged in the tail; (C) Stage 3 (S3), Body Length≈21mm. 29 dph, more IB of greater length gradually emerged in the tail; (D) Stage 4 (S4), Body Length≈32mm. 42 dph, all of the IB in the tail have a mature morphology and length. IB have also emerged throughout the body of the fish from the tail to the head.

Fig. 2. Sampling area for the study (rectangular area)

All animals and experiments were conducted in accordance with the "Guidelines for Experimental Animals" of the Ministry of Science and Technology (Beijing, China). The

study was approved by the Institutional Animal Care and Use Ethics Committee of Huazhong Agricultural University. All efforts were made to minimize suffering. All experimental procedures involving fish were approved by the institution animal care and use committee of the Huazhong Agricultural University.

2.8 Total RNA isolation and cDNA library construction

Total RNA was isolated from the samples at 4 stages and different tissues using RNAiso Plus Reagent (TaKaRa, China) according to the manufacturer's protocol. RNA quality and quantity were measured using the NanoDrop 2000 (Thermo Scientific, USA) and Agilent 2100 Bioanalyzer (Agilent, USA). All the samples were standardized to 500 ng/μ l. At each stage, two Digital Gene Expression Profiling libraries and one miRNA transcriptome library were constructed. Meanwhile, a reference transcriptome library was constructed by mixing equal volumes RNA from 4 stages. During the QC steps, Agilent 2100 Bioanaylzer and ABI StepOnePlus Real-Time PCR System were used to quantify and qualify the sample library preparations. Finally, the libraries were sequenced using an Illumina HiSeq™ 2000 platform (BGI, Shenzhen, China). All of the raw RNA-Seq data were submitted to the NCBI databases (http://trace.ncbi.nlm.nih.gov/Traces/sra/sra.cgi?view=run_browser) under accession number SRR2335137 for transcriptome data, SRR2338087 for DGE data and SRR2338872 for miRNA data.

2.9 De novo assembly and functional annotation

All reads with low quality or shorter than 18 nt were eliminated. The 5′ or 3′ primer contaminants and polyA tails were removed. The clean sequencing reads were de novo assembled using the Trinity (http://trinityrnaseq.sthisceforge.net/) with Kmer = 25. The TGI Clustering Tool (version 2.1) (http://sthisceforge.net/projects/tgicl/) was used for further processing of sequence splicing and redundancy removal. BLASTx (version

v2.2.26) (E-value cut-off 1e-5) protein database (NR, Swiss-Prot, KEGG and COG) alignment was performed. When results from different databases conflicted, a priority order of NR, Swiss-Prot (http://www.ebi.ac.uk/swissprot/), KEGG (http://www.genome.jp/kegg) and COG (http://www. ncbi.nlm.nih.gov/COG) was followed for annotation. When a unigene was found to be unaligned to the above databases, ESTScan software (http://estscan.sthisceforge.net/) was introduced to decide its sequence direction. Furthermore, biological function annotation and classification were performed by mapping unigenes to each term of the Gene Ontology database (http://www.geneontology.org/), and pathways for biochemical and signal transduction were determined via a KEGG pathway analysis (http://www.kegg.jp/).

2.10 Gene expression profiling of different development stages

After raw data filtering, clean reads of the 8 libraries were mapped to the reference transcriptome using SOAPaligner/soap2 (http://soap.genomics.org.cn/) to obtain unique mapped reads, allowing a maximum of two mismatches in the alignment. The number of unique-match reads was calculated and normalized to RPKM (reads per kb per million reads) for gene expression analysis. Comparison of unigene expression between different stages was performed using DESeq analysis25. Genes with log-fold difference (log2Ratio) ≥ 1 and false discovery rate (FDR < 0.001) were considered to be significantly differentially expressed.

2.11 MiRNA sequencing and differential expression analysis

Fthis small RNA libraries were constructed and sequenced as previously described15. High-quality reads were blasted against the Rfam (ftp://sanger.ac.uk/ pub/databases/Rfam/) database and the GenBank noncoding RNA database (http://blast.ncbi.nlm.nih.gov/) to annotate rRNA, tRNA, snRNA and other ncRNA sequences, and then aligned to exons and introns of mRNA to screen and remove

degraded fragments. Selected sequences were also mapped to the reference transcriptome with a tolerance of one mismatch in the seed sequence to analyze their expression and distribution on the genome by SOAP. Conserved miRNAs were identified through a Blastn search against the miRNA database, miRBase20.0 (http://www.mirbase.org/ftp.shtml) using Mireap software (https://sthisceforge.net/projects/mireap/).

MiRNAs with reads less than 100 were discarded, and miRNA expression levels were normalized by TPM (transcript per million) values (TPM = (miRNA total reads/total clean reads) $\times 10^6$). Comparisons between developmental stages were made to find significantly differentially expressed miRNAs (|log2(fold change) | > 1 and P-value ≤ 0.05). Subsequently, gene expression differences between developmental stages showing complementarity with corresponding miRNA expression values were selected and analyzed with Targetscan (http://www.targetscan.org/) and MiRanda (http://www.microrna.org) to predict the miRNA target. Furthermore, GO terms and KEGG enrichment analysis on differential expressed miRNAs was determined via a hypergeometric test with FDR ≤ 0.05. In addition, detection and interaction analysis of miRNA-mRNA pairs were performed based on the target prediction, function annotation and negative regulation mechanism of mRNA and miRNA. The miRNA-mRNA interaction networks were displayed using visualizing maps.

2.12 Quantitative PCR for miRNA and mRNA expression

To validate the sequencing data, 9 miRNAs and 6 mRNAs showing sustained significant increases or declines in expression over the fthis stages and 13 miRNA-mRNA interaction pairs identified from the pairwise comparison of S1 and S3 (S1 and S3 showing significant differentiation in the number and form of IBs; Fig. 1) were selected, and specific primers were used to quantify the miRNA and mRNA for each stage of development. After acquiring high quality total RNA, miRNAs and mRNAs were reverse transcribed using PrimeScript RT reagent Kit with gDNA Eraser (TaKaRa, Japan, RR047A). Quantitative

real-time PCR analyses on the miRNAs and the mRNAs were performed using the SYBR Green PCR Master Mix (TaKaRa, Japan, RR820A) on a Roche LightCycler 480 System II (Roche, Mannheim, Germany) according to the manufacturer's instructions. M. amblycephala 18s RNA and β -actin were used as internal controls for miRNA and mRNA RT qPCR, respectively. All of the real-time reactions were performed in triplicate and the relative expression levels were measured in terms of threshold cycle value (Ct) and were normalized using the equation $2^{-\Delta\Delta Ct}$, in which $\Delta Ct = Ct_{miRNA/mRNA} - Ct_{18s/\beta\text{-actin}}$. Based on the annotation information of mRNA transcriptome data, it is selected a number of bone-related genes to analyze their expression in different tissues (Supplementary Table S2), with the aim to find IB specific genes.

2.13 Vector Construction and Dual Luciferase reporter assays

The 3′ UTR of tgfbr1a and runx2a containing a miR-133b-3p binding site and the 3′ UTR of tgfbr1a and runx2b containing a miR-206-3p binding site were amplified from genomic DNA by PCR with the primers shown in Supplementary Tables S1-4. PCR products were cloned into pmirGLO using the MSS I and Xho I restriction sites. Dual luciferase reporter experiments were performed in HeLa cell lines (Cell Collection Center for Freshwater Organisms, Huazhong Agricultural University). When the cells reached 60% to 70% confluence in 24-well plates, pmirGLO-3′ UTR (200 ng) was co-transfected with 100 nM negative control or a microRNA mimics (GenePharma, Shanghai, China) using 2 μ L Fugene6 (Promega) according to the manufacturer's instructions. The relative luciferase activity was measured 24 h after transfection by the Dual-Luciferase Reporter Assay System (Promega).

2.14. Phylogenetic Analysis and Genomic Structure Analysis

Synteny maps of the chromosomic regions surrounding human *Bmpr2*, mouse *Bmpr2* and zebrafish *bmpr2a*, *bmpr2b* genes were constructed using human genes as

reference by combining PhyloView and AlignView from Genomicus 81.01 (http://www.genomicus.biologie.ens.fr/genomicus-93.01/cgi-bin/search.pl) (Louis et al., 2015) with Ensembl Comparative Genomics data (http://www.ensembl.org/index.html), which revealed the protein similarity between species. Gene structure and exon sequence homology were also demonstrated based on Ensembl database.

2.15 Fish Strain, Design of bmpr2a and bmpr2b gRNAs for CRISPR/Cas9, Generation and Genotyping of Mutants

The transgenic zebrafish parent labeled with green fluorescent protein for osteoblast-specific transcription factor (Osterix GFP) used in this experiment was provided by Professor Xiao Chongde from Chung Yuan Christian University, Taiwan, China. Fish were kept at 26-28°C under a controlled light cycle (14h light, 10h dark) to induce spawning. The offspring were used for subsequent experiments. Zebrafish *bmpr2a* and *bmpr2b* gRNAs were designed (Table 1) and prepared in according to the study of Miguel et al. (Moreno-Mateos et al., 2015). Purified gRNAs (80 ng/μl) were co-injected with Cas9 mRNA (400 ng/μl) into zebrafish embryos at the one-cell stage. The corresponding primers (Table 1) were used to screen out founders with site mutations by fast DNA extraction method and the adult founders were outcrossed with wild-type fish to obtain F1 fish, which were subsequently genotyped and outcrossed with wild-type fish to obtain F2 fish. Then, heterozygous F2 individuals were self-crossed to obtain homozygous F3 fish.

Table 1. gRNA primer and gene mutation detection primer

Primer ID	Sequence	Production size	Tm
Scaffold	GATCCGCACCGACTCGGTGCCACTTTTT CAAGTTGATAACGGACTAGCCTTATTTTA ACTTGCTATTTCTAGCTCTAAAAC		
bmpr2a sgRNA	AATTAATACGACTCACTATAGGTGGTTCT TCTGGGTCCTGGTTTTAGAGCTAGAAAT AGC		
bmpr2b sgRNA	AATTAATACGACTCACTATAGGGGCAGC AGGATGAGAGTGGTTTTAGAGCTAGAAA TAGC		
bmpr2a mutant check	F: TCTTGACGTTGGACTGATTGCC R: TGTGGACAGCAATTCTACTGTAATTCTA	130bp	62°C
bmpr2a mutant seq	F: TGCCTGGTTGGACTCTGAAA R: CTGACTCTCACACCTCGCTTT	467 bp	62°C
bmpr2b mutant check	F: CATGAGCTTGAACTTCGGTCG R: ATGTCCGGTTTAGGATCCGC	131 bp	60°C
bmpr2b mutant seq	F: CCGTGCACATGAGCTTGAAC R: CGCTGAGGGATACCAACGAA	307 bp	60°C

2.16 Phenotypic and Developmental Observation of Mutant Fish

Zebrafish were anesthetized by buffered tricaine methanesulfonate (MS222, Sigma-Aldrich, USA), and X-ray analysis was performed using Bruker In-Vivo DXS Pro (USA).

Histology analysis: After fixing the wild and mutant fish in 4% paraformaldehyde for 24 h, the tissues were dehydrated through a series of graded ethanol solutions (70-100%) and cleared in xylene at room temperature. The tissues were then impregnated in paraffin at 60°C. Transverse sections (5 μm thick) were prepared following the normal procedures. Hematoxylin-Eosin (H-E) staining was subsequently used to observe the histological structures of skeleton (Nie et al., 2017).

Mineralized bone was stained with Alizarin Red using a modified protocol from lab of P. Eckhard Witten in Ghent University (Belgium) for larvae and adult fish (details in Supplementary File 2). The stained specimens were analyzed and photographed under an Olympus SZX2 Stereo Microscopes (Japan).

Osterix GFP-labeled embryos and larval fish at different developmental stages were observed and photographed under a Leica M205 FA Fluorescent Stereo Microscope (Leica Microsystems GmbH, Wetzlar, Germany).

2.17 Comparative Transcriptome Analysis

Total RNA was isolated from the 15 dpf (days post-fertilization) wild and mutant larval fishes with three biological replicates using RNAiso Plus Reagent (TaKaRa, China) according to the manufacturer's protocol. After RNA quality and quantity control, 6 transcriptome equencing libraries were generated using NEBNext® Ultra™ RNA Library Prep Kit for Illumina® (NEB, USA) following manufacturer's recommendations and index codes were added to attribute sequences to each sample. After cluster generation, the library preparations were sequenced on an Illumina Hiseq platform After quality control of raw data, paired-end clean reads were aligned to the zebrafish reference genome (ftp://ftp.ensembl.org/pub/release-92/fasta/danio_rerio/) using Hisat2 v2.0.4 (Kim et al., 2015). HTSeq v0.9.1 was subsequently used to count the reads numbers mapped to each gene and then FPKM of each gene was calculated (Trapnell et al., 2010). Differential expression analysis of two conditions/groups (two biological replicates per condition) was performed using the DESeq R package (1.18.0) (Wang et al., 2010). Genes with an adjusted P-value <0.05, which adjusted using the Benjamini and Hochberg's approach for controlling the false discovery rate, were defined as differentially expressed genes (DEGs). GO and KEGG enrichment analysis of differentially expressed genes were then performed. Using GOseq R package (Young et al., 2010), GO terms with corrected P-value <0.05 were considered significantly enriched by differential expressed genes. KOBAS software (Mao et al., 2005) was used to test the statistical

enrichment of differential expression genes in KEGG pathways (http://www.genome.jp/kegg/).

2.18 Quantitative real-time PCR for BMP-Smad Pathway Genes and Skeletal Development-Related Genes

cDNA of *bmpr2b* mutants and wild fish (15dpf) were used for quantitative real-time PCR (qRT-PCR), which was performed according to SYBR Green Premix Ex Taq (TaKaRa) using a QuantStudio 6 Flex real-time PCR System (Applied Biosystems, ABI, USA) according to the manufacturer's instructions. The relative expression levels of the target genes were normalized to the housekeeping gene *β-actin*, and further calculated using the double-standard curve method. Detailed information of primers used in the study was showed in Table 2.

Table 2. Primers for quantitative gene expression

Gene	Sequence	Production size (bp)	Tm (℃)
bmpr1aa:	F: AGTGCTTAAGGGCCATGCTA R: TCCACTGATCCAAGTCCACA	298	60
bmpr1ab	F: GATGCCACAAACAACACCTG R: GCAACCAAAGTGAAGCAACA	299	60
bmpr1ba	F: GCTCATGACAGAGTGTTG R: CTGCGTCAACTTCTCCTGC	286	60
bmpr1bb	F: GAGGCAGATGGGTAAACTG R: CTCCTGTGTTCTGTTGAG	327	60
smad1	F: ATGGAGCTGACCATAAAGCAAC R: CACTGTTCTAGTCTCTAAGCTAG	282	60
smad5	F: CTTTGAGGCCGTCTATGAGC R: GGGTGCTTGTCACATCTTGT	102	60
smad8/9	F: TGGTGTTCGGTGGCGTAT R: ATGGTGGAGTTGCGGTTG	158	60
smad4	F: GGGCGAGACCTTCAAAGTGC R: TCAGACAGCGAACCCACACG	203	60
acvr2aa	F: GGCATTCGGAGTGTTCCTCA R: GCCTCTTGTCCTTGTCTCCC	155	60

Gene	Sequence	Production size (bp)	Tm (℃)
acvr2ab	F: CTGCTACGACAGCAGTGAGT R: GGCTCAACCGTCTCTGGATT	117	60
acvr2ba	F: CTGGCTCGACGACTTCAACT R: CGGCAGGTGTGTGAATCTCT	121	60
acvr2bb	F: TTACGCGTCATGGCTGAACT R: CAGAAGAACACCTGCGGACT	129	60
Osteocalcin (*ocn*)	F: ACTGCACCTGGAGACCTGAC R: TTTATAGGCGGCGATGATTC	114	60
entpd5	F: ATATGCCTGAAAAGGGTGGA R: TACTTCTTTGACCTCATTCAGCAG	170	60
spp1	F: TGTGAAGCGCTCAGCAAG R: CATCTGCCTCCTCAGTGTCA	176	60
runx2a	F: GACGGTGGTGACGGTAATGG R: TGCGGTGGGTTCGTGAATA	174	60
runx2b	F: CGGCTCCTACCAGTTCTCCA R: CCATCTCCCTCCACTCCTCC	150	60

2.19. Protein Expression Analysis by Western Blot

The protein expression of the genes that had antibodies available in the lab were analyzed using western blot, which was conducted by separating protein fragments using gel electrophoresis followed by transfer to a polyvinylidene difluoride membrane. The membrane was probed with primary BMPR1A (Rabbit, Abcam), BMPR1B (Rabbit, Abcam), SMAD4 (Rabbit, CST), RUNX2 (Mouse, Abcam), OCN (Mouse, Abcam) antibody against GADPH (Abcam) and stained with horseradish peroxidase (HRP)-conjugated secondary antibodies (HRP-Goat anti Rabbit, ASPEN; HRP-Goat anti Mouse, ASPEN). Finally, band intensities were quantified using UN-SCAN-IT gel analysis software (version 6). The levels of protein expression were normalized to GADPH expression.

3 RESULTS

3.1. Tissue section and staining observation results

In order to observe the microstructural characteristics of IB, CT and muscle of *M. amblyphala*, three types of tissues were sampled from the 6-month-old *M. amblyphala*. Tissue sections and HE staining was then performed. Microscopic observations showed that the IBs were wrapped by CT, and the morphological characteristics of connective tissue were significantly different from that of muscle (Figure 3-A). The staining results showed that the stained nuclei were concentrated in CT. In addition, Fig. 3-B shows the morphological characteristics of the CT that differentiated into the IBs. The acquisition of these microscopic observations provides important basic information for studying the origin of the differentiation of IBs, and also provides a reference for the analysis of the transcriptome of different tissues in this study.

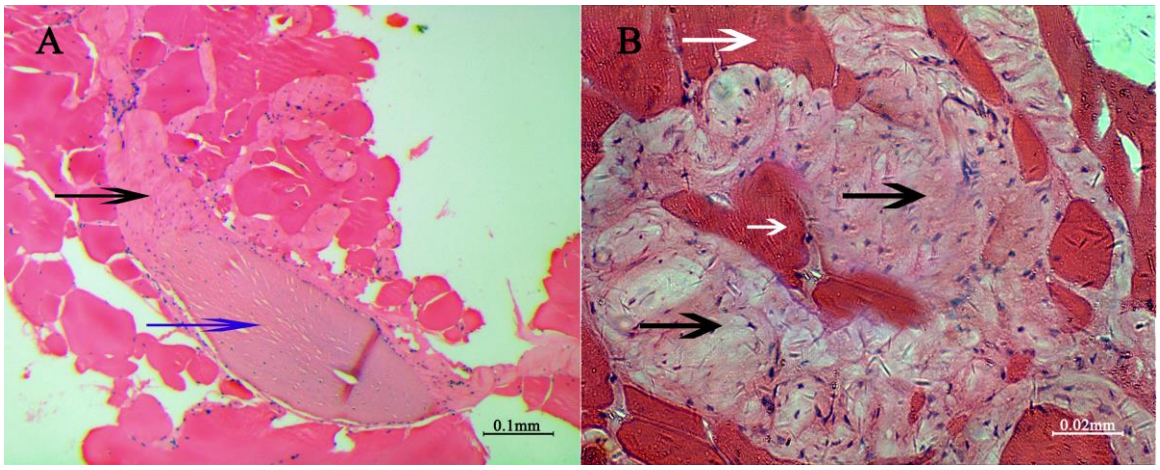

Figure 3. The microstructure of sampled tissues in *M. amblycephala*. (A) Intermuscular bone and encircled connective tissue (connective tissue was indicated by black arrow; the intermuscular bone was indicated by blue arrow); (B) Muscle and connective tissue (white arrow indicated the muscle; black arrow indicated the connective tissue).

3.2 General Features of Small RNAs

In order to identify the miRNAs for IBs of M. amblycephala, the two tissues (IBs and CT, which encircle the IBs) were collected from six-month-old individuals, when the intermuscular bone is actively growing. Two independent RNA libraries were constructed for the IBs and CT and then sequenced using the Illumina HiSeq 2000 platform. A total of 9,544,686 and 9,375,253 raw reads were generated from the IB and CT libraries, respectively. After discarding low-quality reads, 3' and 5' adaptors, sequences with <18 and >30 nt, 9,424,634 (99.07%) and 9,211,591 (98.52%) clean small RNA reads were obtained in the IB and CT libraries, respectively (Table S1-1). Little difference was found in the length distribution of the sequences from the two libraries. Most (>93%) of the small RNAs were 21–23 nt in length, especially 22 nt, which is the typical length of Dicer-derived products, accounting for 64.29% and 72.01% of the total sequence reads in the IB and CT libraries, respectively. These results are similar to the length distribution characteristics of small RNAs in other fish species, such as *C. carpio* (Zhu et al., 2012), *I. punctatus* (Xu et al., 2013) and Japanese flounder (*Paralichthys olivaceus*) (Fu et al., 2011).

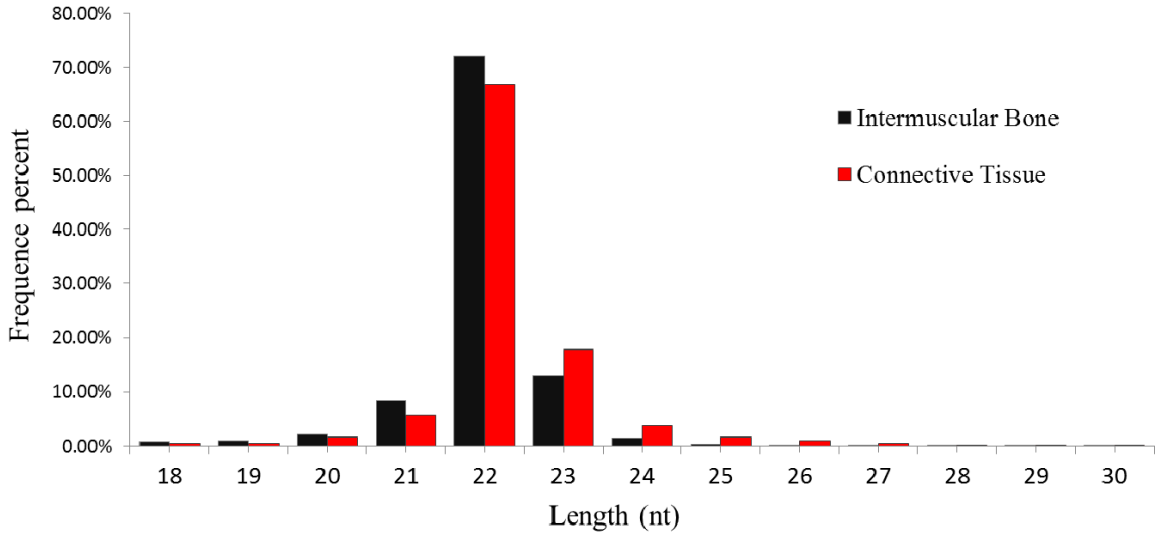

Figure 4. Length distribution of small RNAs in intermuscular bone and connection tissue of *M. amblycephala*

The total number of unique reads from sRNA libraries of IB and CT groups was 168,227 and 249,063, respectively. These unique sequences of two libraries contained 34,314

common sequences. After comparing the small RNA sequences with the NCBI GenBank and Rfam database, rRNA, tRNA, snRNA, snoRNA, scRNA, repeat DNA, exon antisense, exon sense, intron antisense and intron sense sequences were annotated and removed (Figure 4). The remaining reads, including 9,152,701 and 8,884,176 for the IB and CT groups, respectively, consisting of 131,549 and 215,002 unique sequences, respectively, were retained for miRNA analysis.

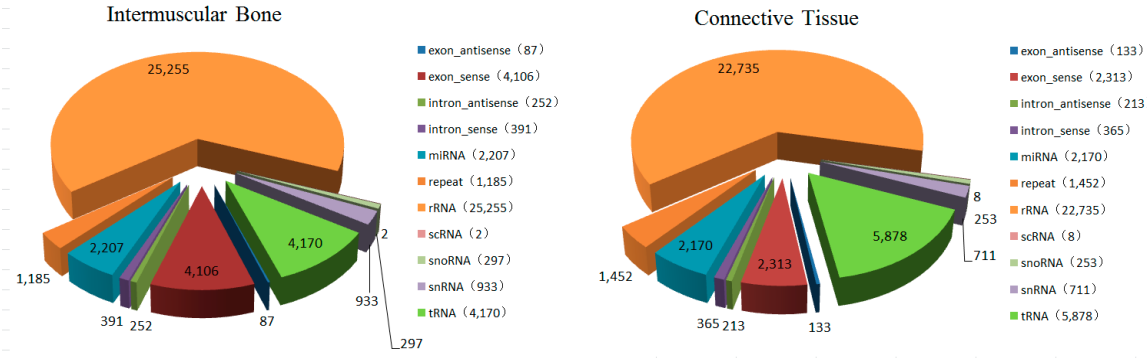

Figure 5 Annotation of small RNAs derived from the Intermuscular bones (IBs) and connective tissue (CT) of *M. amblycephala*.

Due to the lack of genome information for *M. amblycephala*, the selected small RNA sequences were mapped to the genome sequence of zebrafish (*Danio rerio*), which is evolutionarily close to *M. amblycephala*. For the selection of the computing algorithm, it is chosen a tolerance of one mismatch for mapping. Subsequently, for the IB and CT groups, 8,389,883 reads (89.02%) representing 69,307 (41.2%) unique small RNAs and 7,534,341 reads (81.79%) representing 48,844 (19.61%) unique small RNAs, respectively, were mapped to the reference genome (Figure 5).

3.3 Identification of Conserved miRNAs

To identify conserved miRNAs, the sequences of the miRNAs in the libraries of the IB and CT groups were compared with those of the 1250 precursor miRNAs and 831 mature miRNAs from miRBase Version 20.0. This analysis identified 201 and 205 conserved miRNAs in the IBs and CT libraries, respectively. The reads of these miRNAs were

ranged from 1 to 2,796,874, indicating that not only highly-expressed miRNAs, but also weakly-expressed miRNAs were identified by Illumina small RNA deep sequencing. After grouping identical sequences, a total of 218 unique mature miRNAs were identified, which belong to 97 families, including 188 miRNAs that overlapped between the two libraries, 13 and 17 miRNAs that were detected only in the IB and CT libraries, respectively.

For the identified and validated miRNAs from two groups, the ten most abundant miRNAs in the IBs were miR-1, let-7a, miR-206, let-7b, let-7c, miR-199-3p, miR-21, let-7f, let-7d and miR-199a-3p, accounting for 94.86% of the total reads mapped to miRBase. Eight of these miRNAs were also among the ten most abundant miRNAs (miR-1, miR-206, let-7a, let-7b, let-7c, miR-199-3p, miR-21, miR-22a, let-7f, let-7g) identified in the CT library, which accounted for 94.28% of the total reads mapped to miRBase. For these miRNAs that have already been identified and validated, miR-1 has the highest expression in both libraries. This phenomenon was in agreement with other studies of miRNAs (Nielsen et al., 2010; Novello et al., 2013), showing that miR-1 was the crucially expressed miRNAs in skeletal muscle development, human osteosarcoma origin, proliferation and cell cycle control. miR-206, previously viewed as a muscle-specific miRNA (Kim et al., 2006; Sweetman et al., 2008), was demonstrated as a key regulator for the process of osteoblast differentiation. The expression of miR-206 decreased over the cthisse of osteoblast differentiation, and overexpression of miR-206 in osteoblasts inhibited their differentiation; conversely, knockdown of miR-206 expression promoted osteoblast differentiation (Inose et al., 2009). Therefore, it is speculated that the high expression of miR-206 in IB and CT libraries could be related to the development and differentiation of IBs. Previous studies have shown that the target genes of identified miRNAs could be involved in the basic biological reactions and organ system development. For instance, miR-21 contributes to myocardial disease by stimulating MAP kinase signaling in fibroblasts (Thum et al., 2008), and it was known that downregulation of miR-21 biogenesis by estrogen action results in osteoclastic apoptosis (Sugatani and Hruska, 2013). A previous study also found that miR-22 regulated the adipogenic and osteogenic differentiation of human adipose tissue-derived mesenchymal stem cells in opposite directions, which indicated that miR-22 was decreased during the process of adipogenic

differentiation, but increased during osteogenic differentiation (Huang et al., 2012). Similarly, miR-199a-3p had been also reported to play a functional role in osteosarcoma cell growth and proliferation (Duan et al, 2011). Transfection of precursor miR-199a-3p into osteosarcoma cell lines significantly decreased cell growth and migration. Restoring miR-199a-3p's function may provide therapeutic benefits in osteosarcoma. These findings may be able to assist us better in explaining the development mechanism of IBs. In addition, seven miRNAs of the let-7 family, including let-7a, let-7b, let-7c, let-7d, let-7e, let-7f and let-7g, were present at high frequencies in both libraries. This result was similar to many previous studies about miRNAs in fish species (Fu et al., 2011; Mondol and Pasquinelli, 2012; Wang et al., 2012; Johnson et al., 2007), which demonstrated that the let-7 miRNAs are important regulators for extensive biological processes. Interestingly, the expression of let-7d had a significant difference in IBs and CT. Huleihel and Ben-Yehudah (Huleihel and Ben-Yehudah, 2014) had examined the effects of transfection on fibroblast responsiveness to transforming growth factor-β (TGF-β) and found that let-7d transfection significantly attenuated high-mobility protein induction by TGF-β. Notably, TGF-β was an important factor in osteoblast differentiation and bone formation [38]. Therefore, it is conjectured that let-7d may play a key role in the differentiation process between IBs and CT through regulating protein synthesis of osteoblast differentiation and bone formation.

Additionally, the analysis of base bias on the first position of identified miRNAs with a certain length and on each position of all identified miRNA was performed, respectively. Results showed that the identified sequences being 18–25 nt in length from two libraries have a strong bias for U in the first nucleotide (Figures S2 and S3). Furthermore, a total of 25 duplex-like miRNA:miRNA* pairs were detected from 4377 unique sequences. It had been reported that miRNA/miRNA* ratios may vary dramatically at different stages of development, as some miRNA* sequences could be reported as mature functional miRNAs with abundant expression. In this study, is also found that some miRNA*s were detected at obviously high levels in two libraries, like miR-199-3p, miR-199a-3p, miR-140-3p and mam-miR-133a-3p. Previous studies (Andreassen, 2013; Ramachandra

et al., 2008) have described the same phenomenon and indicated that the miRNA*s may play a functional role in regulating gene expression.

3.4 Statistics of Multiple IsomiRs in *M. amblycephala*

Recently, deep sequencing revealed that the same miRNA precursor can generate multiple isoforms of miRNA (isomiRs), which vary in length and/or sequence, due to exonuclease-mediated trimming, a shift of cleavage sites of Drosha and Dicer, miRNA editing or 3'-end nontemplated nucleotide addition. In the present study, the phenomenon of multiple isomiRs was again observed. Some isomiRs, detected with single nucleotide substitutions, including transition and transversion, possibly represent the result of pre-miRNA editing. These end-sequence variations are interesting, as they may allow miRNA variants to perform distinct roles through influencing the formation of the miRNA/target mRNA hybrid duplex. Of the twelve types of single nucleotide substitutions observed in the two libraries, the most prominent were T to A (12.50%), T to C (11.76%), A to G (10.51%) and G to A (10.21%) (Figure 3), which was similar to several previous studies (Li et al., 2011). Meanwhile, prior reports had demonstrated that sequence variations may be the result of post-transcriptional modifications of RNA (Ebhardt et al, 2009). Therefore, it is presumed that the nucleotide substitutions in this study may be attributed to post-transcriptional modifications of RNA.

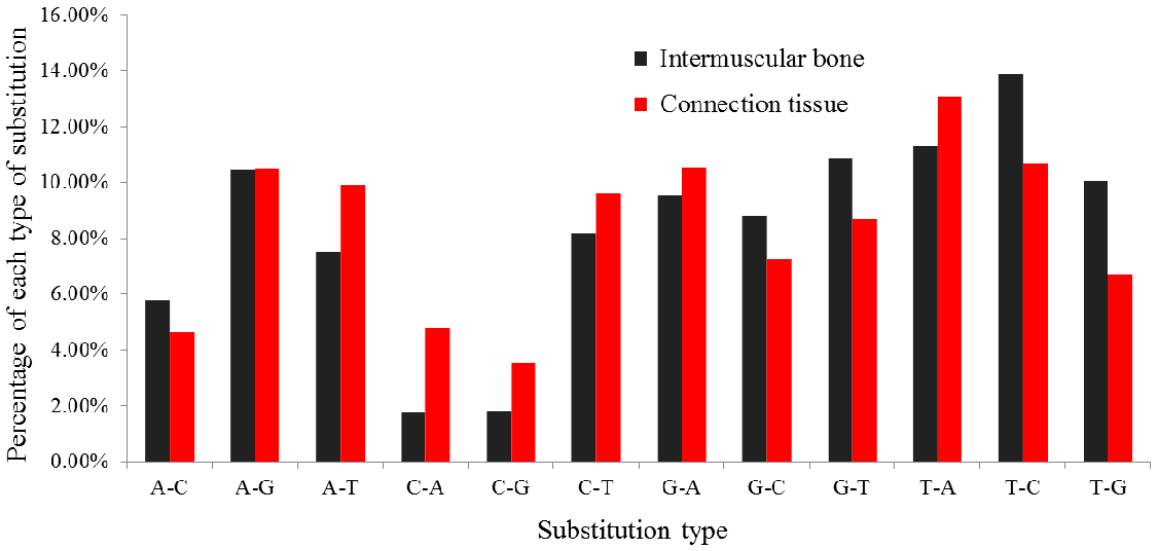

Figure 6. Histogram displaying the single nucleotide substitutions in the miRNAs seed region sequence when aligning un-annotated sRNAs tags with mature miRNAs from miRBase20.0. The x-axis represents the substitution type from genome to RNA (small RNA sequence). The y-axis represents the percentage comparing of the observed count of each type to the total count of all substitution types.

Furthermore, another type of isomiR was observed with additional 5' or 3' non-template nucleotides, which may have longer, shorter or consensus lengths considering the canonical miRNA sequences (Ebhardt et al, 2009; Kuchenbauer et al, 2008). The most abundant nontemplated nucleotide added at the 3' terminal ends of mature miRNA were uridine. A typical example was mam-let-7d-3p, in which the length varied from 19–25 nucleotides, similar to other miRNAs identified in this study (Figure 6). A similar phenomenon has previously been widely reported in many species included fish, maize and mouse, showing that essentially, all miRNAs have length and/or end-sequence variation. Different from the nucleotide substitutions, these length variations were thought to be the result of inexact Drosha and Dicer processing. Additional 3' non-template nucleotides in isomiRs may play a key role in miRNA: target interactions. IsomiRs with 3' additions increased miRNA stability in Drosophila and weakened the effectiveness of some specific miRNAs, and isomiRs could also accumulate to a considerable level and

downregulate their target genes in organisms (Fernandez-Valverde et al, 2010; Burroughs et al., 2010; Yang et al, 2011; Laqtom et al, 2014).

Summarily, more future studies are required to functionally validate the conclusion and the significance of isomiRs.

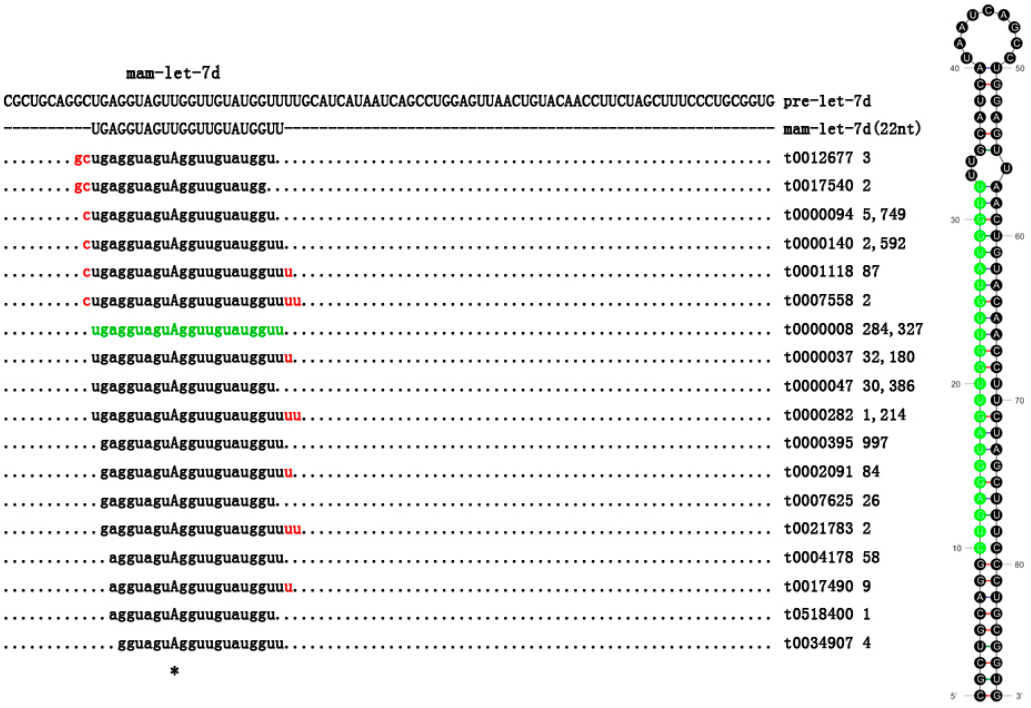

Figure 7. A portion of the miRNA precursor and details of mam-let-7d isomiRs, including sequence count. The most abundant mature miRNAs are indicated by the sequence in green. The non-templated nucleotide additions were indicated in the red. * indicated the single nucleotide mutation loci.

3.5 Differentially Expressed miRNAs

Among these conserved 218 miRNAs identified by RNA-Seq, 44 conserved miRNAs in M. amblycephala were differentially expressed ($p < 0.01$) by comparing with miRNA expression patterns between two libraries (Table S3). Of the 44 differentially-expressed miRNAs, 24 miRNAs and 20 miRNAs had higher expression in the CT and IB groups, respectively, as shown by differential expression analysis, which suggested that miRNAs play an important role in regulating diverse biological processes during the development

of IBs. The expression of miRNA in two samples was shown by plotting a log2-ratio figure and scatter plot (Figure 7). These differentially-expressed Int. J. Mol. Sci. 2015, 16 10693 miRNAs were sequenced at varying frequencies. For instance, mam-miR-199-3p, mam-miR-199a-3p, mam-miR-128 and mam-let-7d were detected with relatively high sequence counts in both libraries. In contrast, the sequencing frequencies of some miRNAs (mam-miR-363, mam-miR-30b and mam-miR-551) were low in both of the libraries.

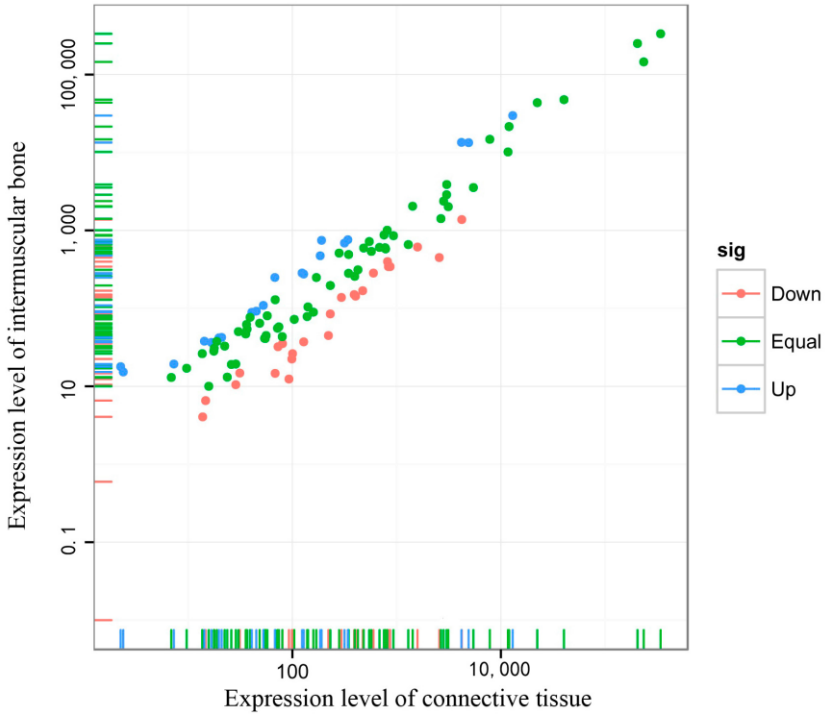

Figure 8. Scatter plot map for miRNA expression levels in the IBs and CT of M. amblycephala. Each plot represents an individual miRNA. This reflects the proportion of miRNAs that have a greater number in IBs and CT, respectively.

Quantifying the differentially expressed miRNAs in the different tissues is an important initial step to investigate the fundamental functions of these miRNAs. It is used stem-loop RT-PCR to validate and profile the expression of the 11 differentially-expressed miRNAs in nine tissues of M. amblycephala, including muscle, brain, liver, spleen, kidney, gonad, rib, IBs and CT (Figure 8). The results indicated that the mam-miR-221, mam-miR-222a, mam-miR-92a and mam-miR-26a were expressed at relatively high levels in IBs and CT, and this result suggests that these miRNAs may play roles in the connective tissue

differentiation and IB formation of *M. amblycephala*. Simultaneously, it is found the expression of mam-miR-125a and -26a was almost significantly high in all tissues. Ubiquitous expression of these miRNAs indicates that they were involved in many fundamental functions. For example, mam-miR-125a not only affected genes involved in the mitogen-activated protein kinases (MAPKs) signaling pathway (Harrera et al., 2009), but also may act as an NF-κB inhibitor upon TLR stimulation and inhibits erythroid differentiation in leukemia and myelodysplastic syndromes (MDS) cell lines (Gañán-Gómez et al., 2014).

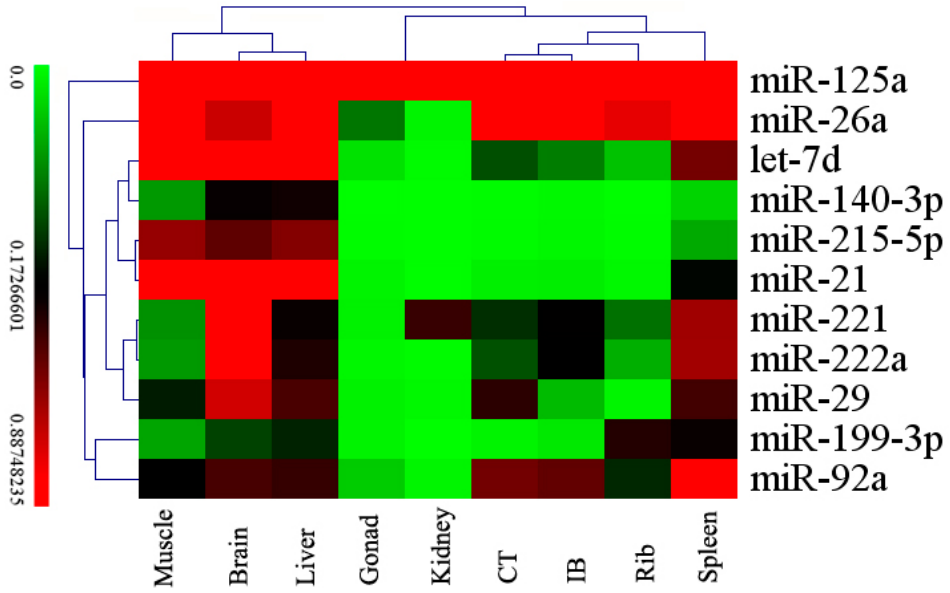

Figure 9. Heat map showing the 11 differentially-expressed miRNAs expression patterns in nine tissues measured by stem-loop RT-PCR. Relative expression levels of the 11 differentially-expressed miRNAs were measured in terms of threshold cycle value (Ct) and were normalized to 5S rRNA. The expression data were analyzed by hierarchical clustering for both tissues and miRNAs.

3.6 Prediction of Potential Targets of Differentially-Expressed miRNA

The identification of miRNA targets is a crucial step to further understand the regulatory functions of miRNAs. Strong base pairing between the seed region of a miRNA and the UTR of its target mRNA is important for its degree of regulation. Hence, many target

prediction algorithms enforce strong seed complementarity and evolutionary conservation in the complementary region of potential targets. As such, to improve the accuracy of target gene prediction results and to limit the validation requirements, targets were identified by both MiRanda (Enright et al., 2003) and TargetScan (Lewis et al. 2003) and were present in the results of comparative transcriptome sequencing analysis. A total of 2,084,911 unique targets, including 49,962 EST sequences of *M. amblycephala*, were predicted for the 44 highly significant differently-expressed miRNAs ($p < 0.01$), which were identified in this study.

3.7 Function Analysis of Target Genes of Differentially-Expressed miRNAs

The identified target genes of differentially-expressed miRNAs were subjected to a GO analysis, which classifies miRNA-gene regulatory networks on the basis of molecular function, cellular component and biological process. The GO analysis of identified predicted target genes revealed 21,082, 20,087 and 20,627 genes, respectively, classified into 877 molecular function ontology terms, 388 cellular component ontology terms and 3633 biological process ontology terms (Table S5). It was noteworthy that the GO terms of miRNAs between IBs and CT were highly present in: cell 83.60%, intracellular 74.10% and organelle 61.00% of the cellular component; cellular processes 75.70%, single-organism processes 57.40%, metabolic processes 55.90% of biological processes; and binding 76.40%, catalytic activity 44.70% and organic cyclic compound binding 31.80% of molecular functions.

The pathways of predicted target genes, which were actively regulated by miRNA in M. amblycephala, were also identified and classified according to KEGG functional annotations. Notably, the most overrepresented miRNA targets belonged to the metabolic pathways, which perform a variety of anabolic and catabolic tasks, such as lipid, carbohydrate, amino acid and energy metabolism. A similar phenomenon has previously been widely reported in many studies (Schuster et al., 2000; Choi et al., 2012), showing

that the pathways serve energy conversion, macromolecular compounds synthesis, and so on. The Wnt signaling pathway (2.14%) had previously emerged as a key regulator of developmental processes, including skeletal patterning. Mouse genetics confirmed the importance of canonical Wnt signaling in the regulation of bone homeostasis. Activation and inhibition of the pathway, respectively, lead to increased and decreased bone mass and strength (Glass et al., 2005). The importance of Wnt signaling for bone has also been highlighted since then in the general population in numerous genome-wide association studies (Baron et al., 2013). TGF-β regulates a large variety of cellular activities, which acts as a potent inhibitor of the terminal differentiation of epiphyseal growth plate chondrocytes during the formation of endochondral bone (Li et al., 2005). In this study, 424 (1.46%) target genes of the differential miRNAs were mapped to the TGF-β signaling pathway. Another pathway targeted by the differential miRNAs was the MAPK signaling pathway (3.17%), which is not only known to be involved in the regulation of muscle differentiation by affecting the activities of myogenic transcription factors, as well as controlling the expression of structural muscle genes (Keren et al., 2006), but also essential for skeletogenesis and bone homeostasis. In mice, the p38 MAPK pathway is necessary for normal skeletogenesis, and deletion of any of the MAPK pathway member-encoding genes, MAPK kinase 3 (Mkk3), Mkk6, p38a or p38b, profoundly reduced bone mass secondary to defective osteoblast differentiation (Greenblatt et al., 2010). In fish, the activation of MAPK is absolutely indispensable for muscle cell proliferation (Fuentes et al., 2011). Meanwhile, 419 (1.45%) target genes of the differential miRNAs were directly mapped to the osteoclast differentiation pathway. In addition, the pathway data also highlighted associated with human T-lymphotropic virus type 1(HTLV-I) infection, dilated cardiomyopathy, Epstein-Barr virus infection, herpes simplex infection and other diseases, suggesting that genes involved in cellular immune, cell cycle progression and cell proliferation are targeted by the differential miRNAs. Furthermore, pathways associated with the regulation of actin cytoskeleton, focal adhesion, biosynthesis of secondary metabolites, endocytosis, phagosome, tight junction, vascular smooth muscle contraction and protein processing in endoplasmic reticulum were all significantly enriched, indicating the role of the differentially-expressed miRNAs

in the regulation of cell motility, cytoskeleton, cell nutrition, communication between cells and the extracellular matrix.

On the whole, the results indicated that these differentially-expressed miRNAs were abundant and functionally involved in regulating the development and differentiation of IBs and CT, as well as providing an opportunity for further functional validation of miRNA in the regulation of IB development.

3.8 Assembly and annotation of reference transcriptome

To obtain a reference transcriptome for the IBs' development in *M. amblycephala*, a RNA-Seq library was constructed using RNA from samples of fthis development stages. A total of 92,991,884 raw reads were generated through high-throughput sequencing. After quality control, approximately 7,882,445,160 nt of high-quality data with a Q20 percentage of 98.11% and GC percentage of 48.70% was available for analysis (Table 3). With the Trinity de novo assembler, a total of 127,712 contigs were generated, with an average length of 301 bp and an N50 of 437 bp. A total of 52,918 unigenes were further generated with an average length of 635 bp and an N50 of 865 bp (Table 3). The size distribution of these contigs and unigenes of total of 46,569 unigenes were successfully annotated through alignment to reference databases. In total, 33,354 (63.03%), 45,648 (86.26%), 29,753 (56.22%), 24,094 (45.53%) and 9,072 (17.14%) unigenes could be annotated by NR, NT, Swiss-Prot, KEGG and COG database, respectively, with 6,349 (12.00%) unigenes showed no homology to known sequences deposited in these databases (Table 3).

Table 3. Assembly and annotation results of transcriptome sequencing

Category	Number	Database	Number of unigenes
Total Raw Reads	92,991,884	NR	33,354
Total Clean Reads	87,582,724	NT	45,648
Q20 percentage	98.11%	Swiss-Prot	29,753
GC percentage	48.70%	KEGG	24,094
Total number of contigs	127,712	COG	9,072
Total length (nt) of contigs	38,443,923	GO	22,222
Mean Length (nt) of contigs	301	Total Number of annotated unigenes	46,569
N50 of contigs	437		
Total number of unigenes	52,918		
Total length (nt) of unigenes	33,582,035	None annotated unigenes	6,349
Mean length (nt) of unigenes	635		
N50 of unigenes	865		

Based on the NCBI nr database, E-value distribution and homology percent of the unigenes was performed and mostly of them showed strong homology to available database sequences. Meanwhile, 30,258 (90.72%) unigenes were annotated to 5 top-hit species (*Brachydanio rerio, Oreochromis niloticus, Oryzias latipe, Fugu rubripes, Tetraodon nigroviridis*), especially D. rerio (81.41%). A total of 22,222 M. amblycephala unigenes were classified into 3 gene ontology (GO) categories (cellular component, biological process and molecular function and 24,094 unigenes were mapped into 258 KEGG pathways. Metabolic, regulation of actin cytoskeleton, cancer and focal adhesion pathways dominated the KEGG functional analyses. In addition, some pathways related to osteocyte differentiation, such as the MAPK (mitogen-activated protein kinase), Wnt signaling pathway, osteoclast differentiation and TGF-β (transforming growth factor beta) signaling pathways, were highly represented in the results of the KEGG functional analyses.

Based on the annotation, hundreds of bone-related genes, such as FGFRs, SOXs, Runx2, TGFβ s, BMPs, SMAD, Osteocalein, MMP, cathepsin K, Col1a1/2, Col2a1, ColXa1, IGFs and so on, were identified in the IB transcriptome. These genes have a well-recognized function in formation and differentiation of cartilage and bone26. For example, the combination of SOX5, SOX6, and SOX9 suggests that the signals necessary for induction

of permanent cartilage are present in the transcriptome27. BMP signaling is known to be involved in fish in fin growth, scleroblast differentiation28, tissue calcification29, and in mammals BMP and Ihh/PTHrP signaling interact to coordinate chondrocyte proliferation and differentiation30. At least 30 collagens isoforms have been identified in bone and are important in skeletal development31. TGFβ has a role in osteoblast differentiation and bone formation32. The identification in the transcriptome of abundant bone-related genes supports that this present transcriptome is closely related to the bone, which justifies the enrichment of the transcriptome for IBs. (Zhu et al., 2012)

3.9 Expression profiling of IBs development-dependent genes

In order to identify the functional genes in response to development of IBs, 8 DGE (digital gene expression profiling) libraries have been generated from 4 developmental stages with two biological replicates. The mapping results for the 8 libraries (4 developmental stages) are shown in the Table 2. The distribution of unique reads in the 8 DGE libraries was compared as an assay of gene coverage. Similar coverage was obtained for all 8 libraries. More than 34% of the unigene sequences in every library have a gene coverage of more than 70%, which is determined as the ratio of the base number in a gene covered by unique mapping reads to the total bases number of that gene. Sequencing saturation analysis showed the number of unique tags reached a plateau shortly after the number of clean reads reached 20 million. Therefore, the 8 libraries fully represent the transcripts expressed in each developmental stage. Principal component analysis (PCA) showed that the biological replicates had very similar expression levels, suggesting good reproducibility of the method.

Table 4. Alignment results of 8 libraries mapping to the reference transcriptome

Sample ID	Total reads	Total basepairs	Total mapped reads	Unique match	Multi-position match	Total unmapped reads
StageI-1	14,010,101 (100.00%)	1,893,716,998 (100.00%)	13,518,462 (96.49%)	8,802,813 (62.83%)	4,715,649 (33.66%)	491,639 (3.51%)
StageI-2	15,412,123 (100.00%)	2,149,413,540 (100.00%)	14,947,070 (96.98%)	9,564,804 (62.06%)	5,382,266 (34.92%)	465,053 (3.02%)
StageII-1	12,371,018 (100.00%)	1,739,928,464 (100.00%)	12,028,229 (97.23%)	7,172,029 (57.97%)	4,856,200 (39.25%)	342,789 (2.77%)
StageII-2	15,891,229 (100.00%)	2,332,924,677 (100.00%)	15,533,624 (97.75%)	9,456,435 (59.51%)	6,077,189 (38.24%)	357,605 (2.25%)
StageIII-1	15,194,682 (100.00%)	2,104,759,656 (100.00%)	14,838,649 (97.66%)	8,411,453 (55.36%)	6,427,196 (42.30%)	356,033 (2.34%)
StageIII-2	12,908,078 (100.00%)	1,758,036,319 (100.00%)	12,612,680 (97.71%)	6,935,639 (53.73%)	5,677,041 (43.98%)	295,398 (2.29%)
StageIV-1	16,179,709 (100.00%)	2,200,713,831 (100.00%)	15,877,084 (98.13%)	9,491,808 (58.66%)	6,385,276 (39.46%)	302,625 (1.87%)
StageIV-2	18,600,312 (100.00%)	2,583,939,574 (100.00%)	18,324,379 (98.52%)	10,852,126 (58.34%)	7,472,253 (40.17%)	275,933 (1.48%)

Comparison of adjacent developmental stages S1-vs-S2, S2-vs-S3 and S3-vs-S4 detected 36 up-regulated and 113 down-regulated genes, 173 up-regulated and 319 down-regulated genes, 99 up-regulated and 320 down-regulated genes, respectively (Fig. 10A, Table 4). Pairwise comparisons between nonadjacent developmental stages S1-vs-S3, S2-vs-S4 and S1-vs-S4 detected 148 up-regulated and 575 down-regulated genes, 86 up-regulated and 426 down-regulated genes and 97 up-regulated and 711 down-regulated genes, respectively (Fig. 10A). Venn diagrams displayed no overlapping DEGs for the three adjacent pairwise comparisons, while 57 overlapping DEGs were identified with nonadjacent pairwise developmental stage comparisons (Fig. 10B). These results indicated that comparisons of nonadjacent developmental stages can obtain more key DEGs, which may play an important role during long-term development of IBs.

The analysis of specific expression genes (SEGs) found 59, 239, 569 and 470 development-dependent specific expression genes in the S1, S2, S3 and S4 stages, respectively. The number of SEGs increased with the development of IBs, which showed that more unigenes expressed and functioned with the appearance and development of

IBs. The identification of SEGs related to development stages may provide key genomic information to explore the mechanism of IB development.

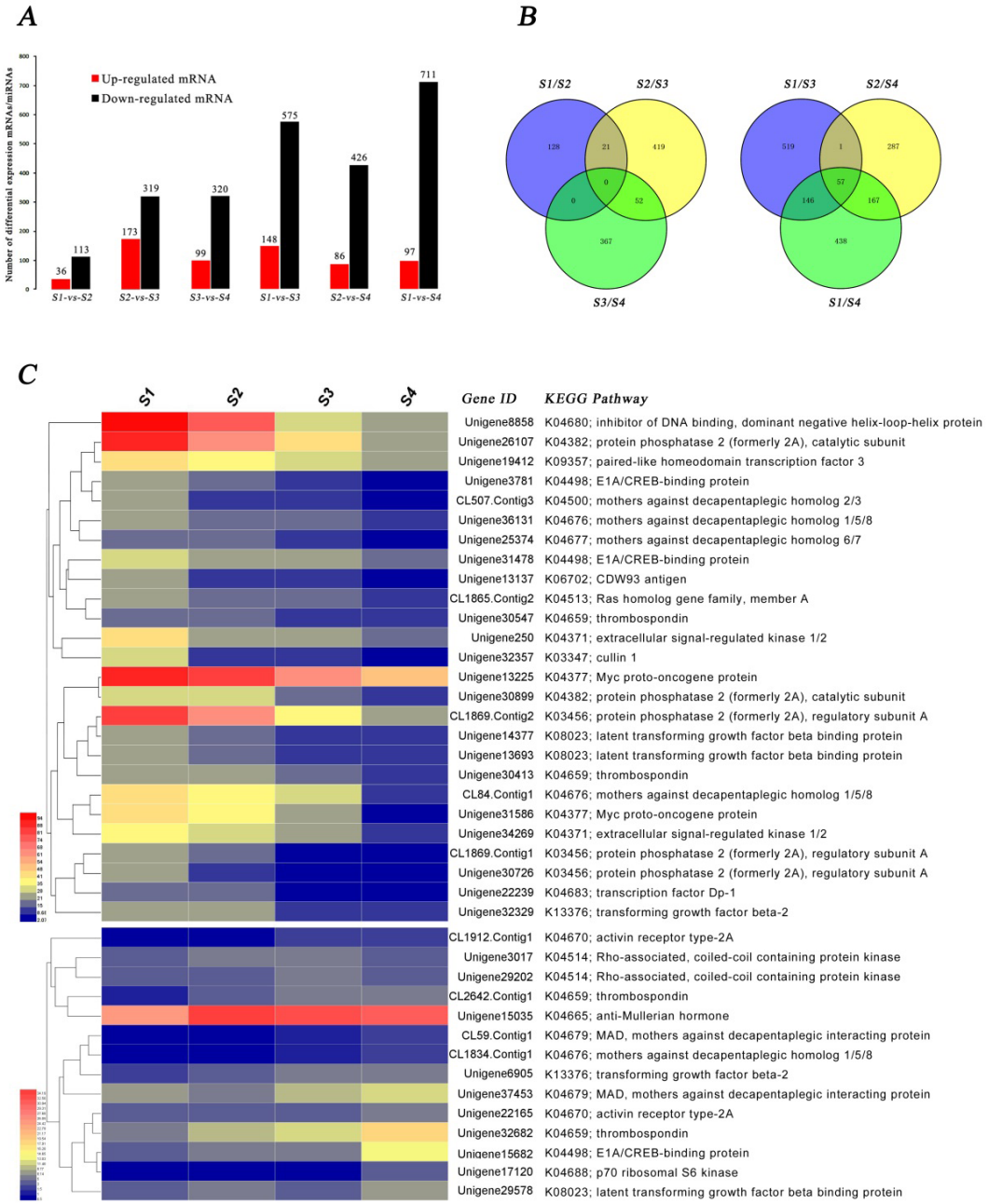

Figgure 10. Differentially expressed profiles for mRNA. (A) The number of up/down-regulated differentially expressed genes in each comparison analysis group; (B) Venn diagram of differential expression mRNAs between adjacent/nonadjacent pairwise comparisons; (C) Hierarchical cluster analysis for mRNAs belonging to the TGF-β pathway and having a sustained decreased/increased expression level from stages S1 to S4.

3.10 Functional analysis of DEGs and SEGs during the fthis developmental stages

GO categorization of DEGs in the six pairwise comparisons were all significantly enriched in cellular process, cell, cell part, binding and single-organism process, indicating the similarity in the major processes that respond to different developmental stages of IBs. Through aligning to the KEGG database, which categorizes gene functions with emphasis on biochemical pathways, a total of 13, 92, 52, 184, 121 and 184 DEGs involved in 12, 35, 31, 50, 55 and 52 pathways were predicted in the pairwise comparison of S1-vs-S2, S2-vs-S3, S3-vs-S4, S1-vs-S3, S2-vs-S4 and S1-vs-S4, respectively. The metabolic pathway containing the most DEGs was ko01100, which performs a variety of anabolic and catabolic tasks, affecting energy conversion, macromolecular compounds synthesis and so on33. Other pathways with an abundance of DEGs included those involved with the biosynthesis of secondary metabolites (ko01110), protein processing in endoplasmic reticulum (ko04141) and ribonucleotide metabolism (ko00240, ko00230). Similar results were obtained for GO annotation and KEGG analysis of SEGs in fthis development stages.

In order to narrow the focus of this analyses to genes likely to be relevant to bone tissue development, it si performed a detailed analysis of expression levels for genes involved in the TGF-β pathway, which is a known important factor in osteoblast differentiation and bone formation32. Twenty-six TGF-β genes were found to show a sustained decline in expression levels, while 14 TGF-β genes showed sustained increases in expression from stages S1 to S4. By referring to the KEGG map of the TGF-β pathway, it is found that the TGF-β pathway cooperated with the MAPK and extracellular signal-regulated kinase (ERK) pathways to regulate and control osteoblast differentiation (Fig. 11). It is noteworthy that Unigene34269 and Unigene250 were down-regulated in the ERK 1/2 pathway and Unigene32329 was down-regulated in TGF-β 2 pathway. Unigene39770 and Unigene20588, which belong to the BMP (bone morphogenetic protein) signaling pathway, were differentially expressed in S1 and S3. Previous studies have reported that

ERK plays a significant role in survival of osteoclasts and BMP promote differentiation of meschenchymal cells into chondrocytes and osteoblasts

.

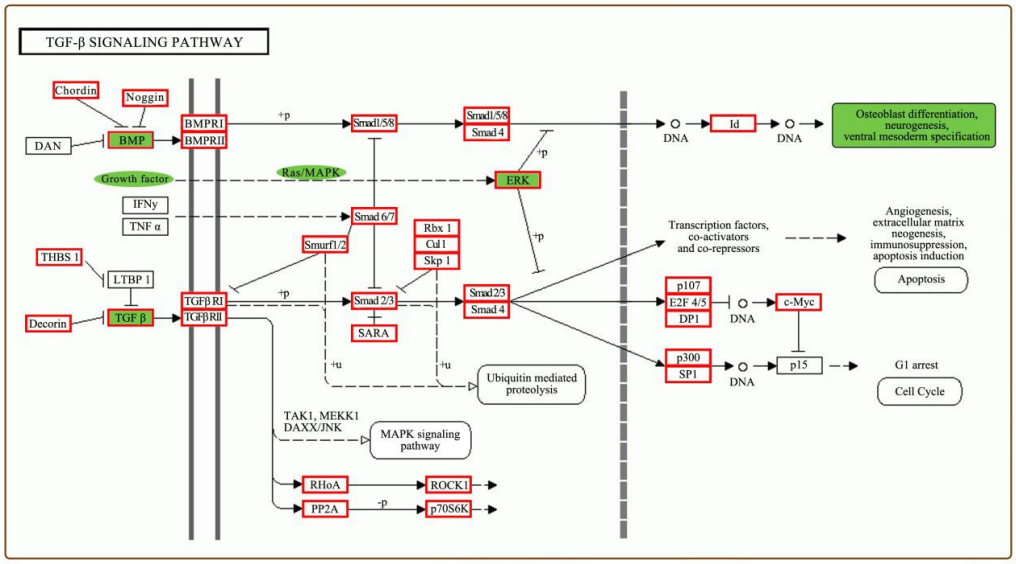

Figgure 11. Map of a portion of the TGF-β pathway. Red rectangles represent active gene expression. Green areas represent key signaling pathways and factors involved in the osteoclast differentiation.

3.11 Sequence and expression profiling of IB development-dependent microRNAs

A total of 12,105,829, 11,468,831, 12,420,544 and 12,472,082 raw reads were successively collected from fthis libraries, respectively. After discarding low-quality reads, 3′ and 5′ adaptors and sequences with < 18nt, 11,807,206, 11,222,117, 12,142,432 and 12,042,698 clean small RNA reads were obtained in the S1, S2, S3 and S4 libraries, respectively. Little differences in the length distribution of the sequences from the this libraries (> 75%) in all libraries. The total number of unique reads from S1, S2, S3 and S4 were 100,606, 78,655, 121,567 and 91,580, respectively. Through mapping, 10,432,263 (88.36%), 9,957,281 (88.73%), 10,714,729 (88.24%) and 10,470,015 (86.94%) clean reads representing 20,890 (20.76%), 14,952 (19.01%), 20,108 (21.96%) and 28,282 (23.26%) unique sRNAs were mapped to the reference transcriptome. After NCBI

Genebank and Rfam database alignment, rRNA, tRNA, snRNA and snoRNA were annotated and removed. For further miRNA analysis, a total of 420 known miRNAs and 41 novel miRNA candidates were generated. Among them, 375, 360, 358 and 385 known miRNAs and 22, 19, 14 and 23 novel miRNAs were found in the S1, S2, S3 and S4 libraries.

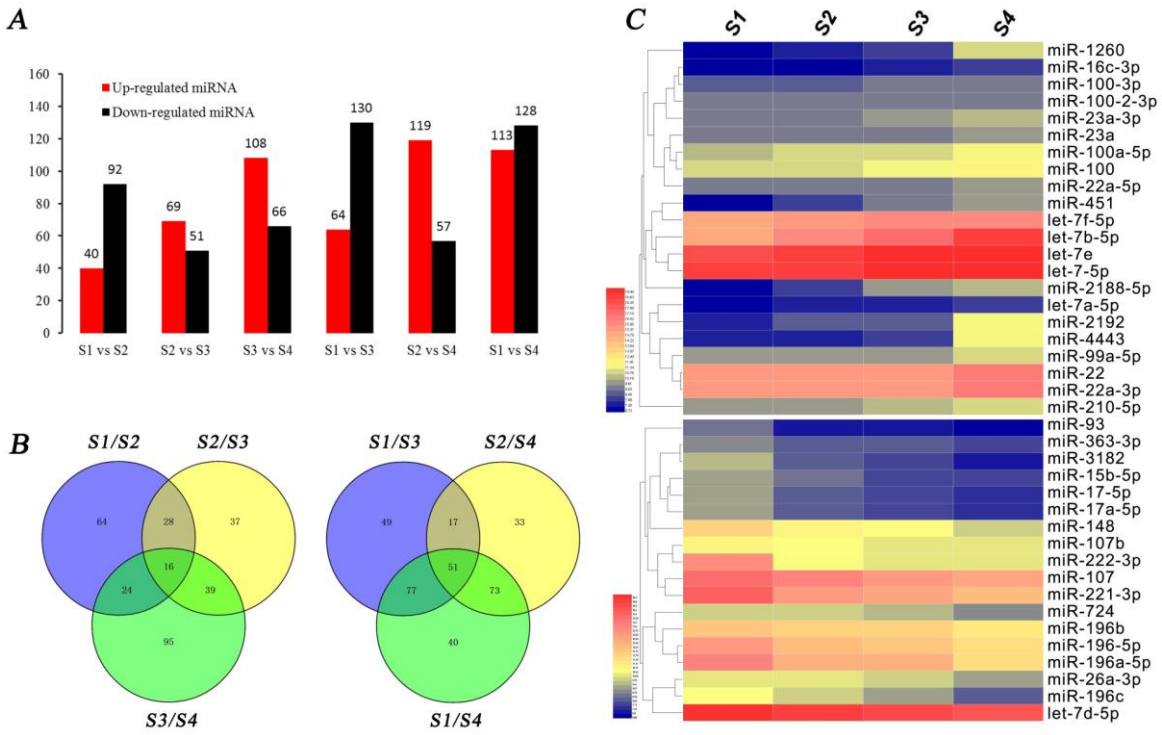

Figgure 12. Differentially expressed profiles for miRNAs. (A) Number of up/down differential expression miRNAs in each comparison analysis group; (B) Venn diagram of miRNA differential expression between adjacent/nonadjacent pairwise comparisons; (C) Hierarchical cluster analysis of miRNAs, having a sustained decreased/increased expression from stages S1 to S4.

To evaluate the time cthisse and development-dependent miRNA activities across the fthis development stages of IBs, it is performed a time cthisse differential expression miRNA analysis by comparing each two adjacent developmental stages (Supplementary Table S10). Using |log2Ratio| ≥ 1, P < 0.05 and reads ≥ 100 as the cut-off, it is identified 132 (40 up-regulated and 92 down-regulated), 120 (69 up-regulated and 51 down-regulated) and 174 (108 up-regulated and 66 down-regulated) differentially expressed miRNAs in adjacent pairwise comparisons of S1-vs-S2, S2-vs-S3 and

S3-vs-S4 (Fig. 12A). In nonadjacent pairwise comparisons, 194 (64 up-regulated and 130 down-regulated), 176 (119 up-regulated and 57 down-regulated) and 241 (113 up-regulated and 128 down-regulated) differentially expressed miRNAs were identified in S1-vs-S3, S2-vs-S4 and in S1-vs-S4, respectively (Fig. 12A). Similar to the mRNAs, comparisons of nonadjacent developmental stages obtained more differentially expressed miRNAs (Fig. 12A), and miRNA expression showed a long-term slowly increase/decrease with the IB development. Through Venn diagram analysis, 16 and 51 overlapped differentially expressed miRNAs were identified in the three adjacent pairwise comparisons and three nonadjacent pairwise comparisons, respectively (Fig. 12B). In order to further understand the regulatory functions of miRNAs, a total of 52,918 unique targets of *M. amblycephala* were predicted for the 420 known miRNAs and 41 novel miRNAs including 362 highly significant differently expressed miRNAs.

Furthermore, in order to obtain significant miRNAs, which expression has a sustained increase/decline trend with the development of IBs, a comprehensive analysis was performed using standardized reads data from fthis stages. Twenty-two miRNAs with sustained increased expression and 18 miRNAs with sustained decreased expression from S1 to S4 stages were detected (Fig. 12C). Functions of these miRNAs in differentiation and development of bone have been verified in many species. For instance, prior studies provided evidence that let-7 miRNAs and miR-140 play major roles in endochondral bone development38. Let-7 and miR-22 had also been shown to be positive regulators of bone development, promoting osteogenesis and suppressing adipogenesis of MSCs in vitro (Wei, et al.,2014; Huang, et al., 2012). MiR-100, miR-26a and miR-148 play important roles in osteogenic differentiation and osteoclastogenesis, respectively (Yang, Z. et al., 2012; Cheng, P. et al., 2013; Luzi, E. et al., 2008). A previous study also found that over-expression of the Hox-cluster miR-196 in zebrafish embryos reduces the number of ribs and somites. Reciprocally, miR-196 knockdown could evoke extra ribs and (He et al., 2011) somites. Therefore, some of the miRNAs that are differentially expressed between these important developmental stages are likely to have important roles in affecting osteoblast differentiation and osteogenesis.

3.12 Analysis of miRNA-mRNA interaction

The investigation of individual miRNA-target interactions and the miRNA-target interaction network has been an exciting and challenging field of study. In general, increased miRNA activity has been found to reduce the expression of mRNA targets, and vice versa (Wang and Li, 2009; Cheng and Li, 2008). Therefore, integrated analysis of miRNA and mRNA expression profiles over the fthis developmental stages is an effective way to identify functional miRNA-mRNA interaction pairs involved in specific biological processes (Pei et al., 2013; Liu et al, 2016)

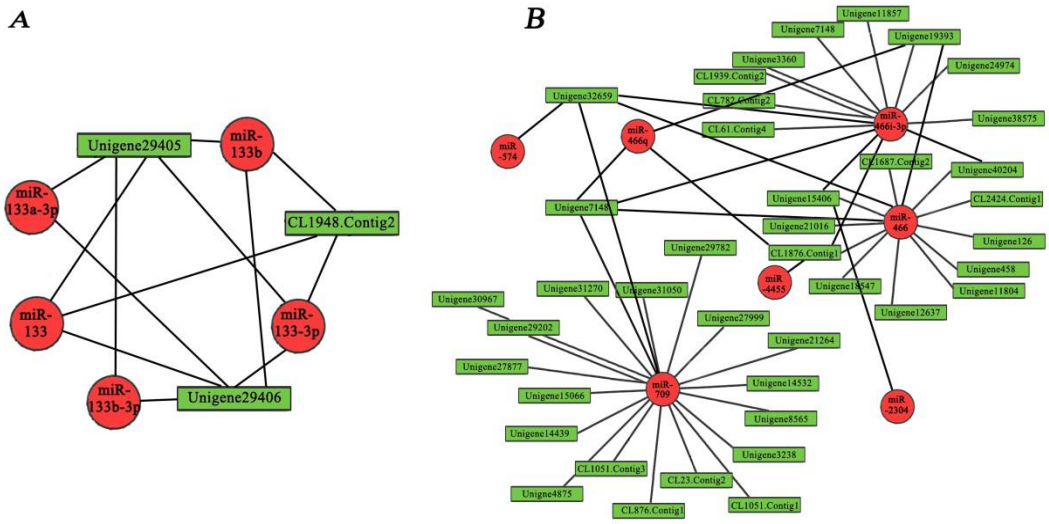

Figgure 13. miRNA-mRNA interaction diagrams. (A) MiRNA-mRNA interaction pairs associated with the miR-133 family; (B) Visualization of a portion of the miRNA-regulated network.

Through the simultaneous analysis of expression profiles for miRNA and target mRNA involved in IB development, it is identified 201, 31, 92, 219, 93 and 500 miRNA-mRNA interaction pairs from six pairwise comparisons (S1-vs-S2, S2-vs-S3, S3-vs-S4, S1-vs-S3, S2-vs-S4 and S1-vs-S4), respectively. For the miRNA-mRNA interaction pairs, it is found that some miRNAs were closely related to bone formation and differentiation, such as miR-133/133a/133b, miR-222 and miR-396049–51. The interaction map of this study performed that CL1948.Contig2 (S1-S4) was down-regulated with the up-regulated of miR-133, miR-133-3p and miR-133b, while unigene29405 and unigene29406 interact

with miR-133, miR-133-3p and miR-133b (Fig. 13A). This suggests that these miRNA-mRNA interaction pairs may function in IB formation. Furthermore, in order to detect the functional characteristics of miRNA-mRNA interaction pairs, the mRNAs involved in interaction pairs were subjected to a GO analysis and KEGG functional annotation. The mRNAs identified in these pairs included those involved in the TGF-beta signaling pathway, Osteoclast differentiation, MAPK signaling pathway, Wnt signaling pathway and Calcium signaling pathway. For instance, CL712.Contig1 (S1–S2, S2–S3, S1–S3), Unigene28219 (S3–S4), Unigene2429 (S1–S3), Unigene20803 (S2–S4, S1–S4) and Unigene6271 (S1–S4) were mapped to the TGF-β signaling pathway; Unigene7819 (S1–S2, S1–S3, S1–S4), Unigene41990 (S3–S4, S2–S4, S1–S4), Unigene271 (S3–S4, S1–S4) and CL782.Contig2 (S1–S3, S1–S4) were simultaneously mapped to the Osteoclast differentiation and MAPK signaling pathway. Similarly, other genes like Unigene34104 (S1–S2, S1–S3), Unigene25273 (S2–S3) and CL618.Contig10 (S1–S4) were mapped to the Calcium signaling pathway and Unigene31459 (S3–S4, S2–S4, S1–S4) was mapped to the Wnt signaling pathway. Previous research has suggested that TGF-β and Wnt are involved in many cellular processes affecting osteoblast differentiation and bone formation (Chen et al, 2012; Katagiri and Takahashi, 2002; Glass et al., 2005; Baron and Kneissel, 2013). Another pathway targeted by the mRNAs was the MAPK signaling pathway, which is not only known to be a major regulator of skeletal muscle development (Keren et al, 2006; Fuentes et al., 2011) but is also essential for bone development and maintenance (Greenblatt et al., 2010). In addition, Ca2+ signals play key roles in osteoblast function (Chen et al., 2000; Than and Han, 2013). Collectively, the existing literature supports that many of the miRNA-mRNA interaction pairs identified in this study are likely to be involved in regulating development and differentiation of bone.

3.13 Quantitative analysis of miRNA and mRNA expression

Quantitative PCR results for 9 miRNAs and 6 mRNAs revealed similar changes in expression to that detected using RNA-seq data (Fig. 14). A similar result was also observed in the validation of the miRNA-mRNA interaction pairs, and 12 of 13 interaction pairs have a same expression pattern with the sequencing data except one of them performed a down-down regulating pattern (Fig. 15). The result is acceptable and it confirmed the credibility of molecular resthisces and sequencing data identified in this study. Because extensive researches performed that hundreds of miRNAs interact with thousands of target mRNAs to maintain proper gene expression patterns under various physiological functions, as the results it is showed. The complexity of the miRNA-mRNA interaction network presents a great challenge for researchers to reveal the roles for specific miRNAs or miRNA-mRNA interactions in specific biological processes60. For instance, miR-709, miR-466 and miR-466i-3p constituted a complex interaction network with unigene32659, unigene7148, unigene15406 and many other miRNAs and mRNAs (Fig. 13B). Furthermore, miRNA-mRNA interaction is only one of the multiple mechanisms influencing the regulation of gene expression and this results will not be sensitive in instances when multiple factors, in addition to miRNA-mRNA interactions are involved (Than and Han, 2013; Reddy et al, 2008). Moreover, in order to explore IB specific genes, it is performed expression analysis of 65 bone-related genes in IBs, muscle and rib tissues. However, the present results indicated that it was not possible, despite repeated attempts to demonstrate IB specific localization of gene from the transcriptome. The failure to demonstrate IB specific gene expression may be because of the fact that the transcriptome contained genes not only for IB, particularly since genes inducing IB development may be expressed in associated tissues, such as muscle. Clearly further research will be required to confirm the function of genes involved in IB development.

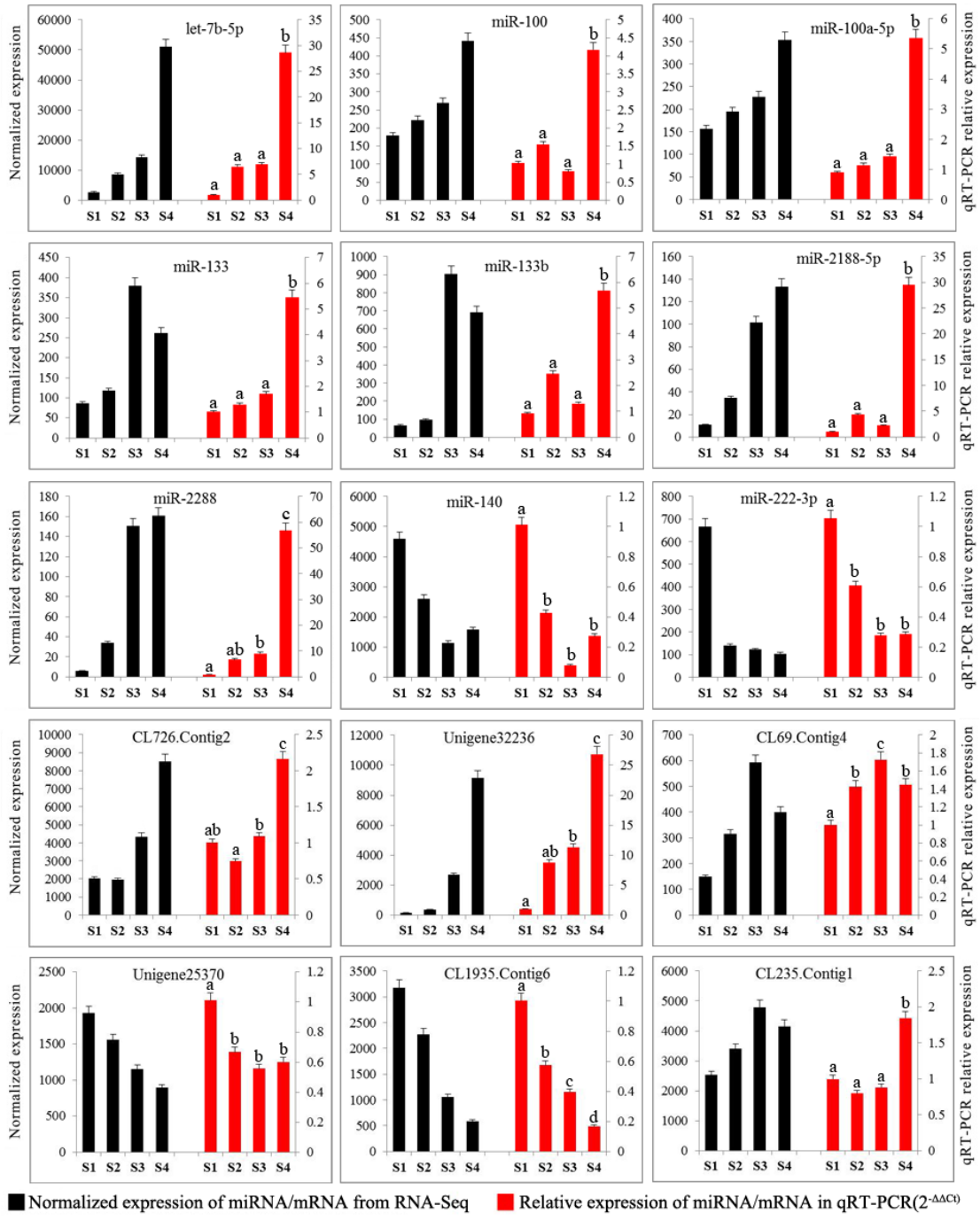

Figgure 14. Comparison of expression levels for the 9 detected miRNAs and 6 mRNAs using RNA-Seq and qRT-PCR

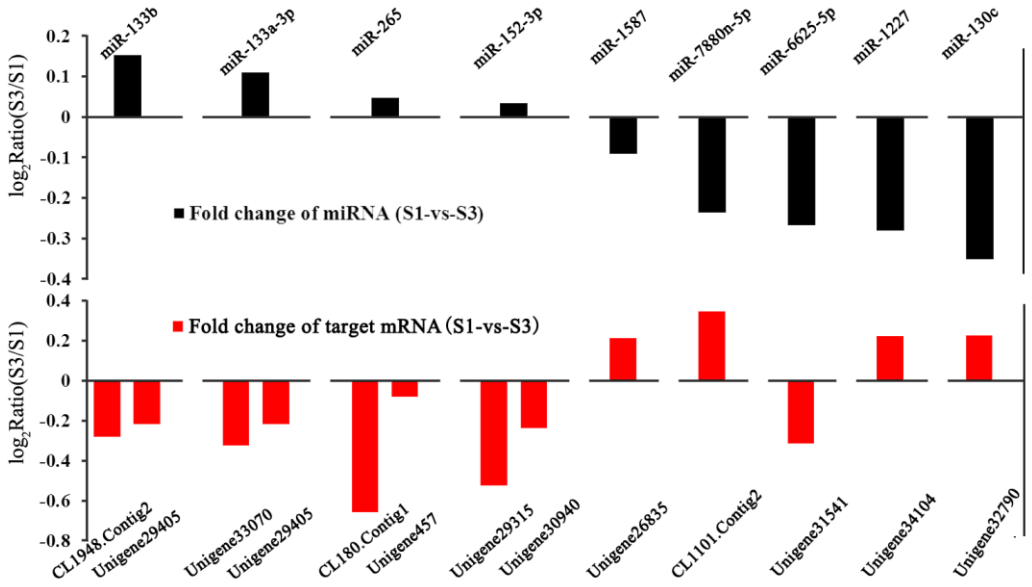

Figure 15. Verification of expression patterns of miRNA-mRNA interaction pairs using qRT-PCR

3.14 Target verification of miR-133b-3p and miR-206-3p

Previous research supports that the miR-133 family and miR-206 were involved in bone formation and differentiation (Hanna et al, 2012). Tgfbr1a and runx2 genes, which functioned in skeletal development (Flores et al, 2004), were identified as downstream targets of the miR-133b-3p/miR-206-3p cluster, with complementary binding sites detected on the 3′ UTRs (Fig. 16A). To evaluate the functions of miR-133b-3p/miR-206-3p at target 3′ UTRs, dual-luciferase reporter constructs carrying tgfbr1a or runx2 3′ UTR (wild-type or empty) were cotransfected with miR-133b-3p mimics or miR-206-3p mimics. The results showed that luciferase activity for the wild-type construct (GLO-tgfbr1a, GLO-runx2a) was significantly reduced by miR- 133b-3p mimics and miR-206-3p mimics, but not by that of the empty construct (pmirGLO) (Fig. 16B, C). The wild-type construct GLO-runx2b was not reduced by miR-206-3p mimics (Fig. 16C), which showed the inaccuracy of software prediction and the necessity of experimental verification.

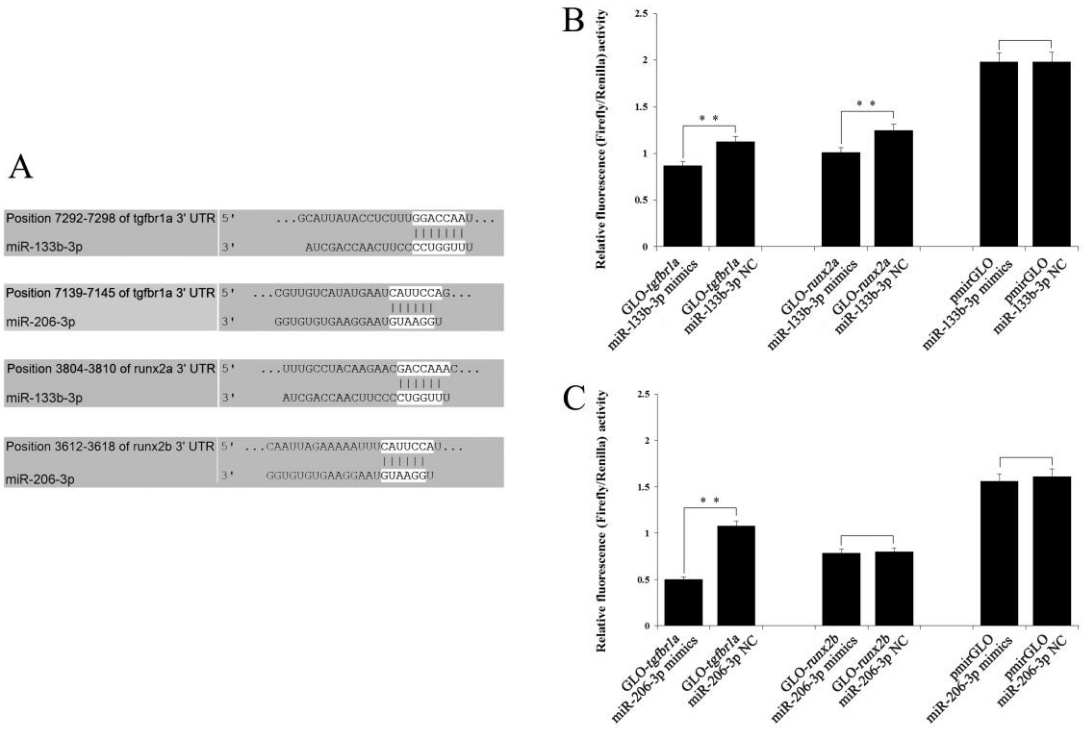

Figgure 16. Target verification of miR-133b-3p and miR-206-3p. (A) MiRNA seed sequences and their complementary sequences on 3' UTR; (B) miR-133b-3p mimics were cotransfected with *tgfbr1a* or *runx2a* 3' UTR dual-luciferase reporters into HeLa cells. ; (C) miR-206-3p mimics were cotransfected with *tgfbr1a* or *runx2b* 3' UTR dual-luciferase reporters into HeLa cells. Firefly luciferase activities were detected and normalized to renilla luciferase (internal control). Results represent means ±SE (n = 4，**$P \leq 0.01$).

3.15 Chromosome synteny analysis and conservation analysis of *bmpr2* genes

Phylogenetic analysis chronologically showed that the *bmpr2* orthologs, which evolved from the same ancestor gene family of vertebrates, was duplicated and differentiated into *bmpr2a* and *bmpr2b* in fishes in the clupeocephala duplication (fish-specific genome duplication; ~300 million years ago) after euteleostomi speciation (~420 million years ago) (Figure 17A). The results of chromosome synteny analysis showed that although the number of the syntenic genes flanking human/mouse *Bmpr2* and zebrafish *bmpr2a/2b* is

limited, the gene synteny is consistent with *bmpr2a* and *bmpr2b* arising during the teleost-specific whole genome duplication event (Figure 17B). Finally, zebrafish Bmpr2b has higher amino acid (AA) similarity (78%) to human BMPR2 than that does Bmpr2a (64%) (Figure 17B).

In addition, sequence and structure analysis of *Bmpr2*/*bmpr2a/b* gene of human/zebrafish also showed that the zebrafish *bmpr2b* and the human *Bmpr2* gene are highly homologous. Although three genes have the same exon number of 13, zebrafish *bmpr2b* (152.60kb) is closer to human *Bmpr2* (192.77kb) in gene length, which is significantly larger than that of zebrafish *bmpr2a* (90.75 kb) (Figure 17C). More remarkably, the sequence from the 5th to the 12th exon of human *Bmpr2* and zebrafish *bmpr2b* is highly homologous with an identity of 76% (Figure 17C), which suggest a relatively high level of conservation between human *Bmpr2* and zebrafish *bmpr2b*.

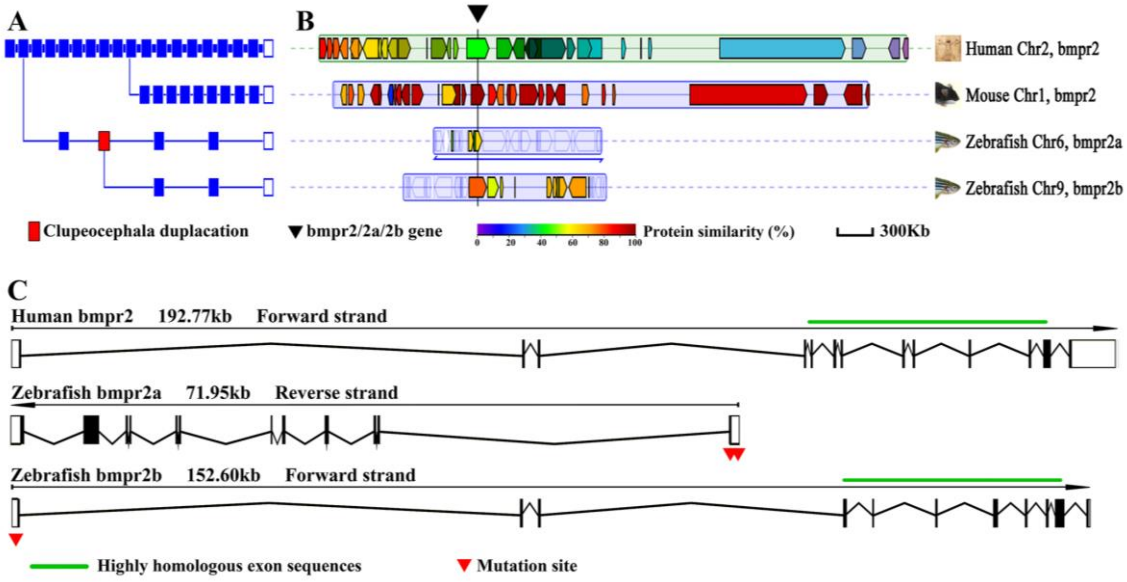

Figgure 17. Phylogenetic analysis and conservation analysis of *bmpr2* gene. (A) Phylogenetic analysis. The blue boxes indicate speciation, and the red boxe indicates fish-specific genome duplication. (B) Synteny maps comparing the genes flanking *bmpr2* among human (*H. sapiens*), mouse (*M. musculus*) and zebrafish (*D. rerio*) chromosomes (equally proportional to genome scale). The black triangle and vertical lines indicate the location of the *bmpr2* gene on the chromosome. The color indicates the protein similarity between the given gene and the human homologous gene. (C) Structural characteristics and homologous comparison of human *bmpr2* and zebrafish *bmpr2a*/*2b*. The black

polyline and rectangular box represent introns and exons respectively (equally proportional to gene scale). Highly homologous exon sequences are marked with green lines. The red triangles indicate the mutation sites.

3.16 Generation of *bmpr2a* and *bmpr2b* mutant zebrafish

In order to explore whether differences in function of skeletal development had occurred between the orthologous genes, it is constructed the *bmpr2a* and *bmpr2b* mutant zebrafish using CRISPR-Cas9 technology. Two *bmpr2a* nonsense alleles with 7bp deletion (*bmpr2a*$^{-7}$) and 10bp deletion (*bmpr2a*$^{-10}$) in the first exon were generated (Figure 17C), which both caused frame-shift mutations at the 22nd and 21nd AA, respectively, and premature transcription termination event at the 79nd and 78nd AA. One *bmpr2b* nonsense alleles with 44 bp deletion (*bmpr2b*$^{-44}$) in the first exon were also generated (Figure 1C). The *bmpr2b*$^{-44}$ nonsense allele resulted in an initiation codon deletion and translation termination. Both *bmpr2a* and *bmpr2b* mutations occurred in the front of the highly conserved domain including transmembrane domain and serine/threonine kinase domain (Deng et al., 2000). Considering that the phenotypic consistency of different mutant lines of the same gene was confirmed in subsequent experiments, the homozygous mutant lines of *bmpr2a* and *bmpr2b* were refer as *bmpr2a*$^{-/-}$ and *bmpr2b*$^{-/-}$, respectively, unless otherwise stated.

3.17 Zebrafish with normal IBs

Alizarin red staining observation for the *bmpr2a* and *bmpr2b* zebrafish IBs showed that there was no significant change in the IB phenotypes of the two mutant zebrafishes. Regardless of length, quantity, and morphological analysis, the development of IB of *bmpr2a*$^{-/-}$ and *bmpr2b*$^{-/-}$ is similar to that of wild-type individuals. The results showed that the loss of zebrafish *bmpr2a* and *bmpr2b* gene functions would not lead to changes in the physical phenotype of the IBs.

-

3.18 Zebrafish showed varying degrees of mineralized bone malformations

Adult *bmpr2b*$^{-/-}$ zebrafish show different types and degrees of mineralized bone malformations in different body parts, while *bmpr2a*$^{-/-}$ zebrafish have completely normal bone development. In *bmpr2b*$^{-/-}$ mutants, the abnormally arched back and curved tail can be seen intuitively, which are completely different from wild-type and *bmpr2a* mutants (Figure 18A). Within the skeleton X-ray scanning revealed that *bmpr2b*$^{-/-}$ mutant adult fish have a varying degrees of mineralized bone malformations including severe curvature of vertebral column (Figure 18B). Additionally, it is observed the histologic features of the vertebral deformity through longitudinal histological sections, which results showed compressed and deformed vertebral bodies in *bmpr2b*$^{-/-}$ mutants, as opposed to regularly formed vertebrae in wild fish (Figure 18C).

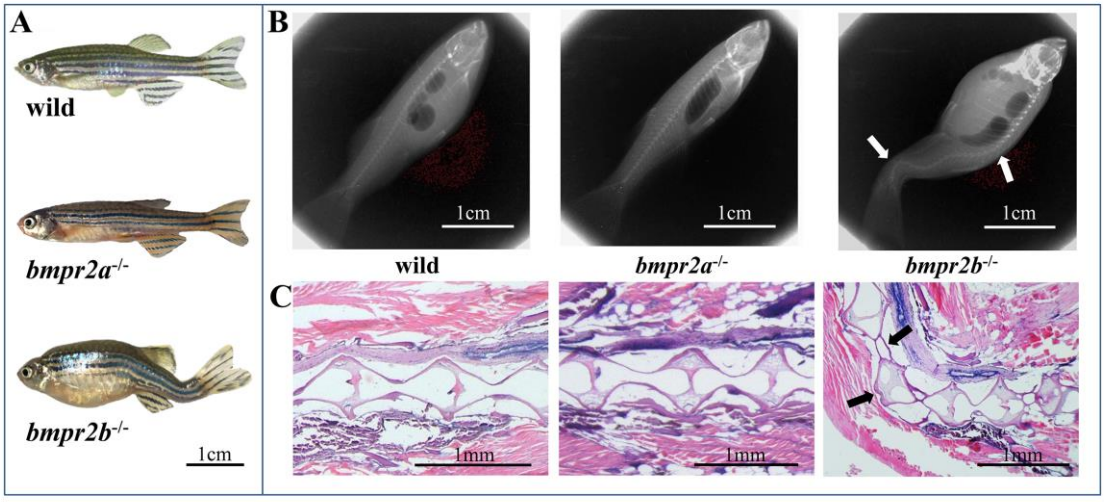

Figgure 18. Phenotype observation of *bmpr2a*$^{-/-}$ and *bmpr2b*$^{-/-}$ zebrafish at 4 month old. (A) External physical characteristics of wild and mutant zebrafish. (B) Overall skeletal phenotype analysis of wild and mutant zebrafish by X-ray scanning. The white arrow indicates deformed bone tissue. (C) Observation of vertebra characteristics by longitudinal section. The black arrows indicate abnormally developed vertebrae in *bmpr2b*$^{-/-}$.

Whole-mount Alizarin Red staining for mineralized bone further illustrated that the skeletal system of *bmpr2b*$^{-/-}$ mutants has various abnormal characteristics (Figure 19A). Phenotypic observations of different batches of fish showed that 80% of bmpr2b$^{-/-}$ individuals had different degrees of mineralized bone malformation. Different from wild phenotypes (Figure 19B), abnormal mineralization of *bmpr2b*$^{-/-}$ mutants result in unusual bowing and kinking ribs and bone callus formation in ribs, which was similar with the callus agglomerations after fractures (Figure 19C). Irregularly shaped bone hyperplasia is also observed in neural and haemal arches of vertebra. In addition, abnormally hyperplastic irregular bone also appears in the intervertebral disc, which can lead to the deformation of the spine of zebrafish. Bowing and kinking was also observed in the caudal fin endoskeleton (Figure 19C). In addition, the staining results of mineralized bones at different early developmental stages indicate that *bmpr2b*$^{-/-}$ zebrafish began to show different degrees of mineralized bone deformities at 15dpf (Figure 20).

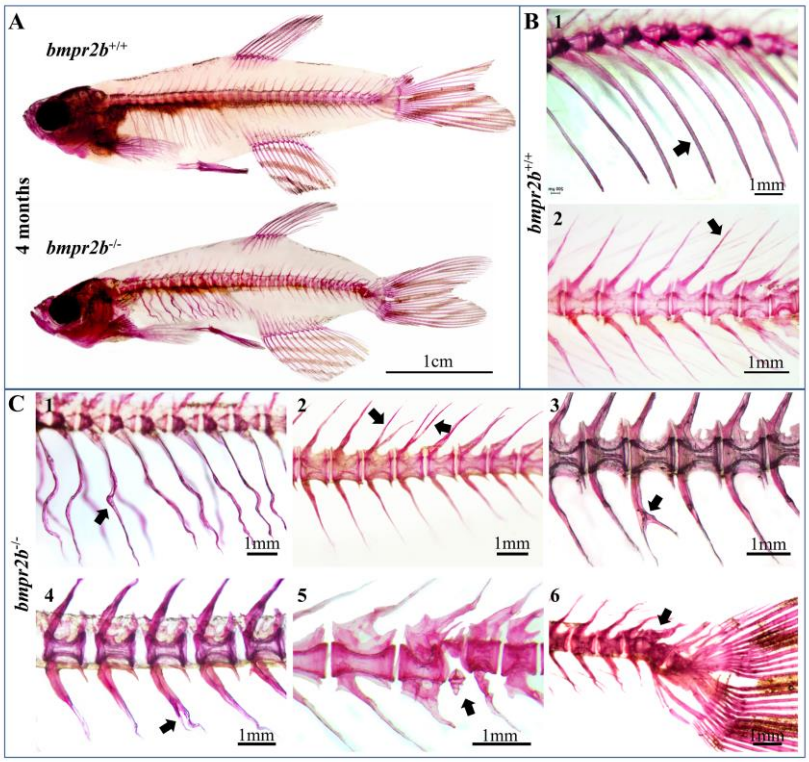

Figgure 19. Alizarin red staining for mineralized bone of 4 month adult *bmpr2b*$^{+/+}$ and *bmpr2b*$^{-/-}$ zebrafish. (A) Overall mineralized bone phenotypes of *bmpr2b*$^{+/+}$ and *bmpr2b*$^{-/-}$ zebrafish. (B1-B2) The normally mineralized bone in wild zebrafish, such as the rib, vertebra, neural and haemal arches indicated by the arrows. (C1-C6) Various types of

mineralized bone malformations in *bmpr2b*$^{-/-}$ mutants. Such as unusual bowing and kinking ribs, hyperplasia in neural and haemal arches and intervertebral disc, bowing and kinking in the caudal fin endoskeleton, etc.

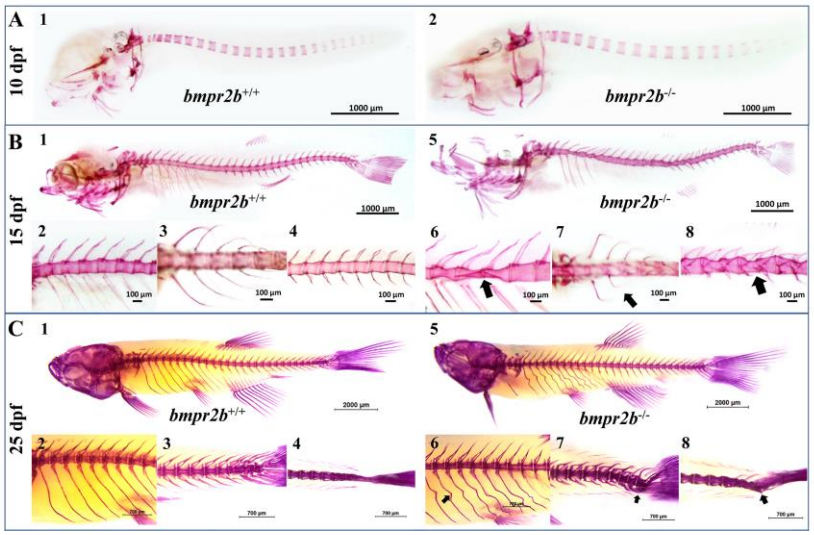

Figgure 20. Observation of bone in *bmpr2b*$^{+/+}$ and *bmpr2b*$^{-/-}$ zebrafish at different developmental stages. (A) No obvious mineralized bone deformity appeared in the 10dpf *bmpr2b*$^{+/+}$ and *bmpr2b*$^{-/-}$ zebrafish. (B) Partially mineralized bone deformity appeared in 15dpf *bmpr2b*$^{-/-}$ zebrafish, such as collapse and contraction of the vertebrae, asymmetrically developed ribs, dysplastic neural and haemal arches, which were indicated by the black arrows. Bone development of *bmpr2b*$^{+/+}$ zebrafish was normal. (C) *Bmpr2b*-/- zebrafish showed more severe mineralized bone malformation in the 25dpf.

3.19 Expression of BMP-Smad signaling molecule significantly Down-Regulated in *bmpr2b*$^{-/-}$ mutants

Considering the important regulatory role of BMP signaling pathway in the bone development of vertebrates and the key role of *bmpr2* gene in signal transduction, it is analyzed the expression of BMP-Smad signaling molecules in 15 dpf wild and *bmpr2b*$^{-/-}$ mutant individuals (malformed phenotypes appear in mutants). As the receptor activated by *bmpr2* in the canonical BMP-Smad pathway, zebrafish BMP type 1 receptor have more abundant homologous genes including *bmpr1aa* and *bmpr1ab*, *bmpr1ba* and

bmpr1bb. Compared to the expression level in the wild samples, the overall expression level of bmpr1a (*bmpr1aa*, *bmpr1ab*) and bmpr1b (*bmpr1ba*, *bmpr1bb*) were all down-regulated in the *bmpr2b*$^{-/-}$ mutant samples (Figure 21A), which also determined by the protein expression analysis (Figure 21D). The significance analysis also showed that the *bmpr1aa* and *bmpr1ba* expression was extremely down-regulated after the *bmpr2b* deletion (Figure 21A), which indicated that *bmpr1aa* and *bmpr1ba* may be the main BMP type 1 receptor mediating BMP-Smad signal in zebrafish. Meanwhile, gene expression analysis of R-Smad factors revealed that *smad1* and *smad5* had similar expression abundance in wild and mutants; however, *smad8/9* was significantly down-regulated in *bmpr2b*$^{-/-}$ mutants (Figure 21B). The gene and protein expression of *smad4* was also significantly down-regulated in the *bmpr2b*$^{-/-}$ mutants (Figure 21B, 21D). The results indicated that Smad8/9 may be the primary co-Smad activated by type 1 receptor that forms complexes with Smad4 to translocate into the nucleus and regulate transcription of target genes through interaction with transcription factors and transcriptional coactivators.

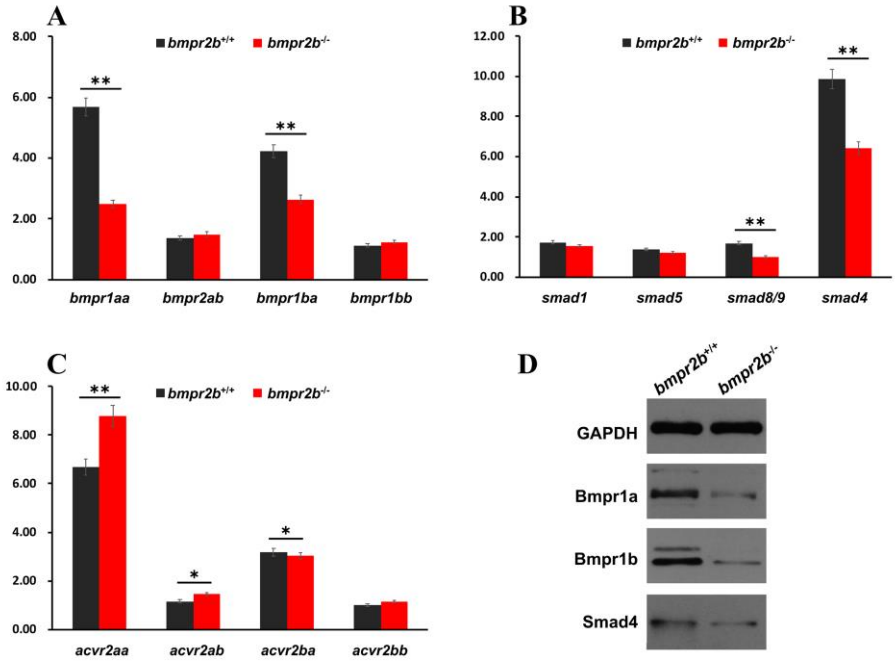

Figgure 21. Expression analysis of BMP pathway molecules in *bmpr2b*$^{+/+}$ and *bmpr2b*$^{-/-}$ samples. (A-C) Quantitative expression analysis of BMP pathway molecules. P-value <0.05 is represented by *. P-value <0.01 is represented by **. (D) Western blot analysis of BMP pathway proteins.

In addition, except that BMPR2 is specific for BMPs, TGF-β/Smad signaling pathway still has type II receptors ACVR2A and ACVR2B, which are shared by activins, myostatin and BMPs. These two type II receptors can also bind to most BMP ligands, affecting the binding preference of BMPs to type I receptors and regulating intracellular gene expression through signal transduction of SMAD molecules (Yu et al., 2005). So, it is conducted the expression analysis of fthis type II activin receptor genes in the wild and *bmpr2b*$^{-/-}$ individuals. Noteworthily, except for *acvr2ba*, three *acvr2* genes (*acvr2aa*, *acvr2ab*, *acvr2bb*) showed up-regulated expression. In particular, the expression level of *acvr2aa* was the highest in both samples and significantly up-regulated in mutant samples (Figure 21C). These results showed that *bmpr2b* deletion may cause compensatory up-regulation of activin receptor type II, but it was not enough to offset the phenotypic changes caused by the loss of *bmpr2b*.

The *bmpr2b* mutants show not only multiple types of bone tissue hyperplasia, but also severe bone tissue defects. The normal development and maintenance of bone tissue is the regulation result of multiple functional genes. The above results have shown that loss of *bmpr2b* leads to significant changes of BMP-Smad signal, which may subsequently lead to abnormal expression of multiple genes with positive or negative regulation of bone mineralization. In order to explain the complex phenotypes in mutants, it is performed quantitative expression analysis for several genes possessing specific functions in bone development such as *ocn*, *runx2*, *entpd5* and *spp1*. The results indicated that the expression of these genes was significant down-regulation in mutants (Figure 22A-E). The protein expression levels of *ocn* and *runx2* also showed consistent changes (Figure 22F). These results indicated that loss of *bmpr2b* function leads to down-regulation of many bone development-related genes, which revealed the potential regulatory role of *bmpr2b* in bone mineralization mediated by BMP-Smad pathway.

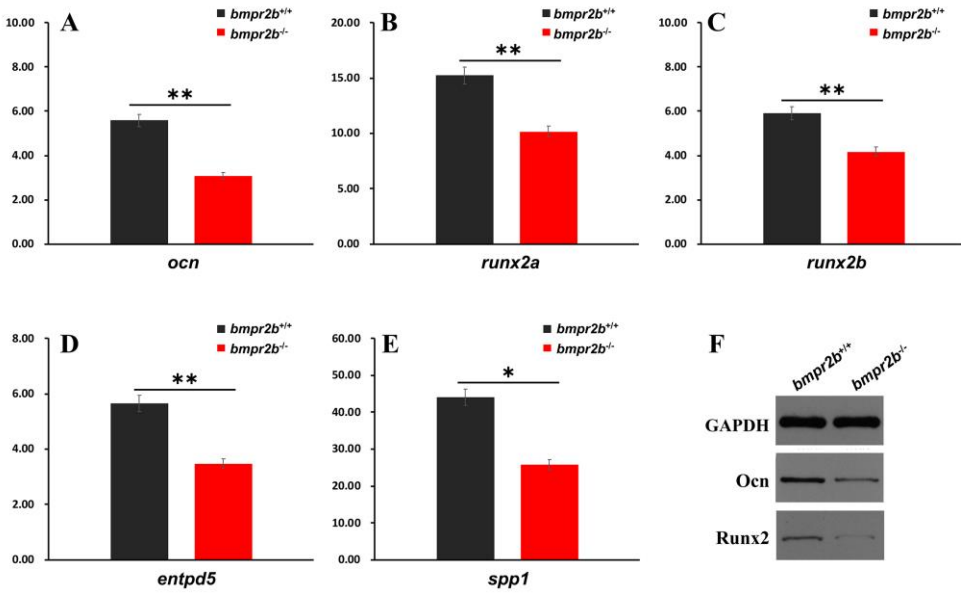

Figgure 22. Expression analysis of genes related to bone development in *bmpr2b*$^{+/+}$ and *bmpr2b*$^{-/-}$ samples. (A-E) Quantitative expression analysis of genes related to bone development. *P*-value <0.05 is represented by *. *P*-value <0.01 is represented by **. (F) Western blot analysis of proteins involved in bone development.

4 DISCUSSION

Unlike humans and mice, which have only one *bmpr2* gene, zebrafish has two *bmpr2* orthologous genes, *bmpr2a* and *bmpr2b*. This provides an excellent material for us to explore the evolution and functional differentiation of fish genes. Previous genome replication studies have shown that the main fate of copies of genes may be to be lost, silenced, sub-functionalized or to produce new functions (Lynch and Force, 2000; Zhou et al., 2006). For instance, the results of sequence analysis, genome query and evolution analysis of three cloned Spindlin genes (*OlSpinA*, *OlSpinB*, *OlSpinC*) in medaka indicate that all of them belong to the phenomenon of gene duplication and have obvious differences in sequence and function (Wang et al., 2005). In this study, the results of phylogenetic analysis showed that FSGD also led to the gene replication of *bmpr2* in zebrafish, forming *bmpr2a* and *bmpr2b*. The synteny analysis of the zebrafish *bmpr2a* and *bmpr2b*, as well as the human and mouse *bmpr2*, revealed a shared synteny, supporting the presence of a common ancestral. However, the limited number, different location and arrangement of the syntenic genes flanking *bmpr2*/*2a*/*2b* also revealed the differentiation of orthologous genes at the level of chromosome structure. But the higher nucleic acid and protein similarity gives us reason to believe that zebrafish *bmpr2b* has more similar functions to human *bmpr2*, while the significantly reduced gene scale and changed protein coding of *bmpr2a* indicate that it is likely to evolve into new functions. Subsequently, the distinct skeletal phenotypes in *bmpr2a*$^{-/-}$ and *bmpr2b*$^{-/-}$ mutants also proved that the functions of *bmpr2a* and *bmpr2b* diverged in evolution, and also indicated that the functional study of *bmpr2b* gene in zebrafish was of more reference value to reveal the role of human *bmpr2* gene in bone development.

Previous studies have focused on the function of *bmpr2b* in early embryonic development, for instance, morpholino-mediated knockdown of *bmpr2a* and *bmpr2b* showed that they are required for the establishment of concomitant cardiac and visceral LR asymmetry in the zebrafish embryo (Monteiro et al., 2008), MO knockdown of *bmpr2b* disrupts both vasculogenesis and angiogenesis in a dose dependent fashion up to 72 hpf, but no vascular defects were identified in control MO or *bmpr2a* injected embryos (Washko et al.,

2009). Unlike previous studies, here it is performed a long-term phenotype observation of *bmpr2b* mutant zebrafish from self-fertilization to adulthood. The results showed that bone and cartilage tissue developed normally without obviously abnormal phenotype in the early development stage. But, mineralized bone showed different degrees of malformation phenotype with still normally developed cartilage tissue from 15 dpf. This time point is similar to the previous studies which showed that Type I Collagen deficiency of zebrafish caused a consistent clinical phenotype of human Bruck Syndrome (Gistelinck et al., 2016). These results also suggest that the visualization of abnormal skeletal phenotypes may require a longer period of accumulation of effects. Early genetic testing is the best measure for the detection, prevention and treatment of diseases, such as osteoporosis in human caused by an inactivating mutation of the ERα gene (Smith et al., 1994), aromatase deficiency syndrome due to inactivating mutations at the aromatase gene (Morishima et al., 1995; Carani et al., 1997; Bilezikian et al., 1998) and the marked bone loss as a result of estrogen deficiency in women (Riggs et al., 1998; Lindsay et al., 1976). In addition, the malformation phenotype of *bmpr2b* mutant fish skeleton showed a series of characteristics, including impermanent malformation site, inconsistent malformation degree among individuals, coexisting hyperosteogenesis and bone atrophy. These representations have a certain degree of similarity with bone malformation phenotypes caused by Type I Collagen II, enpp1 and SCX gene deficiency in the previous studies (Gistelinck et al., 2016; Apschner et al., 2014; Kague et al., 2019), which indicates that the functional deficiency of *bmpr2b* may lead to the expression disorder of various skeletal development related pathways and genes, which then results in non-consistent and unstable abnormal phenotypes.

Expression analysis showed that the function loss of *bmpr2b* in zebrafish would lead to the down-regulation of type I receptor, especially *bmpr1aa* and *bmpr1ba* had the most significant expression change (Figure 7A). Previous studies have shown that embryonic morphology of mouse *Bmpr2* and *Bmpr1a* mutants is very similar (Beppu et al., 2000) and Bmpr1a and Bmpr1b with overlapping functions are essential in mice cartilage development (Yoon et al., 2005). So, the consistent expression patterns in this study indicated that *bmpr1aa* and *bmpr1ba* may be the main functional type 1 receptors

mediating pathway signals related to bone development, which results not only reified the function of type I receptor in fish, but also provided a reference for the study of functional divergence of its homologous genes. *Smad1* and *Smad5* are required for endochondral bone formation, simultaneous loss of *Smad1* and *Smad5* leads to severe chondrodysplasia, but deletion of *Smad8* does not lead to apparent defects (Retting et al., 2009). Noteworthily, there was no significant change in the expression levels of *smad1* and *smad5* in this study, which explained the normally developed cartilage phenotype. Then the significant expression changes of *smad8* indicated that it might play an important role in the mineralized bone development of zebrafish. The expected significant changes in *smad4* expression once again confirmed its important role in animal bone development (Salazar et al., 2013). Meanwhile, the results also proved that the compensation effect between zebrafish type II receptors, the decreased expression of *bmpr2b* was accompanied by the up-regulated expression of *acvr2*, but the effect of *bmpr2b* deficiency on mineralized bone development could not be completely offset. The expression analysis also showed that the functional deficiency of *bmpr2b* resulted in the significant downregulation of various bone developing-related genes such as *ocn*, *entpd5*, *runx2* and *spp1*, which can regulate skeletal development of animals from different directions, for instance, osteocalcin and *runx2* deficiency leads to increased and repressed bone formation in mice, respectively (Ducy et al., 1996; Otto et al., 1997). Induction of *runx2* expression promoted bone formation (Yang et al., 2011) and *entpd5* mutation can lead to lack of mineralized skeleton in zebrafish (Huitema et al., 2012). The fish osteopontin-like protein also plays a role in hard tissue mineralization (Fonseca et al., 2007). These findings help to explain the complex bone phenotype in *bmpr2b* mutants.

This study revealed that the structure and function of that *bmpr2* homologous gene were different in zebrafish. Functional loss of *bmpr2b* results in abnormal mineralized bone development in zebrafish, but *bmpr2a* is not associated with that. Integrating existing studies, this results also revealed the possible regulatory mechanism of the BMP-Smad molecules involved in bone mineralization under the condition of *bmpr2b* functional deficiency (Figure 23), providing important reference information for the in-depth exploration of animal bone development mechanism and the construction of human bone

disease model.

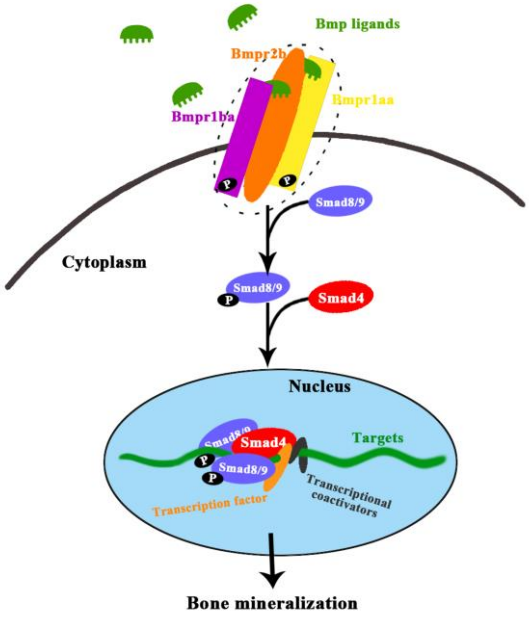

Figgure 23. A working schematic model. BMP ligands-bound type II receptor Bmpr2b mainly binds BMP I receptor Bmpr1aa and Bmpr1ba and phosphorylates them to form activated ligand:receptor complexes, which then mainly binds and phosphorylates Smad8/9. Upon that, Smad8/9 forms complexes with Smad4 and translocate into the nucleus and regulate transcription of target genes through interaction with transcription factors and transcriptional coactivators to affect bone mineralization.

5. CONCLUSIONS

On the whole, the results indicated that these differentially-expressed miRNAs were abundant and functionally involved in regulating the development and differentiation of intermuscular bone and connective tissue, providing an opportunity to further functionally validate miRNA in the regulation of the development of intermuscular bone.

This is the first integrated analysis of miRNA and mRNA related to IBs development in fish species. MiRNA and mRNA expression profiles involved in IB development were revealed over fthis developmental stages. Putative miRNAs/genes associated with IB development were identified in the study. In addition, it isfound that a number of miRNA-mRNA interaction pairs were associated with bone formation and differentiation, adding to knowledge about the regulation of IB development. This study generated fundamental molecular resthisces for fthis developmental stages from emerging to complete formation of IBs, which can be used to improve understanding about the molecular processes affecting IB development.

Key Findings:

1. Revealed the microstructure and potential differentiation relationship of the IB and CT in *M. amblycephala*. Based on the differences of tissue structure and comparative transcriptome analysis, specific expression miRNAs in different tissues and target unigenes were discovered. Through KEGG pathway analysis, a large number of unigenes enriched for skeletal development-related signaling pathways were discovered. The genetic information of IBs were identified from the perspective of tissue differentiation.
2. The correlation analysis of the expression patterns of mRNAs and miRNAs in the fthis key developmental stages of IBs revealed the mRNAs and miRNAs that are specifically expressed at different developmental stages, as well as the differentially expressed genes and miRNAs between different developmental stages, including the TGF-β pathway genes whose expression levels continue to decrease / rise in fthis developmental stages; pathway enrichment analysis found that TGF-β cooperates with MAPK and ERK signaling pathways

to regulate the differentiation of osteoblasts. Research has revealed a great deal of genetic information about IBs from a developmental perspective.

3. miRNA-mRNA interaction analysis revealed a large number of miRNAs and mRNAs related to bone development. Validation of the targeting relationship between skeletal development-related miRNAs and mRNAs based on the dual luciferase reporter gene revealed that miR-133b-3p significantly inhibited the 3'UTR expression of tgfbr1a and runx2a; miR-206-3p significantly inhibited the 'UTR sequence expression. However, the experimental results also showed that the overexpression of miR-206-3p did not cause the suppression of the expression of the wild-type plasmid GLO-runx2b, suggesting the uncertainty of the target genes predicted by the software and the necessity of validation experiments.

4. Functional verification experiments of candidate genes based on CRISPR-Cas9 revealed the role of *bmpr2b* in bone mineralization of zebrafish, but no direct regulatory effect on the IBs phenotype was found.

Research Innovation

1. For the first time, it isobserved the microstructure of the IBs and related tissues, explored their potential differentiation, and constructed the mRNA and miRNA transcriptome database of IBs and potentially differentiated tissues.

2. Based on the characteristics of IBs development, constructed the transcriptome database of mRNA and miRNA, revealing the potential regulatory relationship between miRNA and mRNA in the IB development.

3. For the first time, systematically studied the molecular regulation mechanism of fish IBs by combining morphology, histology, transcriptomics and CRISPR-Cas9 gene editing technology.

6 REFERENCES

Akiyama, H., Chaboissier, M. C., Martin, J. F., Schedl, A., de Crombrugghe, B. (2002). The transcription factor sox9 has essential roles in successive steps of the chondrocyte differentiation pathway and is required for expression of sox5 and sox6. *Genes Dev.* 16, 2813-2828.

Anders, S., Huber, W. (2010). Differential expression analysis for sequence count data. Genome Biol. 11(10), 79–82.

Andreassen, R. (2013). Discovery and characterization of miRNA genes in Atlantic salmon (Salmo salar) by use of a deep sequencing approach. BMC Genomics, 14.

Apschner, A., Huitema, L. F., Ponsioen, B., Peterson-Maduro, J., Schulte-Merker, S. (2014). Zebrafish enpp1 mutants exhibit pathological mineralization, mimicking features of generalized arterial calcification of infancy (GACI) and pseudoxanthoma elasticum (PXE). *Dis. Model. Mech.* 7, 811-822.

Apschner, A., Schulte-Merker, S., Witten, P. E. (2011). Not all bones are created equal - using zebrafish and other teleost species in osteogenesis research. *Methods Cell Biol.* 105, 239-255.

Audic, S.; Claverie, J.M. The significance of digital gene expression profiles. Genome Res. 1997, 7, 986–995.

Baron, R.; Kneissel, M. (2013). WNT signaling in bone homeostasis and disease, from human mutations to treatments. Nat. Med., 19, 179–192.

Beppu, H., Kawabata, M., Hamamoto, T., Chytil, A., Minowa, O., Noda, T. (2000). BMP type II receptor is required for gastrulation and early development of mouse embryos. *Dev. Biol.* 221, 249-258.

Berendsen, A. D., and Olsen, B. R. (2015). Bone development. *Bone* 80, 14-18..

Bing, Z. (1962). On the myoseptal spines of the carp (*Cyprinus carpio* L.). Acta Zool. Sin., 14, 175–178.

Bird, N.; Mabee, P. (2003). Developmental morphology of the axial skeleton of the zebrafish, Danio rerio (Ostariophysi, Cyprinidae). Dev. Dyn., 228, 337–357.

Bizuayehu, T.T.; Babiak, J.; Norberg, B.; Fernandes, J.; Johansen, S.D. (2012). Sex-biased

miRNA expression in Atlantic halibut (*Hippoglossus hippoglossus)* brain and gonads. Sex. Dev., 6, 257–266.

Burroughs, A.M.; Ando, Y.; de Hoon, M.J.; Tomaru, Y.; Nishibu, T. A (2010). Comprehensive survey of 3' animal miRNA modification events and a possible role for 3' adenylation in modulating miRNA targeting effectiveness. Genome Res., 20, 1398–1410.

Chen, C.; Ridzon, D.Z.; Broomer, A.J.; Zhou, Z.; Lee, D.H.; Nguyen, J.T.; Barbisin, M.; Xu, N.; Mahuvakar, V.R.; Andersen, M.R. (2005). Real-time quantification of microRNAs by stem-loop RT-PCR. Nucleic Acids Res. 33.

Chen, G.; Deng, C.; Li, Y.P. (2012). TGF-β and BMP signaling in osteoblast Differentiation and Bone Formation. Int. J. Biol. Sci., 8, 272–288.

Chen, N. X., Ryder, K. D., Pavalko, F. M., Turner, C. H., Burr, D. B., Qiu, J., Duncan, R. L. (2000). Ca($^{2+}$) regulates fluid shear–induced cytoskeletal reorganization and gene expression in osteoblasts. Am. J. Physiol. Cell Physiol. 278(5), C989–997

Chen, X.; Li, Q.; Wang, J. (2009). Identification and characterization of novel amphioxus microRNAs by Solexa sequencing. Genome Biol. 2009, 10.

Cheng, C., Li, L. M. (2008). Inferring microRNA activities by combining gene expression with microRNA target prediction. PloS One 3(4), e1989.

Cheng, P. Chen, C., He, H. B., Hu, R., Zhou, H. D., Xie, H., Luo, X. H. (2013). miR–148a regulates osteoclastogenesis by targeting V–maf musculoaponeurotic fibrosarcoma oncogene homolog B. J. Bone Miner Res. 28, 1180–1190.

Cho, S. H. Oh, B., Kim, H. A., Park, J. H., Lee, M. (2013). Post–translational regulation of gene expression using the ATF4 oxygen–dependent degradation domain for hypoxia–specific gene therapy. J. Drug Target 21(9), 830–836.

Choi, J.W.; Liu, H.; Mukherjee, R.; Yun, J.W. (2012).Downregulation of fetuin-B and zinc-α2-glycoprotein is linked to impaired fatty acid metabolism in liver cells. Cell. Physiol. Biochem., 30, 295–306.

Deng, Z., Morse, J. H., Slager, S. L., Cuervo, N., Moore, K. J., Venetos, G. (2000). Familial primary pulmonary hypertension (gene PPH1) is caused by mutations in the bone morphogenetic protein receptor-II gene. *Am. J. Hum. Genet.* 67, 737-744.

Duan, Z.; Choy, E.; Harmon, D.; Liu, X.; Susa, M.; Mankin, H.; Hornicek, F.

(2011).MicroRNA-199a-3p is downregulated in human osteosarcoma and regulates cell proliferation and migration. Mol. Cancer Ther., 10, 1337–1345.

Ducy, P., Desbois, C., Boyce, B., Pinero, G., Story, B., Dunstan, C. (1996). Increased bone formation in osteocalcin-deficient mice. *Nature* 382, 448-452.

Dunn, W., Duraine, G., Reddi, A. H. (2009). Profiling microRNA expression in bovine articular cartilage and implications for mechanotransduction. Arthritis Rheum. 60(8), 2333–2339.

Ebhardt, H.A.; Tsang, H.H.; Dai, D.C.; Liu, Y.; Bostan, B.; Fahlman, R.P. (2009). Meta-analysis of small RNA-sequencing errors reveals ubiquitous post-transcriptional RNA modifications. Nucleic Acids Res., 37, 2461–2470.

Enright, A.J.; John, B.; Gaul, U.; Tuschl, T.; Sander, C. (2003). MicroRNA targets in Drosophila. Genome Biol., 5.

Fang, L.; Li, X. (2013). A review of research on intermuscular bone formation in lower teleosts. Fish. Sci., 32, 749–752.

Fernandez-Valverde, S.L.; Taft, R.J.; Mattick, J.S. (2010). Dynamic isomiR regulation in Drosophila development. RNA, 16, 1881–1888.

Fisher, S., Jagadeeswaran, P., and Halpern, M. E. (2003). Radiographic analysis of zebrafish skeletal defects. *Dev. Biol.* 264, 64-76.

Flores, M. V., Tsang, V. W. K., Hu, W., Kalev-Zylinska, M., Postlethwait, J., Crosier, P., Fisher, S. (2004). Duplicate zebrafish runx2 orthologues are expressed in developing skeletal elements. Gene Expr. Patterns 4(4), 573–581.

Fonseca, V. G., Laizé, V., Valente, M. S., and Cancela, M. L. (2007). Identification of an osteopontin-like protein in fish associated with mineral formation. *FEBS J.* 274, 4428-4439.

Fu, Y.; Shi, Z.; Wu, M.; Zhang, J.; Jia, L. (2011). Identification and differential expression of MicroRNAs during metamorphosis of the Japanese flounder (*Paralichthys olivaceus*). PLoS ONE 2011, 6, e22957.

Fuentes, E.N.; Björnsson, B.T.; Valdés, J.A.; Einarsdottir, I.E.; Lorca, B.; Alvarez, M.; Molina, A. (2011). IGF-I/PI3K/Akt and IGF-I/MAPK/ERK pathways in vivo in skeletal muscle are regulated by nutrition and contribute to somatic growth in the fine flounder. Am. J. Physiol. Regul. Integr. Comp. Physiol., 300, R1532–R1542.

Fuller-Carter, P. I., Carter, K. W., Anderson, D., Harvey, A. R., Giles, K. M., Rodger, J. (2015). Integrated analyses of zebrafish miRNA and mRNA expression profiles identify miR-29b and miR-223 as potential regulators of optic nerve regeneration. BMC Genomics 16(1), 1–19.

Gañán-Gómez, I.; Wei, Y.; Yang, H.; Pierce, S.; Bueso-Ramos, C. (2014). Overexpression of miR-125a in myelodysplastic syndrome CD34+ cells Modulates NF-κB Activation and Enhances Erythroid Differentiation Arrest. PLoS ONE 2014, 9, e93404.

Gao, Z.; Luo, W.; Liu, H. (2012). Transcriptome analysis and SSR/SNP markers information of the blunt snout bream (Megalobrama amblycephala). PLoS ONE 2012, 7, e42637.

Garyfallia, P. (2013). Let-7 and miR-140 microRNAs coordinately regulate skeletal development. Proc. Natl. Acad. Sci. USA 110(35), E3291– E3300.

Gistelinck, C., Witten, P. E., Huysseune, A., Symoens, S., Malfait, F., Larionova, D. (2016). Loss of Type I Collagen Telopeptide Lysyl Hydroxylation Causes Musculoskeletal Abnormalities in a Zebrafish Model of Bruck Syndrome. *J. Bone Miner. Res.* 31, 1930-1942.

Glass, D.A., II; Bialek, P.; Ahn, J.D.; Starbuck, M.; Patel, M.S.; Clevers, H.; Taketo, M.M.; Long, F.; McMahon, A.P.; Lang, R.A. (2005). Canonical Wnt signaling in differentiated osteoblasts controls osteoclast differentiation. Dev. Cell, 8, 751–764.

Greenblatt, M.B.; Shim, J.H.; Zou, W.; Sitara, D.; Schweitzer, M.; Hu, D.; Lotinun, S.; Sano, Y.; Baron, R.; Park, J.M. (2010). The p38 MAPK pathway is essential for skeletogenesis and bone homeostasis in mice. Clin. Investig., 120, 2457–2473.

Gui, J. F., Zhu, Z. Y. (2012). Molecular basis and genetic improvement of economically important traits in aquaculture animals. Chinese Sci. Bull. 57(15), 1751–1760.

Guo, L., Yu, J., Liang, T., Zou, Q. (2016). miR-isomiRExp: a web-server for the analysis of expression of miRNA at the miRNA/isomiR levels. Sci. Rep. 6.

Hanna, T. (2012). Mechanisms in endocrinology: micro-RNAs: targets for enhancing osteoblast differentiation and bone formation. Eur. J. Endocrinol. 166(3), 359–371.

Harris, M. P., Rohner, N., Schwarz, H., Perathoner, S., Konstantinidis, P., Nüsslein-Volhard, C. (2008). Zebrafish eda and edar mutants reveal conserved and ancestral roles of ectodysplasin signaling in vertebrates. *PLoS Genet.* 4, e1000206.

He, L. et al. Global gene expression patterns of grass carp following compensatory growth. BMC Genomics 16, 184 (2015).

He, X., Yan, Y. L., Eberhart, J. K., Herpin, A., Wagner, T. U., Schartl, M., Postlethwait, J. H. (2011). miR–196 regulates axial patterning and pectoral appendage initiation. Dev. Biol. 357(2), 463–477.

Herrera, B.M.; Lockstone, H.E.; Taylor, J.M. (2009). MicroRNA-125a is over-expressed in insulin target tissues in a spontaneous rat model of Type 2 Diabetes. BMC Med. Genomics, 2.

Hobert, O. (2008). Gene regulation by transcription factors and microRNAs. Science, 319, 1785–1786.

Hu, R., Liu, W., Li, H., Yang, L., Chen, C., Xia, Z. Y., Luo, X. H. (2011). A Runx2/miR–3960/miR–2861 Regulatory feedback loop during mouse osteoblast differentiation. J. Biol. Chem. 286(14), 12328–12339.

Huang, S.; Wang, S.; Bian, C.; Yang, Z.; Zhou, H.; Zeng, Y.; Li, H.; Han, Q.; Zhao, R.C. (2012). Upregulation of miR-22 Promotes osteogenic differentiation and inhibits adipogenic differentiation of human adipose tissue-derived mesenchymal stem cells by repressing HDAC6 protein expression. Stem Cells Dev., 21, 2531–2540.

Huang, Y., Liu, N., Wang, J. P., Wang, Y. Q., Yu, X. L., Wang, Z. B., Zou, Q. (2012). Regulatory long non-coding RNA and its functions. J. Physiol. Biochem. 68(4), 611–618.

Huitema, L. F., Apschner, A., Logister, I., Spoorendonk, K. M., Bussmann, J., Hammond, C. L. (2012). Entpd5 is essential for skeletal mineralization and regulates phosphate homeostasis in zebrafish. *Proc. Natl. Acad. Sci. U S A.* 109, 21372-21377.

Huleihel, L.; Ben-Yehudah, A. (2014). Let-7d microRNA affects mesenchymal phenotypic properties of lung fibroblasts. Am. J. Physiol. Lung Cell Mol. Physiol., 306, L534–L542.

Ikeda, T., Kamekura, S., Mabuchi, A., Kou, I., Seki, S., Takato, T., Chung, U. I. (2004). The combination of SOX5, SOX6, and SOX9 (the SOX trio) provides signals sufficient for induction of permanent cartilage. Arthritis Rheum. 50(11), 3561–3573.

Inose, H.; Ochi, H.; Kimura, A. (2009). A microRNA regulatory mechanism of osteoblast differentiation. Proc. Natl. Acad. Sci. USA, 106, 20794–20799.

Jiang, Y.; Yang, L.; Bao, B. (2008). The epicentrals in several lower teleosts. J. Shanghai Fish.

Univ., 17, 493–496.

Johnson, C.D.; Esquela-Kerscher, A.; Stefani, G.; Byrom, M.; Kelnar, K.; Ovcharenko, D.; Wilson, M.; Wang, X.; Shelton, J.; Shingara, J. (2007). The let-7 microRNA represses cell Proliferation Pathways in Human Cells. Cancer Res., 67, 7713–7722.

Johnson, G.D.; Patterson, C. (2001). The intermuscular system of acanthomorph fish, a commentary. Am. Mus. Novit., 1–24.

Kague, E., Hughes, S. M., Lawrence, E. A., Cross, S., Martin-Silverstone, E., Hammond, C. L., (2019). Scleraxis genes are required for normal musculoskeletal development and for rib growth and mineralization in zebrafish. *FASEB J.* 33, 9116-9130.

Kague, E., Roy, P., Asselin, G., Hu, G., Simonet, J., Stanley, A., (2016). Osterix/Sp7 limits cranial bone initiation sites and is required for formation of sutures. *Dev. Biol.* 413, 160-72.

Kang, L.; Cui, X.; Zhang, Y.; Yang, C.; Jiang, Y. (2013). Identification of miRNAs associated with sexual maturity in chicken ovary by Illumina small RNA deep sequencing. BMC Genomics 2013, 14.

Kang, M.; Zhao, Q.; Zhu, D.; Yu, J. (2012). Characterization of microRNAs expression during maize seed development. BMC Genomics, 13.

Karsenty, G., Wagner, E. F. (2002). Reaching a genetic and molecular understanding of skeletal development. Dev Cell 2(4), 389–406.

Karsenty, G. (2003). The complexities of skeletal biology. *Nature* 423, 316-318.

Katagiri, T., Takahashi, N. (2002). Regulatory mechanisms of osteoblast and osteoclast differentiation. Oral Dis. 8(3), 147–159.

Ke, Z.; Zhang, W.; Jiang, Y. (2008). Developmental morphology of the intermuscular bone in Hypophthalmichthys molitrix. Chin. J. Zool., 43, 88–96.

Keren, A.; Tamir, Y.; Bengal, E. (2006). The p38 MAPK signaling pathway, a major regulator of skeletal muscle development. Mol. Cell. Endocrinol., 252, 224–230.

Kim, D., Langmead, B., Salzberg, S. L. (2015). HISAT: a fast spliced aligner with low memory requirements. *Nat. Methods* 12, 357-360..

Kim, H.K.; Lee, Y.S.; Sivaprasad, U.; Malhotra, A.; Dutta, A. (2006). Muscle-specific microRNA miR-206 promotes muscle differentiation. Cell Biol., 174, 677–687.

Kobayashi, T., Lyons, K. M., McMahon, A. P., Kronenberg, H. M. (2005). BMP signaling stimulates cellular differentiation at multiple steps during cartilage development. *Proc. Natl. Acad. Sci. U S A.* 102, 18023-18027..

Kronenberg, H. M. (2003). Developmental regulation of the growth plate. *Nature* 423, 332-336.

Kuchenbauer, F.; Morin, R.D.; Argiropoulos, B.; Petriv, O.I.; Griffith, M. (2008). In-depth characterization of the microRNA transcriptome in a leukemia progression model. Genome Res., 18, 1787–1797.

Lane, K. B., Machado, R. D., Pauciulo, M. W., Thomson, J. R., Phillips, J. A., Loyd, J. E., (2000). Heterozygous germline mutations in BMPR2, encoding a TGF-beta receptor, cause familial primary pulmonary hypertension. *Nat. Genet.* 26, 81-84.

Lapunzina, P., Aglan, M., Temtamy, S., Caparrós-Martín, J. A., Valencia, M., Letón, R. (2010). Identification of a frameshift mutation in Osterix in a patient with recessive osteogenesis imperfecta. *Am. J. Hum. Genet.* 87, 110-114.

Laqtom, N.; Kelly, L.; Buck, A. (2014). Regulation of integrins and AKT signaling by miR-199-3p in HCMV-infected cells. BMC Genomics, 15,

Leboy, P. S. (2006). Regulating bone growth and development with bone morphogenetic proteins. Ann. NY Acad. Sci. 1068(1), 14–18.

Lewis, B.P.; Shih, I.H.; Jones-Rhoades, M.W.; Bartel, D.P.; Burge, C.B. (2003). Prediction of mammalian microRNA targets. Cell, 115, 787–798.

Li, G.; Li, Y.; Li, X.; Ning, X.; Li, M.; Yang, G. (2011). MicroRNA identity and abundance in developing swine adipose tissue as determined by Solexa sequencing. Cell Biochem., 112, 1318–1328.

Li, L.; Zhong, Z.; Zeng, M. (2013). Comparative analysis of intermuscular bone in different ploidy fish. Sci. China Life Sci., 56, 341–350.

Li, T.; O'Keefe, R.; Chen, D. (2005). TGF-β signaling in chondrocytes. Front. Biosci., 10, 681–688.

Li, X.; Liu, W.; Lu, K.; Xu, W.; Wang, Y. (2012). Dietary carbohydrate/lipid ratios affect stress, oxidative status and non-specific immune responses of fingerling blunt snout bream, Megalobrama amblycephala. Fish Shellfish Immunol., 33, 316–323.

Li, Z. Y., Hassan, M. Q., Volinia, S., Van Wijnen, A. J., Stein, J. L., Croce, C. M., Stein, G. S. (2008). A microRNA signature for a BMP2–induced osteoblast lineage commitment program. Proc. Natl. Acad. Sci. USA 105(37), 13906–13911.

Liu, Y., Zeng, X., He, Z., Zou, Q. (2016). Inferring microRNA-disease associations by random walk on a heterogeneous network with multiple data sthisces. IEEE/ACM Trans Comput. Biol. Bioinform. 1, 1.

Louis, A., Nguyen, N. T., Muffato, M., Roest Crollius, H. (2015). Genomicus update 2015: KaryoView and MatrixView provide a genome-wide perspective to multispecies comparative genomics. *Nucleic Acids Res.* 43(D1), D682-D689.

Lowery, J. W., Intini, G., Gamer, L., Lotinun, S., Salazar, V. S., Ote, S., Cox, K., Baron, R., and Rosen, V. (2015). Loss of bmpr2 leads to high bone mass due to increased osteoblast activity. *J. Cell Sci.*128, 1308-1315.

Lü, Y.; Bao, B.; Jiang, Y. (2007). Comparative analysis of intermuscular bones in lower teleosts. J. Fish. China, 31, 661–668.

Luo, W.; Zeng, C.; Deng, W.; Robinson, N.; Wang, W.; Gao, Z. (2014). Genetic parameter estimates for growth-related traits of blunt snout bream (Megalobrama amblycephala) using microsatellite-based pedigree. Aquac. Res., 45, 1881–1888.

Luzi, E., Marini, F., Sala, S. C., Tognarini, I., Galli, G., & Brandi, M. L. (2008). Osteogenic differentiation of human adipose tissue-derived stem cells is modulated by the miR-26a targeting the SMAD1 transcription factor. J. Bone Miner Res. 23, 287–295.

Lynch, M., Force, A. (2000). The probability of duplicate gene preservation by subfunctionalization. *Genetics* 154, 459-473.

Ma, L.; Dong, Z.; Su, S. (2012). The research progress on intermuscular bones of teleosts. Jiangsu Agric. Sci., 40, 234–235.

Mackay, E. W., Apschner, A., and Schulte-Merker, S. (2015). Vitamin K reduces hypermineralisation in zebrafish models of PXE and GACI. *Development* 142, 1095-1101.

Mao, X., Cai, T., Olyarchuk, J. G., Wei, L. (2005). Automated genome annotation and pathway identification using the KEGG Orthology (KO) as a controlled vocabulary. *Bioinformatics* 21, 3787-93.

Meyer, A., Schartl, M. (2000). Gene and genome duplications in vertebrates: the one-to-fthis (-to-eight in fish) rule and the evolution of novel gene functions. *Curr. Opin. Cell Biol.* 11, 699-704.

Meyer, U., Wiesmann, H. P. (2006). Bone and cartilage engineering. doi: 10.1007/3-540-33606-0.

Minina, E., Wenzel, H. M., Kreschel, C., Karp, S., Gaffield, W., McMahon, A. P., Vortkamp, A. (2001). BMP and Ihh/PTHrP signaling interact to coordinate chondrocyte proliferation and differentiation. Development 128(22), 4523–4534.

Miyazaki, T., Katagiri, H., Kanegae, Y., Takayanagi, H., Sawada, Y., Yamamoto, A., Nakamura, K. (2000). Reciprocal role of ERK and NF-κB pathways in survival and activation of osteoclasts. The Journal of cell biology, 148(2), 333-342.

Miyazono, K., Kamiya, Y., Morikawa, M. (2010). Bone morphogenetic protein receptors and signal transduction. *J. Biochem.* 147, 35-51.

Mondol, V.; Pasquinelli, A.E. (2012). Let's make it happen, the role of let-7 microRNA in development. Curr. Top. Dev. Biol., 99, 1–30.

Monteiro, R., van Dinther, M., Bakkers, J., Wilkinson, R., Patient, R., ten Dijke, P., et al. (2008). Two novel type II receptors mediate BMP signalling and are required to establish left-right asymmetry in zebrafish. *Dev. Biol.* 315, 55-71.

Moreno-Mateos, MA., Vejnar, C. E., Beaudoin, J. D., Fernandez, J. P., Mis, E. K., Khokha, M. K. (2015). CRISPRscan: designing highly efficient sgRNAs for CRISPR-Cas9 targeting in vivo. *Nat. Methods.* 12, 982-988.

Nakamura, H., Hirata, A., Tsuji, T., Yamamoto, T. (2003). Role of osteoclast extracellular signal-regulated kinase (ERK) in cell survival and maintenance of cell polarity. J. Bone Miner. Res. 18(7), 1198–1205.

Nie, C. H., Wan, S. M., Tomljanović, T., Treer, T., Hsiao, C. D., Wang, W. M.(2017). Comparative proteomics analysis of teleost intermuscular bones and ribs provides insight into their development. *BMC Genomics* 18, 147.

Nielsen, M.; Hansen, J.H.; Hedegaard, J.; Nielsen, R.O.; Panitz, F.; Bendixen, C.; Thomsen, B. (2010). MicroRNA identity and abundance in porcine skeletal muscles determined by deep sequencing. Anim. Genet., 41, 159–168.

Novello, C.; Pazzaglia, L.; Cingolani, C.; Conti, A.; Quattrini, I.; Manara, M.C.; Tognon, M.; Picci, P.; Benassi, M.S. (2013). MiRNA expression profile in human osteosarcoma, role of miR-1 and miR-133b in proliferation and cell cycle control. Int. J. Oncol., 42, 667–675.

Otto, F., Thornell, A. P., Crompton, T., Denzel, A., Gilmthis, K. C., Rosewell, I. R.(1997). Cbfa1, a candidate gene for cleidocranial dysplasia syndrome, is essential for osteoblast differentiation and bone development. *Cell* 89, 765-71.

Pan, Q., Yu, Y., Chen, Q., Li, C., Wu, H., Wan, Y.(2008). Sox9, a key transcription factor of bone morphogenetic protein-2-induced chondrogenesis, is activated through BMP pathway and a CCAAT box in the proximal promoter. *J. Cell Physiol.* 217, 228-241.

Patterson, C.; Johnson, G. (1995). Intermuscular bones and ligaments of teleostean fishes. Smithson Contrib. Zool., 559, 1–85.

Pei, H., Ma, N., Chen, J., Zheng, Y., Tian, J., Li, J., Gao, J. (2013). Integrative analysis of miRNA and mRNA profiles in response to ethylene in rose petals during flower opening. PloS one, 8(5).

Perazza, C. A., Menezes, J. T. B., Silva, L. A., Pinaffi, F. L. V., Ferraz, J. B. S., Hilsdorf, A. W. S. (2015). Record of lack of intermuscular bones in specimens of Colossoma macropomum (Characiformes): unusual phenotype to be incorporated into genetic improvement programs. In Abstracts. International Symposium on Genetics in Aquaculture XII Santiago de Compostela, Spain, June 21st-27th, O87 (2015).

Rafael, M. S., Laizé, V., Cancela, M. L. (2006). Identification of Sparus aurata bone morphogenetic protein 2: Molecular cloning, gene expression and in silico analysis of protein conserved features in vertebrates. Bone 39(6), 1373–1381.

Ramachandra, R.K.; Salem, M.; Gahr, S.; Rexroad, C.; Yao, J. (2008). Cloning and characterization of microRNAs from rainbow trout (*Oncorhynchus mykiss*), their expression during early embryonic development. BMC Dev. Biol., 8.

Ran, M., Chen, B., Wu, M., Liu, X., He, C., Yang, A., Zhang, S. (2015). Integrated analysis of miRNA and mRNA expression profiles in development of porcine testes. Rsc Advances, 5(78), 63439-63449.

Reddy, K. L., Zullo, J. M., Bertolino, E., Singh, H. (2008). Transcriptional repression mediated by repositioning of genes to the nuclear lamina. Nature 452, 243–247.

Retting, K. N., Song, B., Yoon, B. S., and Lyons, K. M. (2009). BMP canonical Smad signaling through Smad1 and Smad5 is required for endochondral bone formation. *Development* 136, 1093-104.

Ro, S.; Park, C.; Young, D.; Sanders, K.; Yan, W. (2007). Tissue-dependent paired expression of miRNAs. Nucleic Acids Res., 35, 5944–5953.

Salazar, V. S., Gamer, L. W., and Rosen, V. (2016). BMP signalling in skeletal development, disease and repair. *Nat. Rev. Endocrinol.* 12, 203-221.

Salazar, V. S., Zarkadis, N., Huang, L., Norris, J., Grimston, S. K., Mbalaviele, G. (2013). Embryonic ablation of osteoblast Smad4 interrupts matrix synthesis in response to canonical Wnt signaling and causes an osteogenesis-imperfecta-like phenotype. *J. Cell Sci.* 126, 4974-4984.

Schuster, S.; Fell, D.A.; Dandekar, T. (2000). A general definition of metabolic pathways useful for systematic organization and analysis of complex metabolic networks. Nat. Biotechnol., 18, 326–332.

Smith, A., Avaron, F., Guay, D., Padhi, B. K., Akimenko, M. A. (2006). Inhibition of BMP signaling during zebrafish fin regeneration disrupts fin growth and scleroblast differentiation and function. Dev. Biol. 299(2), 438–454.

Sugatani, T.; Hruska, K.A. (2013). Down-regulation of miR-21 biogenesis by estrogen action contributes to osteoclastic apoptosis. Cell Biochem., 114, 1217–1222.

Sweetman, D.; Goljanek, K.; Rathjen, T.; Oustanina, S.; Braun, T.; Dalmay, T.; Münsterberg, A. (2008). Specific requirements of MRFs for the expression of muscle specific microRNAs, miR-1, miR-206, and miR-133. Dev. Biol., 321, 491–499.

Tachi, K., Takami, M., Sato, H., Mochizuki, A., Zhao, B., Miyamoto, Y., Honda, Y. (2011). Enhancement of bone morphogenetic protein-2-induced ectopic bone formation by transforming growth factor-β1. Tissue engineering Part A, 17(5-6), 597-606.

Tan, X., Weng, T., Zhang, J., Wang, J., Li, W., Wan, H. (2007). Smad4 is required for maintaining normal murine postnatal bone homeostasis. *J. Cell Sci.* 120, 2162-2170.

Tang, M., Mao, D., Xu, L., Li, D., Song, S., Chen, C. (2014). Integrated analysis of miRNA and mRNA expression profiles in response to Cd exposure in rice seedlings. BMC genomics, 15(1), 835.

Than, M., Han, M. (2013). Functional analysis of the miRNA–mRNA interaction network in C. elegans. Worm 2(4), e26894–e26894.

Thum, T.; Gross, C.; Fiedler, J. (2008). MicroRNA-21 contributes to myocardial disease by stimulating MAP kinase signaling in fibroblasts. Nature, 456, 980–986.

Trapnell, C., Williams, B. A., Pertea, G., Mortazavi, A., Kwan, G., van Baren, M. J. (2010). Transcript assembly and quantification by RNA-Seq reveals unannotated transcripts and isoform switching during cell differentiation. *Nat. Biotechnol.* 28, 511-515.

Vieira, F. A., Thorne, M. A., Stueber, K., Darias, M., Reinhardt, R., Clark, M. S., Power, D. M. (2013). Comparative analysis of a teleost skeleton transcriptome provides insight into its regulation. General and comparative endocrinology, 191, 45-58.

Wan, S. M., Yi, S. K., Zhong, J., Nie, C. H., Guan, N. N., Chen, B. X., Gao, Z. X. (2015). Identification of microRNA for intermuscular bone development in blunt snout bream (*Megalobrama amblycephala*). International journal of molecular sciences, 16(5), 10686-10703.

Wan, S.; Yi, S.; Zhong, J.; Wang, W.; Jiang, E.; Chen, B.; Gao, Z. (2014). Development and morphological observation of intermuscular bones in Megalobrama amblycephala. Acta Hydrobiol. Sin., 38, 1143–1151.

Wan, S.; Zhong, J.; Nie, C.; Gao, Z.; Zhang, X. (2015). The complete mitochondrial genome of the hybrid of *Megalobrama amblycephala* (♀) Å~ Megalobrama terminalis (♂). Mitochondria DNA.

Wang, L., Feng, Z., Wang, X., Wang, X., Zhang, X. (2010). DEGseq: an R package for identifying differentially expressed genes from RNA-seq data. *Bioinformatics* 26,136-138.

Wang, X. L., Mei, J., Sun, M., Hong, Y. H., Gui, J. F. (2005). Identification of three duplicated Spin genes in medaka (*Oryzias latipes*). *Gene* 350, 99-106.

Wang, X.; Cao, L.; Wang, Y.; Wang, X.; Liu, N.; You, Y. (2012). Regulation of let-7 and its target oncogenes (Review). Oncol. Lett., 3, 955–960.

Wang, Y. P., Li, K. B. (2009). Correlation of expression profiles between microRNAs and mRNA targets using NCI–60 data. BMC Genomics 10(19), 218.

Washko, D., Macrae, C. A., and Shin, J. T. (2009). Loss of bmpr2b in zebrafish causes augmented bmp-signaling through recruitment of an alternative type 2 receptor. *J. Card. Fail.* 15.

Wei, J., Li, H., Wang, S., Li, T., Fan, J., Liang, X., Zhao, R. C. (2014). let-7 enhances osteogenesis and bone formation while repressing adipogenesis of human stromal/mesenchymal stem cells by regulating HMGA2. Stem cells and development, 23(13), 1452-1463.

Xie, C. (2010). Ichthyology (M); China Agricultural Press: Beijing, China, pp. 56–57.

Xu, X. F., Zheng, J. B., Qian Y. Q., Luo C. (2015). Normally grown and developed intermuscular bone-deficient mutant in grass carp, Ctenopharyngodon idellus (in Chinese). Chinese Sci. Bull. 60(1), 52–57.

Xu, Z.; Chen, J.; Li, X.; Ge, J.; Pan, J.(2013). Identification and characterization of MicroRNAs in channel catfish (Ictalurus punctatus) by using Solexa sequencing technology. PLoS ONE, 8, e54174.

Yan, X.; Ding, L.; Li, Y.; Zhang, X.; Liang, Y. (2012). Identification and profiling of microRNAs from skeletal muscle of the common carp. PLoS ONE, 7, e30925.

Yang, D. C., Tsai, C. C., Liao, Y. F., Fu, H. C., Tsay, H. J., Huang, T. F. (2011). Twist controls skeletal development and dorsoventral patterning by regulating runx2 in zebrafish. *PLoS One* 6, e27324.

Yang, J.; Phillips, M.; Betel, D.; Mu, P.; Ventura, A.; Siepel, A.; Chen, K.; Lai, E. (2011). Widespread regulatory activity of vertebrate microRNA* species. RNA, 17, 312–326.

Yang, Z, Qu, X., Li, H., Huang, S., Wang, S., Xu, Q., Zhao, R. C. (2012). MicroRNA-100 regulates osteogenic differentiation of human adipose-derived mesenchymal stem cells by targeting BMPR2. FEBS letters, 586(16), 2375-2381.

Yi, S. E., Daluiski, A., Pederson, R., Rosen, V., Lyons, K. M. (2000). The type I BMP receptor BMPRIB is required for chondrogenesis in the mouse limb. *Development* 127, 621-630.

Yi, S., Gao, Z. X., Zhao, H., Zeng, C., Luo, W., Chen, B., Wang, W. M. (2013). Identification and characterization of microRNAs involved in growth of blunt snout bream (*Megalobrama amblycephala*) by Solexa sequencing. Bmc Genomics, 14(1), 754.

Yi, S.; Gao, Z.; Zhao, H.; Zeng, C.; Luo, W.; Chen, B.; Wang, W. (2013). Identification and

characterization of microRNAs involved in growth of blunt snout bream (*Megalobrama amblycephala*) by Solexa sequencing. BMC Genomics, 14.

Ying, S., Czymmek, K. J., Jones, P. A., Fomin, V. P., Akanbi, K., Duncan, R. L., & Farach-Carson, M. C. (2009). Dynamic interactions between L-type voltage-sensitive calcium channel Cav1. 2 subunits and ahnak in osteoblastic cells. American Journal of Physiology-Cell Physiology, 296(5), C1067-C1078.

Yoon, B. S., Ovchinnikov, D. A., Yoshii, I., Mishina, Y., Behringer, R. R., and Lyons, K. M. (2005). Bmpr1a and Bmpr1b have overlapping functions and are essential for chondrogenesis in vivo. *Proc. Natl. Acad. Sci. U S A.* 102, 5062-5067.

Young, M. D., Wakefield, M. J., Smyth, G. K., and Oshlack, A. (2010). Gene ontology analysis for RNA-seq: accounting for selection bias. *Genome Biol.* 11, R14.

Yu, P. B., Beppu, H., Kawai, N., Li, E., and Bloch, K. D. (2005). Bone morphogenetic protein (BMP) type II receptor deletion reveals BMP ligand-specific gain of signaling in pulmonary artery smooth muscle cells. *J. Biol. Chem.* 280, 24443-24450.

Yu, Y., Fuscoe, J. C., Zhao, C., Guo, C., Jia, M., Qing, T., Luo, H. (2014). A rat RNA-Seq transcriptomic BodyMap across 11 organs and 4 developmental stages. Nature communications, 5(1), 1-11.

Zeng, X., Zhang, X., Zou, Q. (2015). Integrative approaches for predicting microRNA function and prioritizing disease-related microRNA using biological interaction networks. Brie. Bioinform. 17(2), 193–203.

Zhang, G., Yin, S., Mao, J., Liang, F., Zhao, C., Li, P., Tang, Z. (2016). Integrated analysis of mRNA-seq and miRNA-seq in the liver of *Pelteobagrus vachelli* in response to hypoxia. Scientific reports, 6, 22907.

Zhou, L., Wang, Y., Gui, J. F. (2006). Fish-specific genome duplication. *Zool. Res.* 27, 525-532.

Zhu, Y.; Xue, W.; Wang, J.; Wan, Y.; Wang, S.; Xu, P.; Zhang, Y.; Li, J.; Sun, X. (2012). Identification of common carp (*Cyprinus carpio*) microRNAs and microRNA-related SNPs. BMC Genomics 2012, 13, 413.

7 ADDITIONAL FILES INFORMATION

Additional file 1 miRNA reverse transcription-specific stem-loop primers

miRNA name	Stem loop primer 5'-3'
Mam-miR-125a	CTCAACTGGTGTCGTGGAGTCGGCAATTCAGTTGAGCACAGGTT
Mam-miR-novel14	CTCAACTGGTGTCGTGGAGTCGGCAATTCAGTTGAGCCGCCGCC
Mam-miR-140-3p	CTCAACTGGTGTCGTGGAGTCGGCAATTCAGTTGAGGTCCGTGG
Mam-miR-199-3p	CTCAACTGGTGTCGTGGAGTCGGCAATTCAGTTGAGTAACCAAT
Mam-miR-21	CTCAACTGGTGTCGTGGAGTCGGCAATTCAGTTGAGCCAACACC
Mam-miR-210-5p	CTCAACTGGTGTCGTGGAGTCGGCAATTCAGTTGAGCAATGTGC
Mam-miR-221	CTCAACTGGTGTCGTGGAGTCGGCAATTCAGTTGAGAAACCCAG
Mam-miR-222a	CTCAACTGGTGTCGTGGAGTCGGCAATTCAGTTGAGAGACCCAG
Mam-miR-26a	CTCAACTGGTGTCGTGGAGTCGGCAATTCAGTTGAGAGCCTATC
Mam-miR-29a	CTCAACTGGTGTCGTGGAGTCGGCAATTCAGTTGAGTAACCGAT
Mam-miR-92a	CTCAACTGGTGTCGTGGAGTCGGCAATTCAGTTGAGACAGGCCG

Additional file 2 miRNAs qRT-PCR froward primers

miRNA name	Forward primer
Mam-miR-125a	ACACTCCAGCTGGGTCCCTGAGACCCTTAA
Mam-miR-novel14	ACACTCCAGCTGGGGCGAAGGTGGCTCGG
Mam-miR-140-3p	ACACTCCAGCTGGGTACCACAGGGTAGAACC
Mam-miR-199-3p	ACACTCCAGCTGGGACAGTAGTCTGCACAT
Mam-miR-21	ACACTCCAGCTGGGTAGCTTATCAGACTGG
Mam-miR-210-5p	ACACTCCAGCTGGGAGCCACTGACTAACGC
Mam-miR-221	ACACTCCAGCTGGGAGCTACATTGTCTGCT
Mam-miR-222a	ACACTCCAGCTGGGAGCTACATCTGGCTACT
Mam-miR-26a	ACACTCCAGCTGGGTTCAAGTAATCCAGGA
Mam-miR-29a	ACACTCCAGCTGGGTAGCACCATTTGAAAT
Mam-miR-92a	ACACTCCAGCTGGGTATTGCACTTGTCCCG
Generic reverse primer	TGGTGTCGTGGAGTCG

Additional file 3 miRNA reverse transcription-specific stem-loop primers

miRNA name	Stem loop primer 5'-3'
Mam-let-7b-5p	CTCAACTGGTGTCGTGGAGTCGGCAATTCAGTTGAGAACCACAC
Mam-miR-100	CTCAACTGGTGTCGTGGAGTCGGCAATTCAGTTGAGAAGTTCGG
Mam-miR-100a-5p	CTCAACTGGTGTCGTGGAGTCGGCAATTCAGTTGAGGACACAAG
Mam-miR-2188-5p	CTCAACTGGTGTCGTGGAGTCGGCAATTCAGTTGAGAGGACATG
Mam-miR-133	CTCAACTGGTGTCGTGGAGTCGGCAATTCAGTTGAGTACAGCTG
Mam-miR-133b	CTCAACTGGTGTCGTGGAGTCGGCAATTCAGTTGAGAGCTGGTT
Mam-miR-2288	CTCAACTGGTGTCGTGGAGTCGGCAATTCAGTTGAGAAACCACA
Mam-miR-140	CTCAACTGGTGTCGTGGAGTCGGCAATTCAGTTGAGTCCGTGGT
Mam-miR-222-3p	CTCAACTGGTGTCGTGGAGTCGGCAATTCAGTTGAGAAGACCCA

Additional file 4 miRNAs qRT-PCR froward primers

miRNA name	Forward sequence
Mam-let-7b-5p	ACACTCCAGCTGGGTGAGGTAGTAGGTTGT
Mam-miR-100	ACACTCCAGCTGGGAACCCGTAGATCC
Mam-miR-100a-5p	ACACTCCAGCTGGGAACCCGTAGATCCGAACT
Mam-miR-2188-5p	ACACTCCAGCTGGGAAGGTCCAACCTCACA
Mam-miR-133	ACACTCCAGCTGGGTGGTCCCCTTCAACCA
Mam-miR-133b	ACACTCCAGCTGGGTTGGTCCCCTTCAA
Mam-miR-2288	ACACTCCAGCTGGGAGGTAGTAGGTTGTG
Mam-miR-140	ACACTCCAGCTGGGTACCACAGGGTAGAAC
Mam-miR-222-3p	ACACTCCAGCTGGGAGCTACATCTGGCTACTG
Generic reverse primer	TGGTGTCGTGGAGTCG

Additional file 5 Protocols for fast DNA extraction

1. Put clipped fin into a thin-walled PCR tube (96-well plate format is great). Keep on ice until you ready to proceed.
2. Add 50 ul DNA Lysis Buffer (10 mM Tris pH 8.4; 50 mM KCl; 1.5 mM MgCl2; 0.3% Tween-20; 0.3% NP-40).
3. Incubate 20 min at 94ºC (in PCR machine).
4. Cool reaction to 55ºC
5. Add 5 ul 10 mg/ml ProtK and incubate 1 hr at 55ºC followed by 94ºC for 20 min (also in PCR machine).
6. Store DNA at –20ºC.

Additional file 6 Bone and cartilage staining method

Protocols of alizarin red bone staining:

1. Fix the specimens in 4% paraformaldehyde overnight;
2. Wash specimens 3 times with 1%PBST (0.1% Tween 20), 5 min each time;
3. Prepare the bleach solution: mix 3% H2O2 and 2% KOH according to 1:2;
4. Add bleach solutionto the specimens and process the sample for 10 minutes (depending on the size of the specimens, don't take too long, carefully observe) until the specimens is transparent;
5. Wash specimens 3 times with water, 5 min each time;
6. Transfer the sample to alizarin red staining solution (0.1%) for 1-2 hthis (depending on the size of the specimens, timing observation, adjusting the dyeing time);
7. Wash 3 times with water;
8. Place the sample in 50% glycerol-KOH for transparent, then transfer to 70% and store it in 100% glycerol for examine.

Protocol of Alcian blue cartilage staining:

1. Fix the specimen in 4% paraformaldehyde overnight;

2. Wash specimen 3 times with 1%PBST (0.1% Tween 20), 5-10 min each time;

3. Prepare the bleach solution: mix 3% H2O2 and 2% KOH according to 1:2;

4. Add bleach solution to the specimens and process the sample for 10 minutes (depending on the size of the specimens, don't take too long, carefully observe) until the specimens is transparent;;

4. Wash specimen with water, transfer to Alcian Blue staining solution for staining (2-3 hthiss, depending on the specimen size); Alcian Blue staining solution: 1% concentrated hydrochloric acid, 70% ethanol; 0.1% Alcian blue, final concentration.

5. Wash specimen in acidic ethanol for 1-2 hthiss each time (longer is better);

5% concentrated hydrochloric acid, 70% ethanol;

5% concentrated hydrochloric acid, 50% ethanol;

5% concentrated hydrochloric acid, 30% ethanol;

5% concentrated hydrochloric acid, 15% ethanol;

Wash specimen with water for 5-10 minutes.

6. The sample was digested in 1 mg/ml trypsin, 60% borax solution for 20 minutes to remove background color and tissue interference around the cartilage;

7. Wash specimen with water for 10min

8. Place the sample in 50% glycerol-KOH for transparent, then transfer to 70% and store it in 100% glycerol for examine..

Additional file 7 Wild and bmpr2a mutant zebrafish sequence

Amino acid sequence for wild fish *bmpr2a*：

MAVEGRITILDVGLIAMVVLLGPVAAAQSEQRECAYAEQPQGLAERIGGRGEGLVFHEN
STIRCYQGHRCFGLWGKKNNGVVLVKQGCWTNVGDHQECYDRCVVTNPPSVAQNGT
YRFCCCNKDMCNLNFTEDFPPPSPTTAQPLQSRRLHREEVIVVALATVSMVAVLVILLFF
GYRMLRGRGKHSLHTLNILETALSPPSLDLDNLTLQELIGRGRYGTVYRASLDDRSVAV
KVFISANRQQFTNERMIYRLLLDHENIARFLESEERVGTEGRTEFLLLLEFYPHGSLCTYL
SGRTVDWLSCCRLALSVTRGLAYLHTEIQRGDVYKPAVSHRDLNSRNVLVKTDGSCVIS
DFGLSMILTGKRPPGHGEEDNSAISEVGTVRYMAPEVLEGAVNLRDCESALKQVDVYA
LGLVYWETFMRCADLFPGETVPAFQLAFQAEVGNHPTIEDMQALVSREKERPKFPEAW
KENSLTVHSLKETMEDCWDQDAEARLTAQCAEERLAELLLIWDREKSASPALNHSTAL
QTPKVGSVLEHSSTNTEDHEGADKPLHNDTSVEQTSAGGTNPAEKKKNCINYEWQQA
QSRQSGTESSSATPVSESCNATHPPPVATNLCAQLTREDLEIPKLDPSEVQRNMRESS
DESLMEHSQKQFCSPETSASHGPFYPLMKMVSEVSGSQGSSRHGDTPITILPKQQNVP
KRPSSLSLHVKPGKTSTSTSSSLRMKFGKLGKSNLKKVEMGVAKSSVVNATHEARLITV
ANNDAAAAMNKYATEPAAESAGSSANEDLTFGLLNTSPDEQEPLLRREAHPDNANNNN
SNNNNGEGDGDGETEGGGEGGENNESVGPTGDASSSSTVEPVVLPGPCSASTAIPPQ
AQSQTQTHGEALLRQNRVRRPERPNSLDLSITTLPLLGGRSVGDGTEGSGDKIKKRVKT
PYALKKWRPASWVITTDTLDAEVNNNSRHGGGLGQNQNQAGTSRPKSASAVYLGSRG
GSRFSDPNDCDF*

Amino acid sequence for *bmpr2a*$^{-/-,-10bp}$ mutant，frame-shift mutations at the 21nd AA and premature transcription termination event at the 78nd AA:

MAVEGRITILDVGLIAMVVLWLLHRVSRGSVRTQSSHRVWPSGLVGVGKDLSFMRTLPF
AVIKDTAALDSGAKKIME*Y**SKVAGRMLVTTRSAMTAVW*PTHRQWLRMGHTDSAAAI
KTCAT*TSQRTFHLLPRPLHSPFNRADCTERKS*LLP*QLCPWLLSSSFCFFLGIAC*EDV
VNTHCIL*IYWRRHFLLLLWIWTTSHCRS*LAGAGTVQCIVLRWMTDL*Q*KFSFLLTASS
SLMSV*FIASSWITRT*RAS*RARSASAQKVGQSFSFCWSFILMALCARI*AAGLWTG*AA
AVWLCL*PEGWRTYIQRYSEGMCINRLSPTGI*TAGMCWLRRTARV*SVTLDCP*F*QER
GRLVMEKRTTVPSVR*VQCGTWLQKCWKGL*I*GIVSLR*NKWMFMHWVWFTGRPSCA
VQIFSQVKQCQLFSWHSRQRWAIILP*RTCRRLCPEKKKDPNSQKPGKRIA*RCIL*KRR
WKTAGIRTQKPD*QLSVRRSDSPNCSSSGTEKNQPVLLLTTALHCRHLK*VLSLNTHPQ
TLKTMKVLINHSTMTPQWSKPQQEELIPQRRKRTASTMSGSRPNHDSLAQKAPPLLLS
QSPAMPRILHQWPPISVLS*HEKTWRYQNSTRAKSRGT*ERARTRALWNIHRNSSALLK
RQPPTARFILS*RWFLRFRGHKDPVGMGTPL*PSYLSSRTSLRDPVASVST*SLGKHPPR
RLHRCG*SSESLESQI*RRLRWVWLKAVW*MRRMKPG*LQLPTTMRRQQ*INMQQNQQ
PSQQEVQPTRT*PSAS*TPVPMSRSLC*EERRILTMQTTTTAITTMVREMVMERQRVEE
REERTMRVSVRQGMLRRLLRWSRLCCLARVLLQPPFLHRPKARHRH

Amino acid sequence for *bmpr2a*$^{-/-,-7bp}$ mutant，frame-shift mutations at the 22nd AA and premature transcription termination event at the 79nd AA:

MAVEGRITILDVGLIAMVVLLWLLHRVSRGSVRTQSSHRVWPSGLVGVGKDLSFMRTLP
FAVIKDTAALDSGAKKIME*Y**SKVAGRMLVTTRSAMTAVW*PTHRQWLRMGHTDSAA
AIKTCAT*TSQRTFHLLPRPLHSPFNRADCTERKS*LLP*QLCPWLLSSSFCFFLGIAC*ED
VVNTHCIL*IYWRRHFLLLLWIWTTSHCRS*LAGAGTVQCIVLRWMTDL*Q*KFSFLLTAS
SSLMSV*FIASSWITRT*RAS*RARSASAQKVGQSFSFCWSFILMALCARI*AAGLWTG*A
AAVWLCL*PEGWRTYIQRYSEGMCINRLSPTGI*TAGMCWLRRTARV*SVTLDCP*F*QE
RGRLVMEKRTTVPSVR*VQCGTWLQKCWKGL*I*GIVSLR*NKWMFMHWVWFTGRPSC
AVQIFSQVKQCQLFSWHSRQRWAIILP*RTCRRLCPEKKKDPNSQKPGKRIA*RCIL*KR
RWKTAGIRTQKPD*QLSVRRSDSPNCSSSGTEKNQPVLLLTTALHCRHLK*VLSLNTHP
QTLKTMKVLINHSTMTPQWSKPQQEELIPQRRKRTASTMSGSRPNHDSLAQKAPPLLL

SQSPAMPRILHQWPPISVLS*HEKTWRYQNSTRAKSRGT*ERARTRALWNIHRNSSALL
KRQPPTARFILS*RWFLRFRGHKDPVGMGTPL*PSYLSSRTSLRDPVASVST*SLGKHPP
RRLHRCG*SSESLESQI*RRLRWVWLKAVW*MRRMKPG*LQLPTTMRRQQ*INMQQNQ
QPSQQEVQPTRT*PSAS*TPVPMSRSLC*EERRILTMQTTTTAITTMVREMVMERQRVE
EREERTMRVSVRQGMLRRLLRWSRLCCLARVLLQPPFLHRPKARHRHTERLCSDRTE
CADQRDPTLWICPSQHCHY*EAGLSAMGQRGQGIKSRSG*RRLTHLRSGVLPAGLSPL
THWMPKSTTTVVTEEASGRIRIRLGPADLNQLRLSI*AVEEDLASQILMTVTF

Additional file 8 Wild and bmpr2b mutant zebrafish sequence

bmpr2b mRNA for wild fish:

GGAGCTGAAGTTACCGAGAGCGGCCGCGGGAGCTCGACACGATCCGCGGGGCGA
TAATCAACCACAACGGGGAGAAAAGCGCTTATTTAACCGAACAGACCCTGACCGAC
CGGCAATCAGTTTAACGACCATCACACAGTCTACCGACAGTCGCCGCGTTGTTCAT
TACAGGCCTCCGTCGCTTTGGATCGGACTCAATGTCGCTCCTGTTCGGCCGCTTGA
GCTCGACGCCTTCTGCCGCAGGTTTACTTCATTTCAGAGACATCATTTAAGGGATAA
TGCAGGAATAAAACCGGGCACAGTCGGGAAATGTCGGACATGTCGTCAGCTCGTG
AAGCTAAACATCGACTGAAGCGGACTGACACCAAGAAACCTGACCCATATTGAGAT
CCTGAGCTCGAGCATCTGGACCAGAACCAAATATTACATCGAAACTAAATCTTGTTT
ATAAACACAGACGACAACCGAGAGACGCCACACAGCAGGTTTTGAGACCTTTAGTT
TTATTTTAAGATATGCGAGGAAGTGTATTATACATATTAAATGAAGTATAATCGCTCA
AACTCCCAACCAGCATGGAGAAAATGCGTTTATAAGCTGTTTATCGAAACCAAAGGC
ATCTAAAATCATGCGCTGCCTCCAAATCTTCATCTGCACTAACGTTAGTCATTTCGG
ATTGTTTGCTCCGTGCACATGAGCTTGAACTTCGGTCGATAGAAAGAAGAAAGGGG
GAACAGAAAATCTAGTTACTGGAACTTTTTTTTGGAGCTGAATCCATCCAGAAGCGG
CAGCAGGATGAGAGTGCGGATCCTAAACCGGACATCAGTACTGTCACTCGGGCTCT
GCTCACTGCTTCTGCTCAGTGCTGTGGCCGCTGCTCAGAGTGAAGAGCGCGAGCG
GGAGTGTGCTTTTAATGACCAGCACCAGCAGGTGGATGAGCAGAGTGTGGCAGGT
GACTGGCACATCACCAGAGAAAATAACACCATCCTGTGCAGCAAGAGCAGCCGCTG
CTACGGCCTCTGGGAGAAAACACATGACGGAGAGATCCGTCTGGTCAAACAAGGCT

GTTGGACTTACATTGGTGACCAGCAGGACTGCCATGACGACCGTTGCGTGGTTACC
ACAACGCCATCGCAGATCCAGAATGGCACCTACAGATTCTGCTGCTGCAGCACCAA
CATGTGCAACGTCAACTTCACAGAGAACTGGGTGCCCAGTCCCACCAGCACTGCCA
ACCGTGATCAGCCGCCTATACACAGAGATGAGGCCATCTTCATCGCCCTGGCCTCC
GTCTCCATTGTGGCCGTCCTTATTGTCGCGCTGTTCTTTGGCTATCGTGTGATGATG
GGCGAGTGTAAACAGGGCCTGCACAATATGGACATGATAGAGGCTGCGCCATCTG
AACCTTCGCTGGATTTAGACAGTTTAAAGCTCCTCGAACTGATTGGCCGAGGCCGC
TACGGTTCCGTCTACAAGGGGTCTCTTGACGAACGGCCGGTTGCAGTAAAAGTTTT
TACCTATGCCAACCGGCAGAACTTTGTGAATGAGCGCTCCATCTACCGAGTGCCTC
TTCTGGAGCATGAAAACATTGCTCGCTTTATCGTCGGCGATGAGCGGATGACCACT
GACGGACGCATGGAGTACCTGCTGGTCATGGAGTACTACCCTCATGGCTCGCTGT
GCCGCTATCTGAGTCTGCACACGCTGGACTGGGTGAGCTGCTGTCGTCTGGCTCAT
TCACTGACCAGAGGACTGGCCTATCTGCACACTGAGCTCCTGAGAGGAGATATATA
CAAACCTGCCATTTCGCACCGGGATCTAAACAGCCGGAATGTTCTAGTGAAGAACG
ATGGCACCTGTGTGATCAGCGACTTCGGTCTGTCTATGAAGCTGACTGGAAATCGT
CTGGTACGGCCTGGAGAAGAGGAAAACGCCGCCATCAGTGAGGTGGGCACGATCC
GCTACATGGCGCCGGAGGTGCTGGAGGGAGCCGTGAACCTCAGGGACTGCGAGT
CTGCATTGAAACAGGTGGACATGTACGCCATCGGCCTCATCTACTGGGAGACCTTT
ATGAGGTGCACTGACCTTTTTCCAGGAGAGACAGTGCCAGAATACCAGATGGCTTT
CCAGGCCGAGGCGGGAAACCACCCGTCCTTTGAGGACATGCAGGTGTTGGTGTCC
AGAGAGAAACAGAGACCCAAGTTCCCAGAAGCCTGGAAGGAGAACAGCCTGGCTG
TGCGCTCTCTAAAGGAGACTATGGAGGATTGCTGGGATCAGGATGCAGAGGCTCGT
CTGACAGCGCAGTGTGCAGAGGAGCGTATGGCAGAACTGCTGCTGATTTGGGAAA
GGAACAAACCTGTCAGTCCCACCATCAATCCCATGAGCACAGCGCTGCAGAACGAG
AGGAATCTGACCCACAGCCGCAGGGCTCCCAAAATGGGCTCTTACCCAGATTACTC
TTCATCCTCTTACATCGAGGATCATGAGGGCATGGTGAAGAACCTCCCAGGCGACG
TCTCCACGTCTGGCACTTCCTCTGTGGGTGGTGTGGGCGTGAGTGGCAGCAGTGG
GGGCGTTGCAGCGACCGGAGAGAAGAACAGAAACTCCATCAACTATGAAAGACAG
CAAGCTCAGGCGCAAGCTCGACTGCCCAGTCCTGAAACCAGCGGCACAAGTTTGT
CCACCACAACCACCACAACAGGCCTCACACCCAGTACCATCATGACCACCATCTCC

GAATCGGGCCACTCGGAGGACACAGGAGCCGGAGGAAGTGTACCAGTGTGCCTTC
AACTCACAGAGGAAGATCTGGAGACCACCAAACTGGACCCCAAAGAGGTGGACAA
GAACCTGAAAGAAAGTTCTGATGAGAATCTGATGGAGCACTCGCAGAAACAGTTCA
GCGCCCCTGATCCACTCAGCTCGGGCAGCACCAGTCTTTTATACCCACTGATTAAA
CTCGCAGCAGAAGTGACTGGAGGATCTGGAAGTGGTGGACAAACTGATTTCGGGG
TGGGCAGCAGTGGAATGAGCGACACTCCCACAGCCATGTTTCCTCTCCCCAAACAG
CAGAATCTCCCCAAGAGGCCCACTAGCTTACCCCTCAACACCAAAAATCCTGGTAG
GGAGTCTTCGTCGTCTCGATTGAAATTCGGGAAGCACAAGTCCAACCTGAAGCAGG
TGGAGACAGGTGTAGCCAAGATGAACACTGTGGTGGCCGTCGAGCCACACTTGGC
CACCGTCACCAACAATGGACCCAGTGTGCGCAGTGGTGCTGGAGTGGTCGTAGTA
AATGGATATGGAGTGGGCAATGGTGCCAGCTCCTCTGATGCGTTTGGAAACACGAA
CCCCGTCGGGCCACAGGGTGAAGGGGGCGCTCCTCTGCTGCAGAGCCAACTGAG
CGGAGAAGACAGCCGACTCAACATCAACATCAACTCCAGCCCTGATGAACACGAGC
CCCTGCTAAGAAGAGAGCAGCCGGCCGCGCGGGATCACTCCGGTCGCACCAACTC
CAACAACAACAACAGCAACATTCACACCACTGCCACGGTTTGTGCGCTCACCGCTG
CAGACGCCCAGATAGAGGCTTTAACCTGCCTGTCGGGAGCGCCAGACGGAAGGGA
TAATGGGGTTCCATTGAGGCCACCTAAACCCAGAAGACCAGAGCGGCCAAACTCAC
TGGACCTGTCAGCCTCTTCCCAGAATTCTTCTCTTTTAGATGAGGCCGTGTCGCAG
GAGGGAAAGGCCGGATCAGCTGAGAAGATTAAAAAACGTGTGAAGACTCCTTATTC
GTTGAAAAGATGGCGTCCTTCCACATGGGTCGTCTCCACTGATACACTAGATGGAG
AGGTGAACAACAACGGGCACAGCCAGCAGACGATGATGGCAGTAAGTGGAGGTGG
TCACCCAAGCGCTGGCCAATCAAAGTCCAGCATCGCCGTGTTTTTGGTCGGCGGAG
GAACAGCAACAGCTACTCTGACCTCCGATCCTCCAGATATGACCTGCCTGTGA

Bmpr2b mRNA for *bmpr2b*$^{-/-,-44bp}$ mutant，Lost start codon “ATG”:

GGAGCTGAAGTTACCGAGAGCGGCCGCGGGAGCTCGACACGATCCGCGGGGCGA
TAATCAACCACAACGGGGAGAAAAGCGCTTATTTAACCGAACAGACCCTGACCGAC
CGGCAATCAGTTTAACGACCATCACACAGTCTACCGACAGTCGCCGCGTTGTTCAT
TACAGGCCTCCGTCGCTTTGGATCGGACTCAATGTCGCTCCTGTTCGGCCGCTTGA
GCTCGACGCCTTCTGCCGCAGGTTTACTTCATTTCAGAGACATCATTTAAGGGATAA

TGCAGGAATAAAACCGGGCACAGTCGGGAAATGTCGGACATGTCGTCAGCTCGTG

AAGCTAAACATCGACTGAAGCGGACTGACACCAAGAAACCTGACCCATATTGAGAT

CCTGAGCTCGAGCATCTGGACCAGAACCAAATATTACATCGAAACTAAATCTTGTTT

ATAAACACAGACGACAACCGAGAGACGCCACACAGCAGGTTTTGAGACCTTTAGTT

TTATTTTAAGATATGCGAGGAAGTGTATTATACATATTAAATGAAGTATAATCGCTCA

AACTCCCAACCAGCATGGAGAAAATGCGTTTATAAGCTGTTTATCGAAACCAAAGGC

ATCTAAAATCATGCGCTGCCTCCAAATCTTCATCTGCACTAACGTTAGTCATTTCGG

ATTGTTTGCTCCGTGCACATGAGCTTGAACTTCGGTCGATAGAAAGAAGAAAGGGG

GAACAGAAAATCTAGTTACTGGAACT~~TTTTTTTGGAGCTGAAT~~CC~~ATCCAGAAGCGG~~

~~CAGCAGGATG~~AGAGT~~~~GCGGATCCTAAACCGGACATCAGTACTGTCACTCGGGCTCT

GCTCACTGCTTCTGCTCAGTGCTGTGGCCGCTGCTCAGAGTGAAGAGCGCGAGCG

GGAGTGTGCTTTTAATGACCAGCACCAGCAGGTGGATGAGCAGAGTGTGGCAGGT

GACTGGCACATCACCAGAGAAAATAACACCATCCTGTGCAGCAAGAGCAGCCGCTG

CTACGGCCTCTGGGAGAAAACACATGACGGAGAGATCCGTCTGGTCAAACAAGGCT

GTTGGACTTACATTGGTGACCAGCAGGACTGCCATGACGACCGTTGCGTGGTTACC

ACAACGCCATCGCAGATCCAGAATGGCACCTACAGATTCTGCTGCTGCAGCACCAA

CATGTGCAACGTCAACTTCACAGAGAACTGGGTGCCCAGTCCCACCAGCACTGCCA

ACCGTGATCAGCCGCCTATACACAGAGATGAGGCCATCTTCATCGCCCTGGCCTCC

GTCTCCATTGTGGCCGTCCTTATTGTCGCGCTGTTCTTTGGCTATCGTGTGATGATG

GGCGAGTGTAAACAGGGCCTGCACAATATGGACATGATAGAGGCTGCGCCATCTG

AACCTTCGCTGGATTTAGACAGTTTAAAGCTCCTCGAACTGATTGGCCGAGGCCGC

TACGGTTCCGTCTACAAGGGGTCTCTTGACGAACGGCCGGTTGCAGTAAAAGTTTT

TACCTATGCCAACCGGCAGAACTTTGTGAATGAGCGCTCCATCTACCGAGTGCCTC

TTCTGGAGCATGAAAACATTGCTCGCTTTATCGTCGGCGATGAGCGGATGACCACT

GACGGACGCATGGAGTACCTGCTGGTCATGGAGTACTACCCTCATGGCTCGCTGT

GCCGCTATCTGAGTCTGCACACGCTGGACTGGGTGAGCTGCTGTCGTCTGGCTCAT

TCACTGACCAGAGGACTGGCCTATCTGCACACTGAGCTCCTGAGAGGAGATATATA

CAAACCTGCCATTTCGCACCGGGATCTAAACAGCCGGAATGTTCTAGTGAAGAACG

ATGGCACCTGTGTGATCAGCGACTTCGGTCTGTCTATGAAGCTGACTGGAAATCGT

CTGGTACGGCCTGGAGAAGAGGAAAACGCCGCCATCAGTGAGGTGGGCACGATCC

GCTACATGGCGCCGGAGGTGCTGGAGGGAGCCGTGAACCTCAGGGACTGCGAGT

CTGCATTGAAACAGGTGGACATGTACGCCATCGGCCTCATCTACTGGGAGACCTTT

ATGAGGTGCACTGACCTTTTTCCAGGAGAGACAGTGCCAGAATACCAGATGGCTTT

CCAGGCCGAGGCGGGAAACCACCCGTCCTTTGAGGACATGCAGGTGTTGGTGTCC

AGAGAGAAACAGAGACCCAAGTTCCCAGAAGCCTGGAAGGAGAACAGCCTGGCTG

TGCGCTCTCTAAAGGAGACTATGGAGGATTGCTGGGATCAGGATGCAGAGGCTCGT

CTGACAGCGCAGTGTGCAGAGGAGCGTATGGCAGAACTGCTGCTGATTTGGGAAA

GGAACAAACCTGTCAGTCCCACCATCAATCCCATGAGCACAGCGCTGCAGAACGAG

AGGAATCTGACCCACAGCCGCAGGGCTCCCAAAATGGGCTCTTACCCAGATTACTC

TTCATCCTCTTACATCGAGGATCATGAGGGCATGGTGAAGAACCTCCCAGGCGACG

TCTCCACGTCTGGCACTTCCTCTGTGGGTGGTGTGGGCGTGAGTGGCAGCAGTGG

GGGCGTTGCAGCGACCGGAGAGAAGAACAGAAACTCCATCAACTATGAAAGACAG

CAAGCTCAGGCGCAAGCTCGACTGCCCAGTCCTGAAACCAGCGGCACAAGTTTGT

CCACCACAACCACCACAACAGGCCTCACACCCAGTACCATCATGACCACCATCTCC

GAATCGGGCCACTCGGAGGACACAGGAGCCGGAGGAAGTGTACCAGTGTGCCTTC

AACTCACAGAGGAAGATCTGGAGACCACCAAACTGGACCCCAAAGAGGTGGACAA

GAACCTGAAAGAAAGTTCTGATGAGAATCTGATGGAGCACTCGCAGAAACAGTTCA

GCGCCCCTGATCCACTCAGCTCGGGCAGCACCAGTCTTTTATACCCACTGATTAAA

CTCGCAGCAGAAGTGACTGGAGGATCTGGAAGTGGTGGACAAACTGATTTCGGGG

TGGGCAGCAGTGGAATGAGCGACACTCCCACAGCCATGTTTCCTCTCCCCAAACAG

CAGAATCTCCCCAAGAGGCCCACTAGCTTACCCCTCAACACCAAAAATCCTGGTAG

GGAGTCTTCGTCGTCTCGATTGAAATTCGGGAAGCACAAGTCCAACCTGAAGCAGG

TGGAGACAGGTGTAGCCAAGATGAACACTGTGGTGGCCGTCGAGCCACACTTGGC

CACCGTCACCAACAATGGACCCAGTGTGCGCAGTGGTGCTGGAGTGGTCGTAGTA

AATGGATATGGAGTGGGCAATGGTGCCAGCTCCTCTGATGCGTTTGGAAACACGAA

CCCCGTCGGGCCACAGGGTGAAGGGGGCGCTCCTCTGCTGCAGAGCCAACTGAG

CGGAGAAGACAGCCGACTCAACATCAACATCAACTCCAGCCCTGATGAACACGAGC

CCCTGCTAAGAAGAGAGCAGCCGGCCGCGCGGGATCACTCCGGTCGCACCAACTC

CAACAACAACAACAGCAACATTCACACCACTGCCACGGTTTGTGCGCTCACCGCTG

CAGACGCCCAGATAGAGGCTTTAACCTGCCTGTCGGGAGCGCCAGACGGAAGGGA

TAATGGGGTTCCATTGAGGCCACCTAAACCCAGAAGACCAGAGCGGCCAAACTCAC

TGGACCTGTCAGCCTCTTCCCAGAATTCTTCTCTTTTAGATGAGGCCGTGTCGCAG

GAGGGAAAGGCCGGATCAGCTGAGAAGATTAAAAAACGTGTGAAGACTCCTTATTC

GTTGAAAAGATGGCGTCCTTCCACATGGGTCGTCTCCACTGATACACTAGATGGAG

AGGTGAACAACAACGGGCACAGCCAGCAGACGATGATGGCAGTAAGTGGAGGTGG

TCACCCAAGCGCTGGCCAATCAAAGTCCAGCATCGCCGTGTTTTTGGTCGGCGGAG

GAACAGCAACAGCTACTCTGACCTCCGATCCTCCAGATATGACCTGCCTG